Analysis and Scaling of Coupled Neutronic Thermal Hydraulic Instabilities of Supercritical Water-Cooled Reactor

Thesis Submitted in
Partial Fulfilment of the Requirements
for the Degree of
Doctor of Philosophy
by

DAYA SHANKAR

DEPARTMENT OF MECHANICAL ENGINEERING
INDIAN INSTITUTE OF TECHNOLOGY
GUWAHATI

CERTIFICATE

It is certified that the work contained in this thesis entitled **Analysis and Scaling of Coupled Neutronic Thermal Hydraulic Instabilities of Supercritical Water-Cooled Reactor** by Daya Shankar, research scholar in the Department of Mechanical Engineering, Indian Institute of Technology Guwahati, India, toward the award of the degree of Doctor of Philosophy, has been carried out under our joint supervision, and that this work has not been submitted elsewhere for a degree.

Dr. Manmohan Pandey
Professor
Department of Mechanical Engineering, Indian Institute of Technology Guwahati, Assam, India
8th October 2018

Dr. Dipankar N. Basu
Assistant Professor
Department of Mechanical Engineering, Indian Institute of Technology Guwahati, Assam, India
8th October 2018

DECLARATION

I declare that the work contained in this thesis entitled **Analysis and Scaling of Coupled Neutronic Thermal Hydraulic Instabilities of Supercritical Water-Cooled Reactor,** submitted toward the award of the degree of Doctor of Philosophy, has been carried out by me under the joint supervision of Dr. Manmohan Pandey and Dr. Dipankar N. Basu, and that this work has not been submitted elsewhere for a degree.

Daya Shankar
Research Scholar
Department of Mechanical Engineering, Indian Institute of Technology Guwahati, Assam, India
8th October 2018

ACKNOWLEDGEMENTS

First, I would like to thank my doctoral advisors, Dr. Manmohan Pandey and Dr. Dipankar Narayan Basu, for their exceptional guidance, expertise, and patience over the years. Their consistent encouragement has helped me make this thesis a work I can be truly proud of. I am immensely grateful to them for providing me with the opportunity to do this research and develop my skills in a field, which has both fundamental scientific value and current practical relevance. Their kindness and grace always gave me determination and will to work.

I wish to express my warm and sincere thanks to my doctoral committee members Late. Prof. Subhash C. Mishra, Prof. Anoop K. Dass, Dr. Anugrah Singh and Dr. Ganesh Natarajan, for giving their valuable suggestions and encouragement during my research work.

I am extremely grateful to IIT Guwahati for providing me with the financial support during the course of my PhD. I would also like to acknowledge all the necessary infrastructure offered by Department of Mechanical Engineering, IIT Guwahati requisite for the smooth running of my research work. I am thankful to all the faculty members and staff members of Department of Mechanical Engineering, IIT Guwahati who helped me in different ways whenever I had any problem.

I would like to recognize the many friends I have made since coming to IIT for their camaraderie and their contributions intentional or otherwise to this thesis. I would like to thank Dr. Vijay Kumar Mishra, Dr. Jai Manik, Milan Krishna Singha Sarkar, Kiran Shakia, A Srinivas Pavan Kumar, Ashif Iqbal, Sandeep Sharma and many others for all the supreme times, and for likely extending the amount of time it took to complete the work contained in this thesis.

Of course, none of this would have been possible without the love of my family; particularly my parents: Smt. Geeta Devi and Shri P.N.Tiwary and. Their life-long support and encouragement has contributed so much to making me who I am, and I simply cannot thank them enough for everything they have done for me.

I reserve my heart full of affection and sincere gratitude to my wife Dr. Beauty Pandey for her love, motivations, patience and inspirations during my research work. I take this opportunity to appreciate and thank her for the hardship she had undergone during the stressful moments of my research work.

I take this opportunity to express my sincere thanks to Dr. Shraddha Basu for her kind hospitality and concern during our tough times. I would also like to thanks Smt. Divya Pandey for her indirect support. I extend my blessings and wishes to Baby Eirene and Master Subham Pandey. I wish both of them a glorious and prosperous future.

I would also like to thanks Prof. Biplab Halder for their encouragement and motivation.

Lastly, I would like to thank the Almighty without whose blessings and strength nothing would had been possible. Thank You Maa Kamakhya, for everything!!

All these contributions through every aspect of my life is pre and post Ph.D can never be expressed in words.

I would also like to apologise if I have missed any name. All your contribution all immensely valuable.

Thank you everyone.

Daya Shankar

October 2018

ABSTRACT

Present thesis work primarily focuses on the analysis of flow instability in one of the most powerful concepts under Generation-IV nuclear reactors; technology, namely, Supercritical water-cooled reactor (SCWR). Safety is the primary concern in the any nuclear reactors. Flow instabilities are one of a kind on which the current researches are going on. The reason behind that is the large density difference of the fluid through the coolant channel. Therefore, a downscaled model is required to study the complex phenomena in laboratory conditions; hence a scaled method is proposed here which is useful for the study of both the natural as well as the forced circulation system. For further analysing about the stability of the system, a simple but quite effective model has been developed as the Lumped Parameter Model (LPM). Using this model, a linear and nonlinear stability analysis have been done for the various parametric conditions. Moreover, the stability analysis due to the seismic effects on SCWR has also been considered by using the same LPM. Two types of seismic wave model have been taken into account for the analysis, first the sinusoidal acceleration and the other more realistic Kanai–Tajimi model which is used for more accurate simulation of the seismic wave. These methods are first time introduced in the SCWR.

Nuclear power plants use the heat generated from nuclear fission in a contained environment to convert water into steam, which further utilized for electricity production. The concept of nuclear power generation had started in 1950. According to European Nuclear Society (www.euronuclear.org), as of November 28, 2016, in 31 countries 450 nuclear power plant units with an installed electric net capacity of about 392 GW are in operation, and 60 plants with an installed capacity of 60 GW are in 16 countries under construction.

SCWR is a concept for an advanced reactor that operates at supercritical pressures and temperatures (25–30 MPa, 500-520 ^{o}C exit temperature). Such a high coolant temperature at turbine inlet provides high thermal efficiency

(~42%) which is substantially higher than any other LWR (~30%). But this is on the cost of large density difference throughout the coolant channel, from the inlet to the outlet (720 kg/m^3 to 90 kg/m^3), which raises a serious concern about flow instabilities in the SCWR. To ensure a proper design of the reactor without any sustainability issue, detailed stability analysis is essential.

It is evident from a meticulous survey of the relevant literature that, while the natural circulation-based systems have received some attention, supercritical channels with the forced flow generally experience a more considerable density variation across the core could not grab the proper attention of the researcher which is also more susceptible towards thermohydraulic instabilities. So, for the study and analysis of the latter system, a lumped parameter-based approach is followed.

The lumped parameter model (LPM) is derived from the basic governing equations of mass, momentum and energy. The basic governing equations, which are in PDE form, can be transformed into an equivalent nonlinear system of ODEs by nodalization and spatial integration. As LPM is computationally inexpensive, hence it is suitable for detailed parametric studies of stability trends. The general transient equations are difficult to solve because of the coupling between the momentum and energy equations and the nonlinear nature of these general equations. Therefore, in the present model Channel Integral (CI) method is used. The integrations of the conservation equations are done over first and second zone of the flow channel respectively, and the resultant system of algebraic and ODEs are employed for both linear and nonlinear analysis.

The Scaling of SCWR system is primely done for identifying a less restrictive model fluid, which can adequately mimic the SCW under the relevant scaled condition of an SCWR, and to define the scaling rules in a generalized way, to preserve the phenomenological physics. The focus is kept on uncoupling the radial scaling from the axial one, as only then a possible combination of system dimensions can be proposed.

US reference design of SCWR (Zhao et al., 2007) is considered as the prototype. Accordingly, the scaled dimensions of the lab-scale facility and corresponding operational settings regarding power, flow rate, and inlet temperature are proposed. The advantages of the proposed methodology over the existing ones have also been stressed upon, along with a discussion on the role of involved dimensionless groups.

A circular forced flow channel of uniform diameter is simulated in the present study, with uniform heat flux on the wall. The channel is subjected to both constant pressure drops and constant mass flow rate boundary conditions for the analysis. The one-dimensional conservation equations for mass, momentum, and energy have been taken. For the sake of generalizations, governing equations are nondimensionalized using the suitable dimensionless parameters. The equations for mass and energy are integrated over the first node, i.e., from inlet until the appearance of the pseudocritical point. Correspondingly, two ODEs can be obtained in terms the location of pseudocritical boundary. Now, again integrating the conservation equations over the second node, from the pseudocritical point to the channel outlet, two ODEs are achieved in terms of the outlet enthalpy. These four equations are sufficient for the mass flow rate boundary condition. However, for pressure-drop, boundary condition, the equation for conservation of momentum is integrated separately over both the zones and added to represent the net pressure drop across the channel. Accordingly, the six ODEs are selected for analysis, along with algebraic equations which are obtained by equating the ODE's of mass and energy equations for the two zones, and the equation of state. In order to capture the sharp variation in thermophysical properties of supercritical water around the pseudocritical point, the equation of state is replaced by fitting a separate rectangular hyperbola for each of the zones.

In order to introduce the power dynamics into framework, mathematical model for point reactor kinetics and a lumped parameter representation of the energy balance across the fuel rod are taken into consideration. The heat

generated inside the fuel rod is convectively transferred to the coolant from the rod surface. Applying energy balance with lumped capacitance approximation for the fuel rod, the state equation for fuel temperature and coolant enthalpy can be expressed in non-dimensional form. Therefore, the initial system of PDEs gets converted to a set of algebraic equations and ODEs, with dimensionless time as the sole independent variable. Finally, the thermal hydraulic part is compared with RELAP and found that the LPM results are more conservative than those predicated by RELAP, which implies that the use of LPM for stability analysis is safe. In addition to this, stability map for the various geometric and neutronic parameters have been generated.

Based on the motivation from the two-zone model, a three-zone model has been studied for the stability analysis. The whole flow region is divided as heavy fluid region (H-F), heavy & light fluid mixture region (H-L-M) and light fluid region (L-F) following the approach proposed by Zhao (2007). After analysing the results, within ± 10 % increases in the stability boundary has been observed, which do not justify the complexity of the formulations. The qualitative behaviour of both the models are similar, hence it is recommended that for the preliminary stability analysis, two zone model is more justified then the three-zone model.

The linear stability of SCWR channels has been studied in past. However, the analysis is valid only for infinitesimally small perturbations. Therefore, there is a need to carry out stability analysis for small finite sized perturbations. Moreover, earlier studies do not consider inclination of these channels, which exist for various applications. The present thesis work has also attempted linear, as well as nonlinear, stability analysis of the channel. The bifurcation analysis is carried out to capture the nonlinear dynamics of the system and to identify regions in the parameter space for which subcritical and supercritical bifurcations exist. The study is carried out for different inclination angles in order to characterize the effect of inclination on the stability of the system. The analysis shows that, at all conditions, a

generalized Hopf point exists. The subcritical and supercritical bifurcations are confirmed by numerical simulation of the time-dependent, nonlinear ODEs for the selected points in the operating parameter space. The identification of these points is important because the stability characteristics of the system for finite perturbations are dependent on them. Both stable and unstable limit cycle has been detected and the boundaries of the unstable limit cycle have also been calculated.

In the SCWR subjected to an earthquake, the oscillating acceleration attributable to the seismic wave may cause the variation of the coolant flow rate and density reactivity in the core, which might result in the core instability due to the density-reactivity feedback. Therefore, it is important to properly evaluate the effect of the seismic acceleration on the core stability from a viewpoint of plant integrity estimation. In this study, the in-house code using LPM two zone model is employed for stability appraisal under the seismic acceleration, considering the one-dimensional neutron-coupled thermal hydraulic equations. The coolant flow in the core is simulated by introducing the oscillating acceleration attributed to the earthquake motion into the momentum equation as external force terms. Both a simple periodic acceleration and the acceleration obtained from the response analysis to the El Centro seismic wave of Imperial Valley earthquake. An artificial earthquake records with a nonstationary Kanai–Tajimi model is also used for more accurate simulation of the earthquake. Finally, the behaviours of the core and coolant are calculated in terms of various parameters of acceleration. The effects of the neutronics, amplitude, and direction of the oscillating acceleration have been discussed. The stability map has been plotted based on these pieces of information.

CONTENTS

NOMENCLATURE

A	Area (m^2)
C	Precursor density (cm^{-3})
C_f	Heat capacity of fuel rod (kJ K^{-1})
C_p	Isobaric specific heat (kJ kg^{-1} K^{-1})
D_h	Hydraulic diameter (m)
f	Friction factor (–)
g	Gravitational acceleration (m s^{-2})
G	Mass flux (kg m^{-2} s^{-1})
h	Enthalpy (kJ kg^{-1})
k	Feedback reactivity (–)
K	Restriction coefficient (m^{-1})
L	Core length (m)
n_f	Number of fuel rods (–)
N_{Eu}	Euler number (–)
N_{Fr}	Froude number (–)
N_{SPC}	Pseudo subcooling number (–)
N_{TPC}	Transcritical phase-change number (–)
p	Pressure (N m^{-2})
P	Power (kW)
q_o''	Heat flux (kW m^{-2})
t	Time (s)

T	Absolute temperature (K)
z	Space coordinate (m)

Greek symbols

α	Heat transfer coefficient (kW m^{-2} K^{-1})
$\bar{\beta}$	Volumetric expansion coefficient (K^{-1})
β	Delayed neutron fraction (–)
γ	Nondimensionalized neutron generation time (–)
ρ	Density (kg m^{-3})
σ	$= \beta/\gamma$ (–)
π_h	Heated perimeter (m)

Subscripts

0	Reference
a	Acceleration
c	Core
f	Fuel rod / Friction
g	Gravitational
i	Inlet
L	Loss
o	Outlet
pc	Pseudocritical
$*$	Dimensionless quantities

LIST OF FIGURES

LIST OF TABLES

अतीत में जो कुछ भी हुआ, वह अच्छे के लिए हुआ, जो कुछ हो रहा है, अच्छा हो रहा है, जो भविष्य में होगा, अच्छा ही होगा. अतीत के लिए मत रोओ, अपने वर्तमान जीवन पर ध्यान केंद्रित करो , भविष्य के लिए चिंता मत करो

Whatever happened in the past, it happened for the good; Whatever is happening, is happening for the good; Whatever shall happen in the future, shall happen for the good only. Do not weep for the past, do not worry for the future, concentrate on your present life.

- Bhagwat Gita.

Chapter 1 INTRODUCTION

1.1 Motivation

Energy is the word, which is always important for the development of any country. Few of the option for power generation are fossil fuel, renewable and nuclear. Moreover, one has to think about long-term perspective for selecting the source of energy, which would meet all the requirements, which is not only in terms of energy but also with respect to environment. There are different sources of renewable energy such as solar, wind, hydro, nuclear etc., Among these, nuclear is also one of the energies which are clean and green, as it is considered a form of low-carbon power.

The concept of nuclear power generation had started in 1950. As of April 2017, 30 countries worldwide are operating 449 nuclear reactors for electricity generation and 60 new nuclear plants are under construction in 15 countries. Nuclear power plants provided 11 percent of the

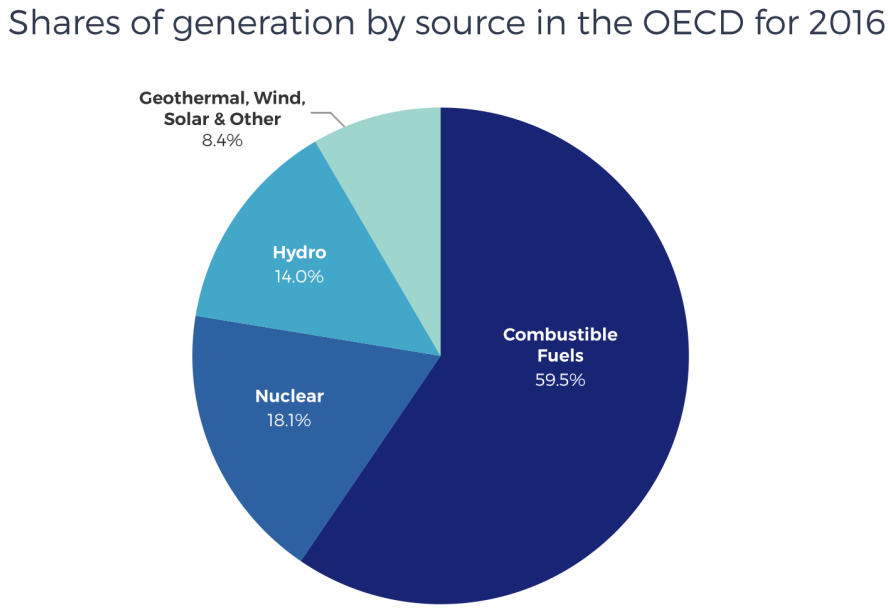

Figure 1-1: Global power generation (https://goo.gl/uDGWgx)

world's electricity production in 2014. In 2016 (Figure 1-1), 13 countries relied on nuclear energy to supply at least one-quarter of their total electricity, with a total net installed capacity of 391, 744 MW (*https://goo.gl/gahmVR*).

In case of nuclear power plant, the boiler is replaced by nuclear reactor, in which nuclear reaction takes place and heat generated due to this reaction given to the primary fluid. This primary fluid in turn, transfers heat to the secondary fluid, which is converted into steam and then expanded into turbine to generate electricity.

There are different types of nuclear reactor starting from Generation I to Generation III+. The first generation was developed during 1950s and 60s as the early prototype reactors. The second generation began in the 1970s in the large commercial power plants that are still operating today. Generation III was developed more recently in the 1990s. Research activities are going on worldwide to develop advance nuclear power plants with high thermal efficiency.

The Generation-IV consortium seeks to develop a new generation of nuclear energy systems for commercial deployment by 2020–2030. Supercritical water-cooled reactors (SCWR) is one of the Generation IV reactors (Figure 1-2). It exhibits excellent heat transfer characteristics and large volumetric expansion near the pseudocritical point, (the “pseudocritical” temperature is defined as the temperature at which the heat capacity of the supercritical fluid attains a maximum), which identifies it as a potential coolant for advanced nuclear reactors. It also promises enhanced thermal efficiency, compact design and economically competitive structure owing to the elimination of several bulky components such as the steam separator, dryer and recirculation channels. Absence of distinct phase change eliminates the constraint associated with the critical heat flux (CHF) as well, however, at the expense of complicated stability behaviour. Operation in the unstable regime is undesirable, as that can lead to diverging thermohydraulic and power oscillations, particularly in natural circulation based systems. That makes it essential to gain a comprehensive insight about the probable operating regime

of such systems under both natural and forced flow situations, with focus on maximizing the flow rate and heat transfer coefficient.

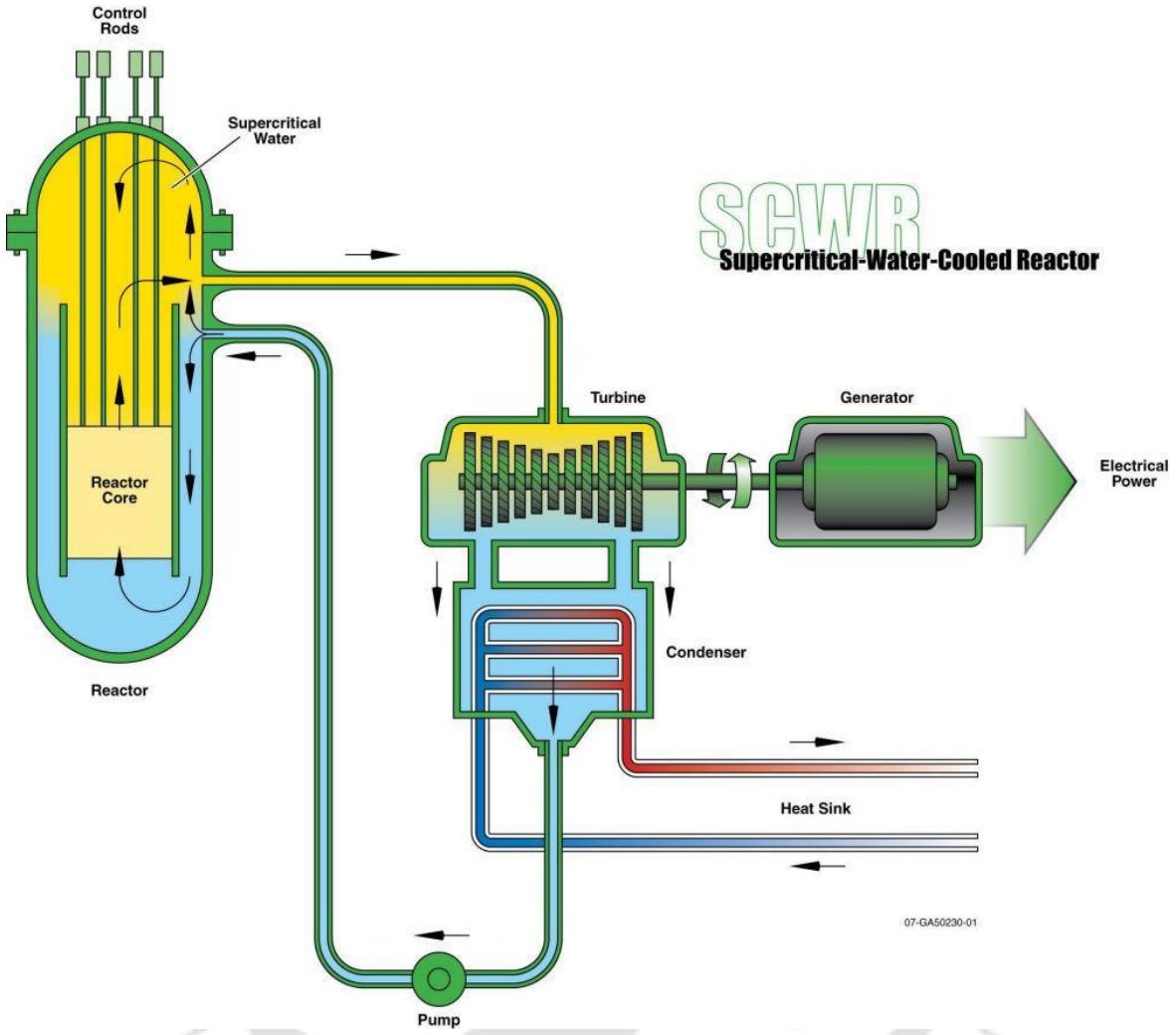

Figure 1-2: Schematics of SCWR (https://goo.gl/qHdFrz)

SCWR is one of the six reactors types that are being investigated international advanced reactor development program. Looking to the trend of coal fired power plants in the last 40 years; it has been observed that there is significant increase in overall efficiency from 37%, which was in 1970s to 46% today. The last 20 years since 1990, in particular, were characterized by an increase of live steam temperature beyond 550 ^{o}C (Abram and Ion, 2008). In comparison with such development, the net efficiency of latest pressurized water reactors (PWR) of around 36% is still close to the efficiency of ~34% of the first generation of light water reactors (LWR) (Schulenberg et al., 2014). SCWRs

are high-temperature, high-pressure water-cooled reactors that operate above the thermodynamic critical point of water (374°C, 22.1 MPa). SCWRs have unique features that may offer advantages compared to state-of-the-art LWRs in the following:

- ✓ SCWRs offer increase in thermal efficiency relative to current-generation LWRs. The efficiency of a SCWR can approach ~ 44%, compared to 33–35% for LWRs.
- ✓ A lower-coolant mass flow rate per unit core thermal power results from the higher enthalpy content of the coolant. This offers a reduction in the size of the reactor coolant pumps, piping, and associated equipment, and a reduction in the pumping power.
- ✓ A lower-coolant mass inventory results from the once-through coolant path in the reactor vessel.
- ✓ No boiling crisis (i.e., departure from nucleate boiling or dry out) exists due to the lack of a second phase in the reactor, thereby avoiding discontinuous heat transfer regimes within the core during normal operation.
- ✓ Steam dryers, steam separators, recirculation pumps, and steam generators are eliminated.
- ✓ The operating costs may be ~ 35% less than current LWRs. The SCWR can also be designed to operate as a fast reactor.
- ✓ The SCLWR reactor vessel is similar in design to a PWR vessel (although the primary coolant system is a direct-cycle, BWR-type system).

Therefore, the SCWR can be a simpler plant with fewer major components.

The SCWR concepts follow two main types, the use of either (a) a large reactor pressure vessel (Figure 1-3) with a wall thickness of about 0.5 m to contain the reactor core (fuelled) heat source, analogous to conventional PWRs and BWRs, or (b) distributed pressure tubes (Figure 1-4) or channels analogous to conventional CANDU and RBMK nuclear reactors.

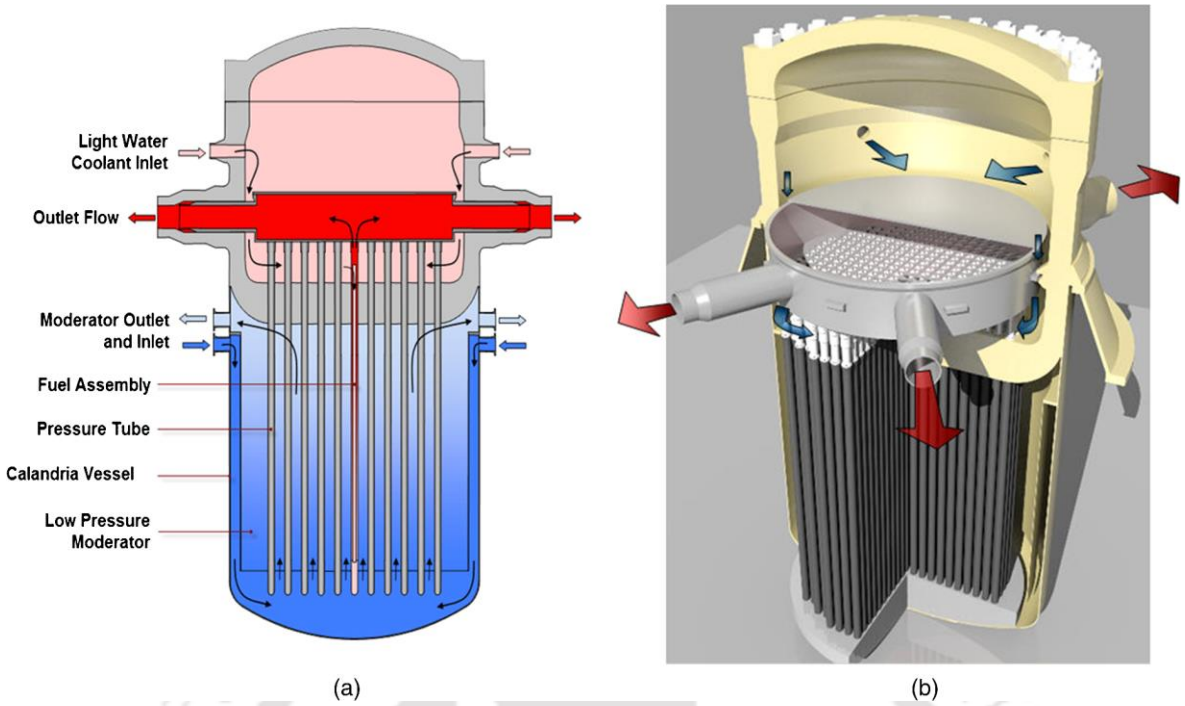

Figure 1-3: Pressure vessel type reactor (Source: google)

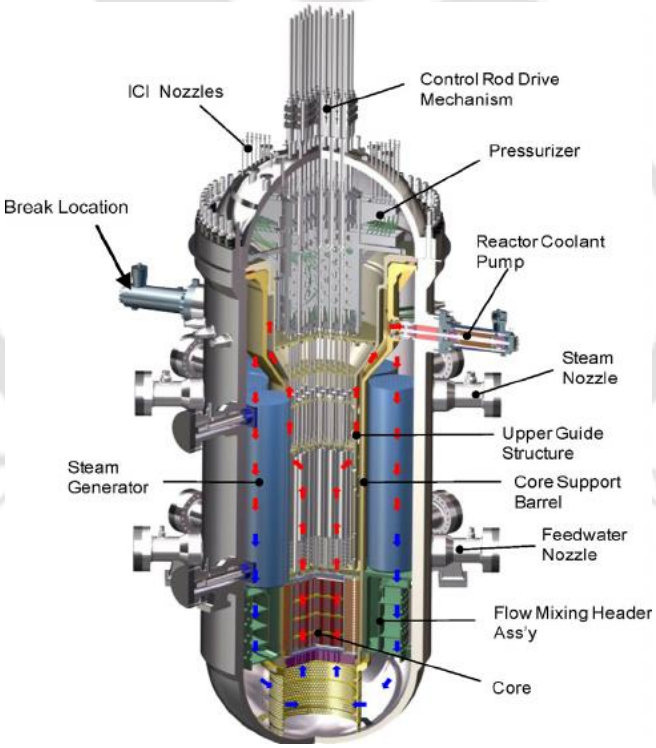

Figure 1-4: Pressure tube type reactor (https://goo.gl/G4RChr)

The pressure-vessel SCWR design is developed largely in the USA, EU, Japan (Ikejiri et al., 2010), Korea and China and allows using a traditional high-pressure circuit layout. The pressure-channel SCWR design is developed

largely in Canada and in Russia to avoid a thick wall vessel. The vast majority SCWR concepts are thermal spectrum reactors. However, a fast neutron spectrum core is also possible (Ikejiri et al., 2010).

Reactor systems are subjected to flow instabilities due to parametric fluctuations, inlet conditions, etc., which may result in mechanical vibrations of the components and system control problems. Supercritical fluids have no definable phase change and, in some respects, behave as single-phase compressible fluids. Thermal hydraulic flow instabilities and oscillations in the near-critical and supercritical region have been known to exist from some time.

The flow oscillation in the nuclear reactor is an interesting phenomenon from the safety point of view. As it may further induce nuclear instabilities due to density-reactivity feedback, which could result in the failure of the control mechanism and lead to a transient event. Flow instabilities can cause damage to the reactor components or lead to their fatigue failure due to oscillatory temperatures. Consequently, the stability behaviour of system under supercritical conditions is of great interest. An understanding of the instabilities in flow systems is therefore necessary in order to explore the stability behaviour of natural circulation as well as forced circulating systems employing supercritical fluids. The flow instability phenomenon in natural circulation and forced circulation loops under supercritical conditions is one of the anticipated reactor engineering challenges that is pertinent to some of the proposed supercritical water reactor designs and their shutdown safety systems; i.e., isolation condenser, decay heat removal. The wide variations in the thermodynamic and physical properties near the pseudocritical point make the supercritical fluid open to various kinds of flow instabilities similar to two-phase fluids.

Flow instabilities are of different types depending on the system configuration and operating conditions. On the basis of primary features such as oscillation periods, amplitudes, and relationships between pressure drop and flow rate, flow instabilities have been classified into several types, which were first

proposed by (Boure et al., 1973) Coupled thermo-hydraulic-neutronics instabilities were reported by (March-Leuba and Rey, 1993). A review of numerical and experimental investigations on two-phase flow instabilities in natural circulation boiling channel were reported by (Prasad et al., 2007). Figure 1-5 presents the summary of the classification of instabilities discussed in (Boure et al., 1973) and (March-Leuba and Rey, 1993).

1.2 Classification of flow instability

Flow instabilities are usually caused by large momentum changes in the system and strongly depend on the thermodynamic, hydrodynamic and geometric behaviour of the system. They may originate as small amplitude oscillations at low power and grow in amplitude with an increase in power, eventually leading to a different operating point or sustained oscillations. There are several microscopic instabilities, which occur locally at the liquid gas interface. E.g. Helmholtz and Taylor instabilities, and are of considerable interest to engineers for various applications. The focus here however will be on the macroscopic instabilities, which involve the entire flow channel dynamics. The instabilities in the flow systems are generally classified as static instabilities or dynamic instabilities. Static instabilities are typically present in a system when small changes in the flow conditions occur and another steady state is not possible near the original steady state. Dynamic instabilities are present in a system when the inertia and other feedback effects play an essential role in the process. Consequently, the system behaves like a servomechanism and knowledge of the steady state laws is not sufficient even for the threshold prediction. The static and dynamic instability is described below.

1.2.1 Static instability

A flow is subject to a static instability if, when disturbed, its new operating conditions tend asymptotically toward the ones that are different from the original ones. In the language of dynamics, it is to say that the original operating point is not a stable equilibrium point, and the system moves to a different equilibrium point which is a stable (Kakac and Bon,

2008). It is characterized by sudden large amplitude excursion of flow to a new stable operating condition. The mechanism and the threshold conditions are predicted using steady-state characteristics of the system. Pressure drop characteristics of a flow channel, nucleation properties, and flow regime transitions play an important role in the characterization of static instabilities.

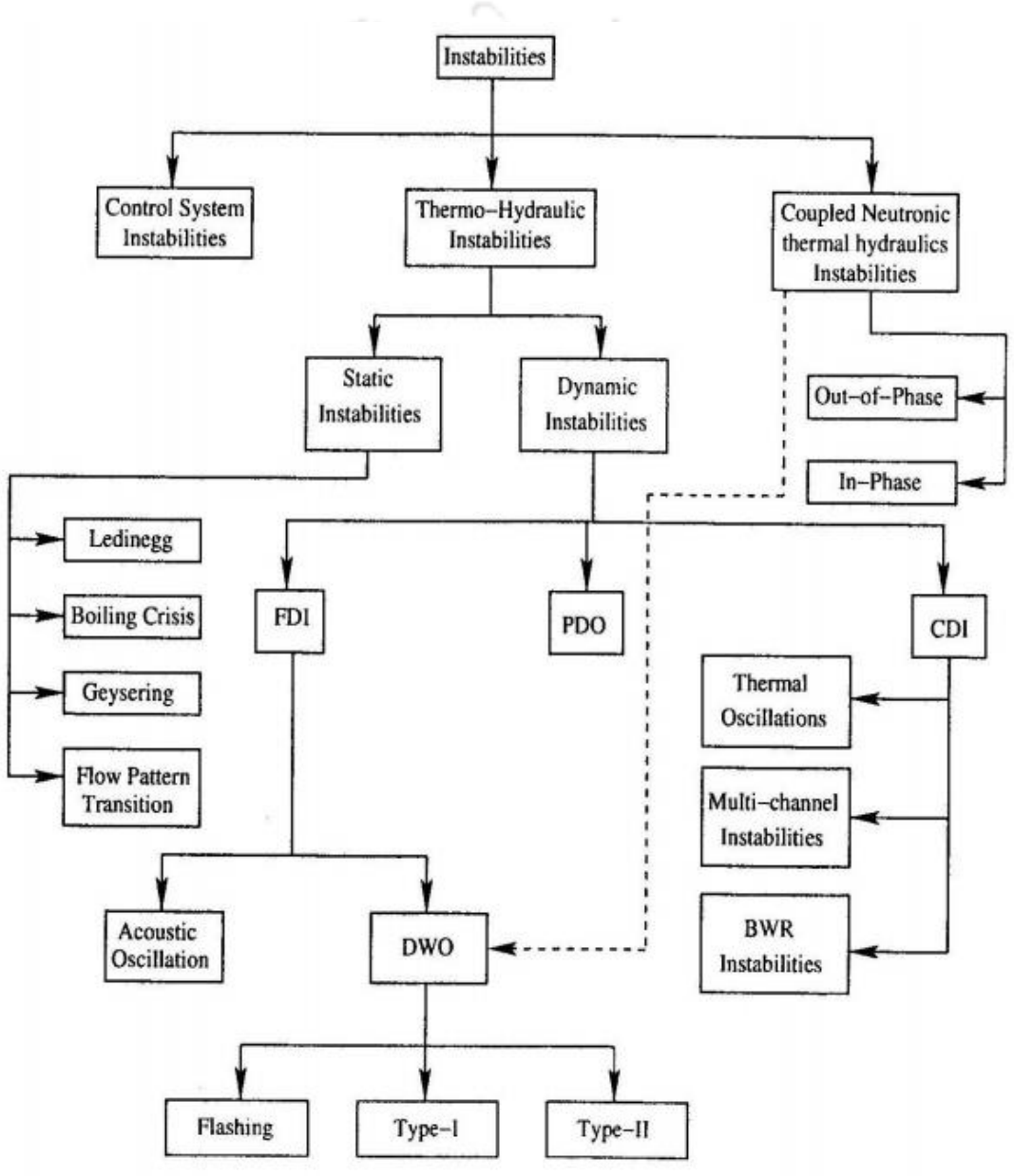

Figure 1-5: Types of flow instability-(Prasad et al. 2007)

Instability, geysering, chugging and vapour burst, etc. are categorized as static instabilities (Boure et al., 1973).

Ledinegg instability: It is also called as flow excursion, is a static instability since this kind of instability phenomenon can be explained by static laws. In addition, it is characterized by a sudden change in the flow rate to a lower value or a flow reversal. This happens when the slope of the channel demand pressure drop vs. flow rate curve (internal characteristics of the channel) becomes algebraically smaller than that of the loop supply pressure drop vs. flow rate curve (external characteristics of the channel). Physically, this behaviour exists when the pressure drop decreases with increasing flow. The criterion or condition for Ledinegg instability to occur is expressed by the inequality (Boure et al., 1973).

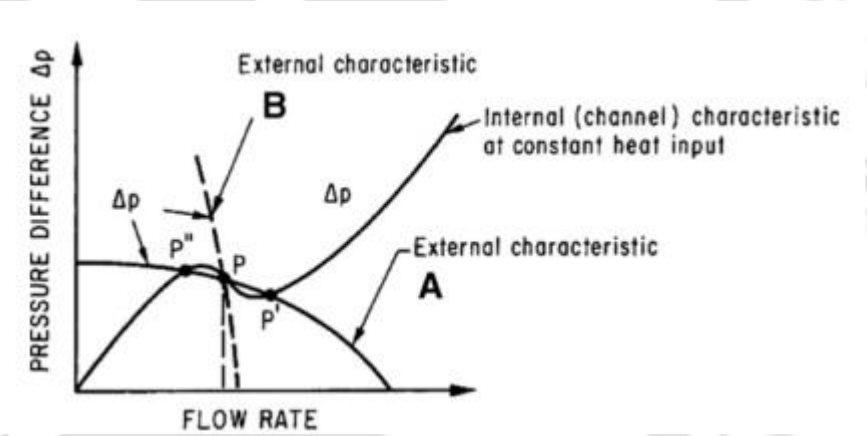

Figure 1-6: Ledinegg instability (Kakac and Bon, 2008)

$$\left[\frac{\partial \Delta P}{\partial G}\right]_{INT} \leq \left[\frac{\partial \Delta P}{\partial G}\right]_{EXT}$$

Where P is the steady-state pressure drop along the flow channel, and G is the mass velocity.

1.2.2 Dynamic instabilities

Dynamic instability is caused by the dynamic interaction between the flow rate, pressure drop, void fraction, etc. The mechanism involves the

propagation of disturbances, which, in two-phase flow, is itself a very complicated phenomenon. Roughly, it can be said that disturbances are transported by two kinds of waves: pressure or acoustic waves, and void or density waves. In any real system, both kinds of waves are present and interact; but their velocities differ in general by one or two orders of magnitude, thus allowing the distinction between these two kinds of pure, primary, dynamic instabilities. The stability boundary of this type is predicted based on the dynamic behaviour or transient (time dependent) characteristics of the system. Density wave oscillations (DWOs), parallel channel instability, pressure drop oscillations (PDOs), etc. fall under this class (Boure et al., 1973). Natural circulation boiling systems are highly susceptible to DWOs and much research was focused on this type of instability.

Density wave oscillations (DWOs): Density-wave oscillation is by far the most studied type of oscillation in two-phase and supercritical flow instability problems, and the amount of published experimental work in this field is overwhelming. A temporary reduction of inlet flow in a heated channel increases the rate of enthalpy rise, thereby reducing the average density. This disturbance affects the pressure drop as well as the heat transfer behaviour. Combinations of geometrical arrangement, operating conditions, and boundary conditions, the perturbations can acquire a 180° out-of-phase pressure fluctuation at the exit, immediately transmitted to the inlet flow rate and become self-sustained.

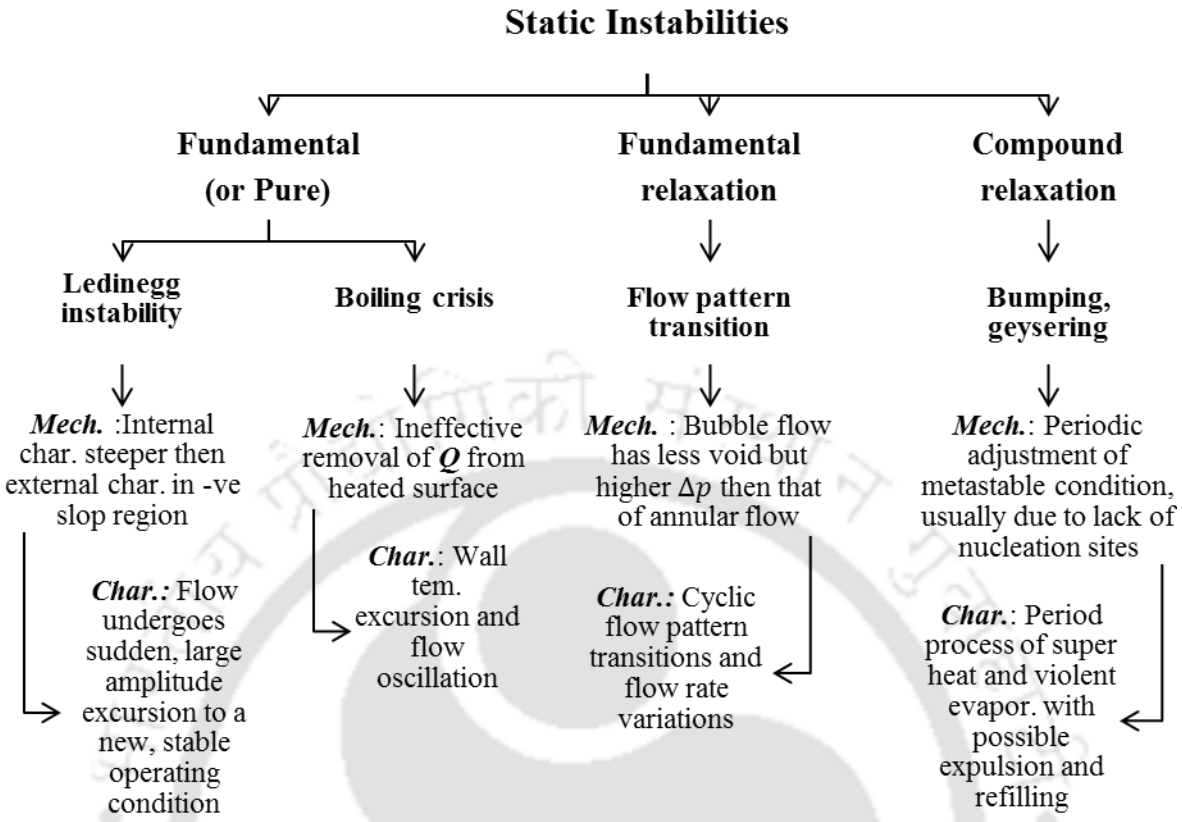

Figure 1-7: Different type of Static Instability

DYNAMIC INSTABILITIES

Fundamental		Compound		Secondary	Phenomena
Acoustic oscillations	DWO	Thermal oscillations	BWR instability	Parallel channel instability	Pressure drop oscillation
MECHANISIM					
- Resonance of pressure wave.	-Delay and feedback effects in relationship between flow rate, density and pressure drop.	- Interaction of variable k with flow dynamics.	- Interaction of void reactivity with flow dynamics and heat transfer.	- Interaction among small numbers of parallel channels.	-Flow excursion initiate by dynamic interaction between channel and compressible volume.
CHARACTERISTICS					
-High freq. (10-100 Hz) related to time required for pressure wave prop. in system.	-Low freq. (1 Hz) related to transit time of a continuity wave.	-Occurs in film boiling.	-Strong only for a small fuel time constant and under low pressures.	-Various modes of flow redistribution.	-Very low freq. periodic process (0.1 Hz).

Figure 1-8: Different types of Dynamic Instability

1.2.3 Coupled neutronics instabilities

Coupled neutronics thermal hydraulic instabilities (or reactivity instabilities) are generated due to reactivity effects of void generated in the core.

Neutronics thermal hydraulic coupling: In boiling water reactors, water serves as the coolant and the moderator. The moderator thermalizes neutrons to increase the probability of neutron participation in the chain reaction. Void generation in the core reduces the moderator quantity (reduction in moderator-to-fuel ratio) and hence, it is moderating capacity. Consequently, the effective multiplication factor k_{eff}, which is a function of moderator-to-fuel ratio, also reduces. This, in a water-moderated system, results in a change in reactivity, and hence a change in reactor power. Thus, there is a direct coupling between neutronics and thermal hydraulics, which is termed as void reactivity feedback.

Feedback mechanism: In the systems, mass flow rate is not an independent variable and depends on the power, operating pressure, and geometry. Thus, a small perturbation in power or any other parameter perturbs the inlet mass flow rate (van Bragt and van der Hagen, 1998a). The three feedback effects are as follow:

1. **Thermal hydraulic feedback through density reactivity in the core**: This affects the reactivity term in neutron kinetics through the density reactivity feedback term.

2. **Fuel dynamics and heat transfer feedback through Doppler reactivity**: This channel acts as a filter of power perturbations and introduces time delays between power production and coolant flow heating.

3. **Power feedback on the core thermal hydraulics**: This is mainly occurring due to the change in the power of the system. This affects the rate of void generation and mass flow rate (in natural circulation system).

1.3 Mathematical modelling

A model is a mathematical representation of the real process in a system. There are different modelling approaches.

Lumped parameter models: It is generally used to study the dynamic behaviour of the system using a low-order model comprising a system of ODEs.

Distributed parameter models: It consist of PDEs with respect to time and space and are used when the spatial variation of the variables has to be studied. These two models are developed from physical principles. There is another empirical approach based on input-output data. These models are valid for the specified operating conditions only. A mathematical model of SCWR includes power dynamics and thermal hydraulics. Power dynamics consists of the kinetics of nuclear chain reaction and heat generation in the fuel rods. Thermal hydraulics comprises mass, energy, and momentum balances for the coolant

1.4 Theoretical analysis of instability

The theoretical prediction in flow systems is typically expressed in the form of a threshold power below which the flow is steady and above which large fluctuations in the flow develop. The stability map typically represented in the dimensionless plane in terms of the following parameters; namely sub-cooled number versus phase number, gravity (dimensionless) versus friction coefficient, or pressure drop versus fluid expansion and many more. There are three main approaches to analyse the stability of flow system based on real time domain analysis, linear and non-linear stability analysis.

1.4.1 Real time analysis

The time domain investigation involves solving the transient mass, momentum and energy conservation equations of the system using some numerical method e.g. finite difference method. The idea is to first solve the discretized form of governing equations for the steady state and then

introduce a perturbation in the steady state solution in terms of the boundary conditions, namely perturbations in the inlet velocity, pressure or the heat flux. The system is said to be unstable if this disturbance grows to a sustained or diverging oscillation with the evolution of time. Time domain analysis is generally computationally very costly because of the stringent minor step restrictions. Furthermore, a large number of computations ought to be run in order to conduct the parametric study of the system. However, with increasing computer potential, it is definitely a promising method since the non-linearity of the system is also taken into account in this approach. One must however be careful about the numerical scheme used in discretization that could lead to certain numerical instabilities, which may not be easily distinguishable from the physical instabilities being investigated.

1.4.2 Linear stability analysis

Linear and nonlinear stability methods are used to predict the stability of any flow system. The method of linear stability consists of linearization of the governing conservation equations along with appropriate constitutive equations by assuming small perturbations about the operating time. Linear stability analysis can be done in the time domain or the frequency domain. The resulting linear equations are mapped to a time domain or frequency domain for analysis. The system stability is then examined by applying the tools of the feedback control system theory. The linearized models can estimate the system threshold of the instability for infinitesimal perturbations. They are simple, economical in terms of computational time, and less prone to numerical instabilities. However, they cannot predict long-term transient unstable behaviour and do not take non-linear terms present in the system into account Therefore, they cannot predict limit-cycle oscillations that are in fact the long-term oscillation behaviour of the system. Hence, in order to predict the effect of large perturbations and their influence on the reactor stability, nonlinear dynamic analysis is required (Prasad et al., 2007).

Table 1-1: Commonly used linear stability analysis codes

Name of Code	Thermal hydraulic model		Neutronics model	Reference
	Channels	TPFM* (Eq.)		
NUFREQ NP	Few	DFM (4)	Simplified 3-D	(Peng et al., 1986)
LAPUR5	1-7	HEM (3)	P-K* & M-P-K*	Otaudy (1989)
STAIF	10	DFM (5)	1-D	Zerreben (1987)
FABLE	24	HEM (3)	P-K	Chan (1989)
ODYSY	Few	DFM (5)	1-D	(Yu et al., 2003)
MATSTAB	All	DFM (4)	3-D	Hanggi (1999)

*TPFM-Two phase fluid model, DFM-Drift flux model, HEM-Homogenies equilibrium model, DFM-Drift flux model, P-K-Point kinetics, M-P-K-Multiple point kinetics.

1.4.3 Nonlinear stability analysis

Non-linear stability analysis involves application of complex mathematical techniques like bifurcation fractal and chaos theory to the flow system. It can provide information about the transient behaviour of the instability near the marginal-stability limits. It can also evaluate the system response to the finite amplitude oscillations and determine the threshold amplitude above which the finite-amplitude oscillations may grow. Although mathematically very challenging, these methods are very promising in predicting the unstable behaviour. However, this method is laborious and special nonlinear techniques such as shooting method, centre manifold reduction method, etc. are applied to study the bifurcation characteristics. Some of the nonlinear stability code is given in Table 1-2. For SCWR, RELAP5

(Debrah et al., 2013) has also been employed for non-linear stability characterizations.

Table 1-2: Commonly used nonlinear stability analysis codes

Name of Code	Thermal hydraulic model		Neutronics model	Reference
	Channels	TPFM (Eq.)		
RAMONA-5	All	DFM (4 /7)	3-D	RAMONA catalogue
RELAP5/MOD3.2	Few	TFM (6)	P-K	RELAP5 manual
RETRAN-3D	4	Slip Eq. (5)	1-D	Paulsen (1993)
TRACG	Few	TFM (6)	3-D	Takeuchi (1994)
ATHLET	Few	TFM (6)	P-K	Lerchi (2000)
CATHARE	Few	TFM (6)	P-K	Barre (1993)
CATHENA	Few	TFM (6)	P-K	Hanna (1998)

*TFM-Two fluid model

1.5 Instability due to seismic effect

Thermal–hydraulic phenomena with supercritical flows are seen widely in various engineering fields, and predictions of complicated phenomena between of flow instability are of practical importance. Evaluation of thermal–hydraulics under seismic conditions becomes of interest since the nuclear accident at Fukushima Daiichi power plant in 2011.

The basic equations and the empirical correlations of safety analysis codes are, however, developed for static conditions, and supercritical flow phenomena under seismic conditions are not known. Fluid flows in reactor

components are externally oscillated. In some reactor components, induced fluid motion results in large pressure impact on structures. Thermal conditions such as heat transfer between fluid and structure are also affected. Variation of supercritical flow conditions may also have an effect upon neutronics in the core, since the coolant density as the neutron moderator is affected (Zhang et al., 2001). Therefore, it is extremely important to study the effect of seismic on the coolant channel for the safety purpose of the system

1.6 Research objectives

To ensure the proper instability analysis of the Gen. IV reactor, SCWR, a methodology of the stability analysis has been developed in this work. Following are the main objectives of the work:

1. To develop a new unified scaling methodology for natural circulation and forced circulation supercritical test facilities.
2. To develop a reduced order transient mathematical model of SCWR for thermal-hydraulics with and without coupled neutronics.
3. Analysis of instabilities and nonlinear dynamics of SCWR using the mathematical model.
4. Stability analysis of SCWR due to the seismic effects.

1.7 Outline of the thesis

The present thesis is divided into nine chapters.

Chapter 1 describes some general terminology used in two-phase and SCWR system. It gives a general discussion an overview. Objective and outline of the thesis.

Chapter 2 describes the literature review on instability in BWR, SCWR and scaling.

Chapter 3 describes the mathematical modelling of SCWR. The detailed description of lumped parameter model (LPM), RELAP model and stability technique along with the model validation has been described. Some other

aspects such as steady-state equations, transient equations and general stability analysis have been describe in detail.

In Chapter 4, primary objectives are to study and identify a less restrictive model fluid, which can properly mimic the SCW under the relevant scaled condition of an SCWR, and to define the scaling rules in a generalized way. Accordingly, the scaled dimensions of the lab-scale facility and corresponding operational settings in terms of power, flow rate and inlet temperature are proposed. The advantages of the proposed methodology over the existing ones have also been stressed upon, along with a discussion on the role of involved dimensionless groups. Finally, the stability analysis using small perturbation (linear stability analysis) has also been described in detail using the transient plots and stability maps of three model fluids.

In Chapter 5, the same validated LPM is used for thermal hydraulic and coupled neutronics stability study, this time using linear stability analysis. Several parameters are determined by non-dimensional analysis of the conservation equations. Finally, a stability map that defines the onset of instability is plotted in that governing parameters plane.

The main focused of Chapter 6, is to analyses the thermal hydraulics aspect by using the three zone LPM. After completed two-zone stability analysis, three zone stability analysis need to be done to predict the effect of increasing the number of zones. It is like the grid independent test. Finally, few parametric analyses have been done to ensure the two-zone model is better as compared to three zone.

After ensuring that the two zone is better than three zone LPM, Chapter 7, focuses on understanding the thermohydraulic and coupled neutronic stability behaviour of a forced flow heated channel. The main focus of this chapter is to carryout stability analysis using large perturbation (Non-linear stability analysis). Various other aspects of nonlinear analysis such as Hops bifurcation, limit cycle, Generalize Hopf Bifurcation, predicting the limit cycle

range etc have been shown and discussed in detailed. Finally, the parametric study has been done using both thermohydraulic and neutronics.

Chapter 8, focuses on the study to provide quantitative and first-hand information useful for determining the significance of the external forcing effect due seismic wave on SCWR system. In order to meet the objective, the transient thermal hydraulic in-house code is used after modified to consider external acceleration in addition to gravity. Few parametric studies have been done, as this work need more rigorous future work, so author keep it for the interested audience.

Finally, In Chapter 9, the conclusion and some future work has been proposed.

Chapter 2 LITERATURE REVIEW

This chapter illustrates the detailed review of the literatures available based on, computational, experimental and analytical works performed by different researchers towards the development and modern advancement in stabilities of Supercritical Water-Cooled Reactor (SCWR), instabilities of boiling water reactors (BWR), Scaling of SCWR for the stability analysis and the mathematical modelling for the stability analysis.

2.1 Instability in SCWR

The first reported work studied the issue of supercritical particularly on heat transfer was found in 1930s. The research was purposed to develop efficient cooling system for turbine blades in jet engines, Schmidt and his associates (Schmidt et al., 1946) examined free convection heat transfer into the fluids at the near-critical point. They observed relatively high free convection heat transfer coefficient (HTC) of fluid at the near-critical state.

After 40 years, a single heated two-phase flow channel, Ishii (1971) had constructed a stability boundary map to provide the stability margin for a specific operating condition. Once the stability boundary had provided, it is very easy for the designers to check the stability feature of their designs based on guidance of the stability maps (Ishii, 1971). A thermal equilibrium two phase model was applied by Ishii (1971). A drift flux model was applied to take into account the non-homogenous feature of the two-phase flow. It was found that the system pressure effects can be absorbed by the stability boundary, which means that the stability boundary is the same for different system pressures. Therefore, once a stability boundary map was constructed for a specific system pressure, it could be applied to other pressures also. Zuber (1966) discussed three mechanism near critical and at super-critical pressures. Saha et al. (1975) improved Ishii's model by using a simplified non-equilibrium two phase flow model. By comparing the model with an experiment conducted by using a Freon-113 boiling loop, further they found

that the model matched the experimental data well. Zuber (1966) did an extensive review and the first in-depth analytical study of the various instability modes of supercritical fluid flow. The stability map proposed by both the researcher become the basis of modern BWR and SCWR stability analysis.

Chatoorgoon, (2001) has studied supercritical flow stability in a single-channel, natural-convection loop is examined using a non-linear numerical code. A theoretical stability criterion is also developed to verify the numerical prediction. He found good agreement between the numerical and analytical results. A different mode of instability identified had been purported to be different from the traditional instabilities associated with the two-phase flow. Along with these, non-dimensional parameters governing supercritical flow instability boundary, derived from an earlier study, are now examined through a numerical experiment comprising 94 simulated cases.

Chatoorgoon, Voodi and Fraser (2005), had done a parametric study by using a range of inlet and outlet K-factors, various inlet temperatures, heated lengths and vertical loop heights. The study reports on the stability of supercritical light water in a natural-convection loop and confirms the validity of non-dimensional parameters for stability predictions.

Yi et al. (2004) studied the stability characteristics of a SCWR core based on the once-through light water-cooled reactor concept proposed by Oka and Koshizuka (2001), by calculating the decay ratio of the system under a pulse perturbation. Zhao et al. (2005) used a three-region model for approximating the variation in density with enthalpy. They defined a few dimensionless scaling groups for analysing thermal hydraulic stability for US reference design of SCWR. A multi-channel stability code in frequency domain (SCWRSA) was developed by Yang and Yang (2005), employing an iterative solution scheme, to calculate the steady state flow distribution among parallel channels under a fixed total flow rate and equal pressure drop boundary condition. (Ambrosini, Di Marco and Ferreri, 2000) and Ambrosini and Sharabi (2008) studied stability of single uniformly heated channel with fixed

inlet and outlet pressures, as they discussed the stability behaviour at different pressures by introducing new sets of non-dimensional numbers for the stability analysis. Sharabi and Ambrosini (2009) predicted the unstable behaviour of heated channels carrying supercritical fluid using a CFD package and analysed a sub-channel of fuel assembly. Subsequently Ampomah-Amoako and Ambrosini (2013) considered the standard $k-\varepsilon$ model, equipped with wall functions, for similar analysis.

Hou et al. (2011) studied dynamic stability characteristics of the fast-spectrum zone of a newly designed mixed-spectrum SCWR (SCWR-M) and that was characterized as a parallel-channel system. Quite a few studies to investigate the dynamical behaviour of supercritical natural circulation loops can also be found in the literature (Chatoorgoon, 2001; Jain and Rizwan-uddin, 2008; Sarkar et al., 2014; Sharma et al., 2010), most of which apply finite difference simulation of the governing equations.

To verify the stability margin of supercritical fluid (SCF) experimentally (Jain 2005) conducted the experiment in a rectangular supercritical carbon dioxide (SCO2) natural-circulation loop at Argonne National Laboratory (ANL). The linear stability analysis has been conducted for three different loop geometries employing water or carbon dioxide as the working fluid. The results for the supercritical water loops displayed stable flow for a more accurate equation of state (EOS); however, the analysis indicated the presence of instabilities for a less accurate EOS. But the analysis still predicts the presence of instabilities for the SCCO2 loop similar to her transient numerical predictions. Finally, it has been found that the stability margin for both water loops and the SCO_2 loop does not correspond with proposed stability criteria from a previous analysis and hence it has been concluded that the phenomenon is a more complex function of both fluid properties and loop geometry.

Chatoorgoon (2008) reports an analytical study of supercritical flow instability in two horizontal parallel channels. The finding is that supercritical flow instability in horizontal channels is driven primarily by the state property variation of density with enthalpy; in particular, the second derivative of

density with enthalpy is a dominant term for the onset of flow oscillations in horizontal flow. In another word, the threshold of supercritical flow instability in horizontal parallel channels occurs, not where $\frac{\partial \Delta p_{ch}}{\partial m^*} = 0$, as is believed for horizontal two-phase flow, but close to where $\frac{\partial^2 \Delta p_{ch}}{\partial m^{*2}} = 0$.

Cai et al. (2009) described study on the procedure of raising the reactor thermal power and the reactor coolant flow rate during the power-raising phase of plant start-up for the supercritical water-cooled fast reactor (SWFR), which is selected as one of the Generation IV reactor concepts. Based on the flow rate distribution, thermal analyses and thermal–hydraulic stability analyses are carried out in order to obtain the available region of the reactor thermal power and the feed water flow rate for the power-raising phase. The criteria for the "available" region is the maximum cladding surface temperature (MCST) and the decay ratio of thermal–hydraulic stability in three "hot" channels; two seed assemblies with upward/downward flow and a blanket assembly. The effects of various heat transfer correlations and axial power distributions are also studied.

Sharma et al. (2010) describes the linear stability analysis model and the results obtained in detail. A computer code SUCLIN using supercritical water properties has been developed to carry out the steady state and linear stability analysis of a supercritical water (SCW) natural circulation loop. The code has been qualitatively assessed with published results and has been extensively used for studying the effect of diameter, height, heater inlet temperature, pressure and local loss coefficients on steady state and stability behavior of a Supercritical Water Natural Circulation Loop (SCWNCL).

Jain et al. (2010) discussed the evolution of unstable and stable behavior along with the nature of flow oscillation in the channels and the effect of pressure on it. Experiments are conducted at constant pressure of one bar and 9 bar. For both the pressures, a single-phase flow condition followed by onset of oscillation due to boiling inception, growth and decay of instability at low power (Type-I), a stable two-phase flow at intermediate power and onset

of instability at high power (Type-II) was observed. Even under the condition of equal heating the flow distribution among the channels is not found to be uniform. This may be attributed to pressure gradients in the header which leads to departure from condition of equal pressure drop among the channels. Range of stable flow domain is found to increase with rise in pressure. Thus stabilizing effect of pressure is confirmed. Channels have slightly different thresholds of instability. This may have its genesis in their steady state flow.

Numerical simulations on a super-critical CO_2 natural circulation loop have been carried out to investigate the flow transitions and instabilities of such systems. It is found for the first time that for the present supercritical CO_2 model there exists a transition heat source temperature at which the system changes from unstable repetitive-reversal flow into stable one-direction flow with the increase of temperature, which is fundamentally different from previous studies for normal fluid. In particular, the critical transition fluid temperature is found to be near the second "pseudo-critical temperature" at around 375 K where the fluid properties experience major transitions with the increase of temperature. Shan et al. (2010) in his work studies the dynamic stability characteristics of the fast-spectrum zone of a newly designed mixed-spectrum SCWR (SCWR-M), which is characterized as a parallel-channel system. A frequency-domain model has been developed for linear stability analysis, and marginal stability bound-arises under several conditions for the parallel-channel system, which indicate that the system normal operational condition is in the stable region. The stability of parallel-channel systems is dominated by the hottest channel. The higher the power density of the hottest channel is, the less stable the system will be. Increasing mass flow is beneficial for the system stability. Finally, they conclude that systems with uniformly axial power distribution are less stable than those with cosine-shaped or stair-shaped axial power distributions. The results of analysis show a good agreement with that of the frequency-domain analyses, and the existence of transitional stable region has been verified. The frequency-domain and time-domain stability analysis model are given in details in this

paper. Both the linear and non-linear stability analyses are done for mixed-spectrum SCWR (SCWR-M). Also the dynamic analyses the transitional stability region has been verified (Hou et al., 2011). Heat transport characteristics of systems, demonstrating the possible appearance of heat transfer deterioration and exploring the effect of buoyancy and flow acceleration on the same, has been the subject of several research studies over last decade (Cheng and Schulenberg, 2001; Jäger et al., 2011; Ruspini et al., 2014).

Yu et al. (2011) predicted the region of instability of natural circulation at supercritical pressure, through a test loop which was built at Tsinghua University. The design pressure of the testing loop is 40 MPa. The height of the loop is 3 m. There are two heaters in the loop. One is called pre-heater and the other is called as heater. The pre-heater is installed horizontally while the heater is installed vertically. Both of them have 2 m length and 20 kW electricity power each. The inner diameter of both heaters are same as 8mmwhile the stainless steel wall thickness is 5 mm. There are two coolers in the loop. Both of the coolers have 2 m length. The cold side temperature can be 40 ^{0}C-150 ^{0}C by adjusting the secondary flow rate. The maximum temperature of coolant in the loop can be 500 ^{0}C. There is a backup pump in the loop to clean up the used water in the loop but it can be bypassed by valve system. The paper presents the information of the test loop and a numerical analysis model for the loop. The paper verified the numerical analysis code by experiment results and using the code to analyse the instability of the loop. The paper concludes conclusion that there will be no Ledinegg instability occurring at supercritical pressure in the loop.

Xiong et al. (2012), concluded on the basis of experiment at Nuclear Power Institute of China (NPIC) on flow instability in two parallel channels with supercritical water, conclusion have been made. This indicates that the asymmetry of flow rate between the parallel channels would be enlarged with relatively higher fluid temperature or total mass flow rate, subsequently making the occurrence of parallel flow instability more difficult in the

experiments. The way of defining the onset of parallel instabilities has been proposed for supercritical water based on the experimental phenomena. In this experiment parametric studies show that the flow becomes more stable with increasing pressure or decreasing inlet temperature in the range of present experiments, and the mechanisms have been discussed compared to that for two-phase flow. Finally, the stability boundaries are illustrated in a two-dimensional plane using two dimensionless parameters proposed for supercritical flow.

Swapnalee et al. (2012), proposed a generalized correlation to estimate the steady state flow in supercritical natural circulation loops based on a relationship between dimensionless density and dimensionless enthalpy reported in literature. Experiments have been performed with supercritical CO_2 and water to validate this generalized correlation. The steady state flow rate data with supercritical CO_2 has been found to be in good agreement with the proposed correlation. The correlation has also been validated using limited number of supercritical water data. Subsequently supercritical natural circulation data for different fluids (Freon-12 and Freon-114) reported in literature has also been compared with the propose correlation. It is observed that the same generalized correlation is applicable for other fluids also. In the present paper, an analysis has been carried out to predict the threshold of excursive instability for both supercritical water and supercritical CO_2. Static instability was not found for CO_2 whereas it was found for supercritical water. The effect of pressure is observed to stabilize the loop. He also observed that due to sharp change of fluid properties such as density at supercritical pressure, Boussinesq approximation is not valid. At higher pressures, instability is observed with very low inlet temperature.

Ampomah-amoako et al. (2013) analysed the results of a systematic methodology aimed at assessing the feasibility of CFD codes of flow instabilities in heated channels containing supercritical fluids. The research makes use of features presently available in CFD models, in the aim to move step-by-step from simple channel cases towards the analysis of more realistic

fuel bundle sub-channels. They use the STAR-CCM+ code has been adopted to solve flow stability problems in circular channels and fuel bundle slices without heating structures, in the aim to characterize the response of CFD models in the analysis of purely thermal–hydraulic instability phenomena. Both static and dynamic instabilities were observed and studied, which provide promising features of CFD codes for such applications. Debrah et al. (2013) used a methodology for the analysis of the flow stability using RELAP5 in natural circulation loops containing fluids at supercritical pressure. It is remarked that the adopted methodology and the related program for linear stability analysis can be applied to any single loop containing a supercritical fluid. The analysis confirmed that lowering the heat transfer coefficient allows to obtain unstable behaviour closer to the observed operating conditions. This suggests that also other closure laws implemented in the code, e.g. for friction factors, should be updated in order to get more reasonable predictions with super-critical water. Lastly, the author concludes that the work performed shows that instabilities in natural circulation loops containing supercritical fluids represent a challenging phenomenon for presently available codes, very sensitive to details in the prediction of heat transfer and hydraulic impedance.

Xiong et al. (2013) have been developed an in-house code applying time-domain approach and done the Comparison between the numerical and experimental results, which shows that the numerical code is capable of predictions, well the stability boundaries quit well. Different ways of geometrical modelling of the test section in the experiments are studied. Based on the validated code, the geometrical simplification is further discussed and a relatively simple as well as the common geometrical configuration is proposed. Discussions also indicated that the entrance and riser sections could not be eliminated with respect to numerical modelling of flow stability. Effects of inlet temperature and total mass flow rate are numerically analysed. Results showed that the inlet temperature has a non-monotonic effect on the threshold power, while the threshold power is roughly proportional to the total mass flow rate no matter the system is symmetrical

or not. Moreover, the results indicate that it would be more difficult to perform flow instability experiments at higher inlet temperature or total mass flow rate. Sharma et al. (2014), have been set up a closed Supercritical Pressure Natural Circulation Loop (SPNCL) to generate data on flow and heat transfer behaviour for supercritical fluids (i.e. water and carbon dioxide) under natural circulation conditions. Experiments were conducted in SPNCL with water as working fluid. Instability was observed over a range of power in the pseudo-critical temperature region for horizontal heater horizontal cooler orientation. Instability was observed at low supercritical pressure range of 22.1–22.9MPa, however it got suppressed at higher pressures. An in-house developed computer code NOLSTA has been used to perform steady state and stability analysis of SPNCL and predictions are compared with experimental data. The heat transfer data generated in the test facility has been compared with various heat transfer correlations for supercritical fluids available in literature. Finally, it describes the experimental results and comparisons in detail. Xi et al. (2014), have been done a three dimensional (3D) numerical simulation using the CFX code to investigate the out of phase oscillation between two heated parallel channels with supercritical water. The numerical procedure is discussed and proper numerical models such as mesh number, coupling method between velocity and pressure, time step, difference scheme and turbulence model are selected. Then, instability boundaries are obtained under different inlet mass flow rates, system pressures, with and without gravity conditions.

Xu et al. (2015), studied the neutronics–thermohydraulic coupling (N–T coupling) calculation on core design, security and stability analysis of supercritical water-coolant reactor (SCWR), and a suitable thermal correlation were also necessary for the N–T coupling calculation. In this paper, the scheme of the U.S. SCWR design and the process of the N–T coupling will be introduced as well as some of different thermal correlations firstly. Then, based on the N–T coupling system ARNT, the U.S. SCWR design is simulated to analyse the influences of thermal correlations on N–T coupling calculation

of SCWR so as to find out which correlation is best. Dutta et al. (2015a) studied the development of numerical models to predict steady and unsteady thermal-hydraulic behaviour of supercritical water flow at various operating conditions. A simple one- dimensional numerical thermal-hydraulic model based on a finite-difference scheme has been developed. A detailed CFD analysis based on two turbulence models, Reynolds Stress Model and k–ω SST model, has also been presented in this paper. Seven experimental cases of steady state and vertically up flowing supercritical water in circular tubes operated at various working regimes, such as normal and deteriorated heat transfer regions, are used to validate the numerical models. Comparisons for steady state flow show good agreement between the numerical and experimental results for all normal heat transfer cases and most of the deteriorated heat transfer cases.

Shen et al. (2017) has studied the heat transfer of supercritical water by both experimentally and numerically. A 2-m long vertical upward smooth tube with a diameter of 19mm was tested at pressures ranged from 11 to 32 MPa, values of mass flux from 170 to 800 and heat fluxes up to 600. Various dimensionless parameters representing effects of property variations, buoyancy and thermal induced acceleration were estimated. Some of them show unique and strong relations to heat transfer coefficient, while no single behavior of independence is obtained with the majority of them. This result indicates additional parameters are required in case these dimensionless parameters are applied to predict super- critical heat transfer. Based on the experimental data, six typical correlations were evaluated. The shear stress transport k-x model was employed to numerical analysis. Results of numerical prediction show a good agreement with experimental data, which proves the suitability of the present model. According to the result, physical mechanisms of both enhanced and deteriorated heat transfer at supercritical pressure are revealed. The integral effect of specific heat and buoyancy effect are the main reasons resulting in the abnormal heat transfer.

Hou et al. (2017) studied, the open natural circulation which is widely used in the designs of advanced nuclear reactor in recent years due to its inherent safety. In this paper, an experimental and analytical investigation was carried out in an open natural circulation loop, to figure out the mechanism of the open natural circulation behaviors. The experimental result showed six different flow modes occur in the loop. There into the mode of steady flashing flow is newly discovered, and it cannot be formed spontaneously in our experiment. Moreover, it is observed from those flow modes that the boiling and the flashing interact with each other strongly, and determine the behaviors of open natural circulation separately or jointly. Therefore, the open natural circulation behaviour can be considered as interaction results of flashing and boiling. To figure out the interaction mechanism, a linear model was conducted to investigate the instability regions caused by only flashing and only boiling respectively. By comprehensive comparing the experimental results and analytical results, the mechanism of the interaction between flashing and boiling, and how the flashing and boiling influence the open natural circulation behaviors were figured out. Moreover, according to those mechanisms, the measurements to form the steady flashing flow are also put forwards.

According to Li et al., (2018), the experimental tests on heat transfer deterioration (HTD) of supercritical water flowing in 4 different kinds of channels, including tube, annular channel, and 2 by 2 bundle, have been carried out on the Supercritical water multipurpose test loop (SWAMUP). The tube is made of Inconel alloy with different inner diameters; the annular channel consists of an Inconel alloy heated inner tube and a 304 stainless steel unheated outer tube. Two kinds of bundles were tested. The first kind of bundle consists of 4 Inconel-718 tubes with different Pitch-to-Diameter ratios, and the 2 by 2 bundle with grid spacers is installed into a square assembly box. The other kind of 2 by 2 bundle consists of 4 heater rods, and the rod bundle with wire wraps is also installed into a square assembly box. The heat transfer of supercritical

water in simple channel like tube is stronger with larger cross-sectional flow area, but it is stronger with smaller cross-sectional flow area in complex channel like bundle. Two kinds of HTDs are observed in tube and annular channel, only the first kind of HTD is observed in bundle. The first kind of HTD occurs only at high ratio of heat flux to mass flow velocity in different channels, and the second kind of HTD is more likely to occur in simple channel, which could be eliminated in bundle by the transverse turbulent flow. The effects of thermal–hydraulic and structural parameters on the second kind of HTD in tube are as follows: the HTD of supercritical water is severer with higher heat flux and the increment of wall temperature is much larger. The HTD occurs earlier and severer with lower mass flow velocity; the HTD delays and the wall temperature rises more slowly when the pressure rises; and the diameter has no evident effect on this kind of HTD. The heat transfer in bundles especially with wire wraps is qualitatively better and more stable than that in other tested channels. In order to avoid the first kind of HTD within the operating condition of SCWR, the low mass flow velocity condition and high heat flux condition should not occur at the same time during operation.

According to Wang et al. (2017), In an experiment has recently been completed to obtain the wall temperature and heat transfer coefficient of water at subcritical pressures in a SCWR sub-channel. The test section was wire-electrode cut to simulate the central sub-channel of a 2 by 2 rod bundle. Experimental parameters covered the pressures of 11–19 MPa, mass fluxes of 700–1300 kg/m^{2}s and heat fluxes of 200–600 kW/m^2. Heat transfer characteristics in single-phase and two-phase regions were analysed with respect to the variations of heat flux, system pressure and mass flux. For a given pressure, it was found that the wall temperature increases with increasing heat flux or decreasing mass flux in the steam-water two-phase region. Departure from Nucleate Boiling (DNB) was observed from the wall temperature profiles in the sub-channel. Experimental results showed that the soaring wall temperature at DNB becomes dramatic with the increase of

pressure. Correlation assessments have also been conducted against the current set of experimental data. The comparisons indicated that the Fang correlation agrees well against the two-phase heat transfer coefficient. Heat transfer difference in the sub-channel at subcritical and supercritical pressures was compared. It was concluded that the wall temperature at sub-critical pressure might be lower or higher than that of supercritical pressure depending on q/G ratio and the occurrence of DNB.

Kiss et al. (2017), the thermal hydraulics of supercritical water under forced-, mixed convection and natural circulation conditions is not fully understood. In order to study the thermal hydraulic behaviour of this fluid under natural circulation conditions a small size, closed experimental loop has been designed and built. The thermal hydraulic phenomenon occurring in the loop can be measured by thermocouples mounted onto the outer surface of the heated tube wall, absolute, differential pressure transducers, and a flow meter; moreover, simultaneously can be visualized by neutron radiography techniques. This paper describes the loop itself, the process of the experiment with the measurement techniques, the data acquisition system applied and the results got during the first measurement series. Based on the results of the first measurement series, it was found that the measured part of the steady state characteristic is independent from the system pressure. A slight dependence of steady state characteristic on the inlet temperature can be identified: the higher the inlet temperature the higher the mass flow rate. The total pressure drop and its components seem to be independent from the system pressure but strongly dependent on the inlet temperature due to the influence of bulk-fluid temperature on the relevant thermophysical properties (density and dynamic viscosity). The pressure drop due to acceleration of flow found to be negligible next to the two dominant components, the pressure drop due to frictional resistance and due to gravity. The coupled evaluation of the radiographic images and the thermophysical properties of water have shown that the main driving force behind the decrease of the neutron attenuation is the decreasing water density as the bulk-fluid temperature

increases. The reverse of this relationship could be exploited during the validation of future Monte Carlo simulations.

Wang et al. (2018) in his paper presents an experimental investigation of the pressure drop and friction factor of supercritical water in an annular channel. The gap and the full length of the annulus are 4mm and 1400 mm, respectively. The experimental pressure ranges from 23 to 28 MPa, mass flux ranges from 700 to 1500 kg/(m^2s), and heat flux on the inner wall ranges from 200 to 1000 kW/m^2. Results showed that the frictional pressure-drop increases significantly with increasing mass flux, particularly when the bulk enthalpy surpasses the pseudo-critical enthalpy. A local hump in the friction factor was observed corresponding to the pseudo-critical enthalpy, which becomes stronger with the decrease of mass flux or pressure. The assessment of correlations demonstrated that constant-property-based correlations fail to predict the friction factor of supercritical water. Hence, an improved correlation was proposed which captures 82.6% of the experimental data within±25% error band.

Li et al. (2018) developed and studied a 3-D numerical of turbulent flow of supercritical water flowing upward in two heated parallel channels with constant applied wall heat flux using a RANS model in ANSYS CFX. Oscillatory flow instabilities were investigated using the standard k-e turbulence model with scalable wall functions. The effects of changes to the grid sizes and the time step size on flow instabilities were studied first. Then the instability thresholds of experimental cases were obtained with the CFX code.

Yang and Shan (2018), studies the flow instability of hydrocarbon fuel. This is an important factor in the design of a regenerative cooling channel due to flow excursion accidents. To explore the mechanism of the instability process, the onset of flow instability (OFI) of cyclohexane were investigated experimentally in horizontal tubes at supercritical pressures. The geometric structure of the test channel, with a tube length of 0.20–0.79m and inside diameter of 1.0–2.0 mm, was studied with regard to static flow characteristics.

Based on the experimental data, a dimensionless analysis was conducted, and a new correlation to predict the OFI for supercritical fluids was obtained.

2.2 Instability in BWR

Boure et al. (1973) were first proposed flow instabilities and classified into several types. Fukuda et al. (1979), Hydrodynamic instabilities of two-phase flow are classified into at least eight types, three of which can be roughly classified into Ledinegg instability. Roy et al. (1988) done an experimental for the study of a Refrigerant-113 boiling flow system. It was undertaken as one part of a research effort the goals of which encompassed both theoretical modelling and experiments. The main objective of the experiments was to generate their own database for validating a dynamic instability model developed in the course of the theoretical effort. March-Leuba and Rey (1993): BWRs are generally susceptible to three types of instabilities, which are classified as (i) Control system instabilities (ii) Thermal hydraulic instabilities and (iii) Coupled neutronics thermal hydraulic instabilities. Rao et al. (1995) Concluded from their analysis that Ledinegg instability does not occur due to neutronics feedback and that it is pure channel thermal hydraulic instability. Finally, another researcher investigated the effect of flow oscillations on CHF for low flow and low-pressure conditions and suggested CHF correction factors based on experimental data for forced and natural circulation flows. They observed that the flow circulation mode (natural or forced) does not affect the CHF as long as the flow is stable. Their analysis is on Pressure drop oscillations (PDOs), they investigated experimentally the characteristics of PDO. They observed that PDO occurs only when there is compressible volume in the loop. They suggested that adding a throttling device upstream of the evaporator and maintaining uniform heat flux in the evaporator are some of the measures that can suppress PDO.

Manera et al. (2003) studied experimentally the stability of NCBWR during start-up conditions, proposed efficient start-up procedures to avoid these instabilities. Lee and Pan (2005) analysis is on parallel channel instabilities, they developed a nonlinear mathematical model to explore the dynamics of a double channel two-phase natural circulation loop under low-pressure conditions. Their study indicates that stability curves are similar to that of single channel systems. Xu et al. (2009) work described here is the validation of TRACE/PARCS for Boiling Water Reactor stability analysis. A stability methodology was previously developed, verified, and validated using data from the OECD Ringhals stability benchmark. The work performed here describes the application of TRACE/PARCS to all the stability test points from cycle 14 of the Ringhals benchmark. The results show that the SI method has a smaller numerical damping than the SETS method. When applying the SI method with adjusted mesh and Courant time step sizes (the largest time step size under the Courant limit), the numerical damping is minimized, and the predicted Decay Ratio (DR) agrees well with the reference values, which were obtained from the measured noise signal. There is good agreement between the decay ratios and frequencies predicted by TRACE/ PARCS and those from the plant measurements. Sensitivities were also performed to investigate the impact on the decay ratio and natural frequency of the heat conductivity of the gap between fuels and clad, as well as the impact of the pressure loss coefficient of spacers. Natural circulation is an important passive heat-removal mechanism in both existing and next-generation light water reactors. Finally, explained thermal and stability analyses are performed for a two-phase natural circulation loop. The homogeneous equilibrium model is employed to describe the two-phase flow in the loop. Subsequently, a linear stability analysis is performed in the frequency domain to establish the stability map of a natural circulation loop.

Dykin et al. (2013) deals with the modelling of Boiling Water Reactor (BWR) local instabilities via so-called Reduced Order Models (ROMs). More specifically, a four-heated channels ROM, which was earlier developed, was

modified in such a way that the effect of local perturbations could also be accounted for. This model was thereafter used to analyse a local instability event that took place at the Swedish Fors-mark-1 BWR in 1996/1997. Such a local instability was driven by unseated fuel assemblies. Comparisons between the results of ROM simulations and actual measurement data demonstrated that the developed ROM was able to correctly reproduce the main features of the event.

2.3 Scaling for instability of fluid in SCWR

Jackson and Hall (1979) identified several important requirements for scaling of heat transfer in supercritical fluid. Starting from the dimensionless versions of the conservation equations, three dimensionless groups were proposed for scaling of pressure, bulk temperature and mass flux. Heat flux and heat transfer coefficient were defined accordingly. Number of recent CFD-based effort can be found (Fu et al., 2012), focussing on the associated mechanism of heat transfer. Pioro and Duffey (2005) reviewed the fluid-to-fluid modelling of heat transfer at supercritical conditions. Based on the phenomenological analysis and distortion approach, a fluid-to-fluid scaling law was proposed, which was subsequently validated using existing test data from various fluids, combined with existing heat transfer correlations. Another important perspective of SCWR operation is the system stability, which is comparable with the well-explored boiling water reactor (BWR). In a typical BWR core, fluid density can change from 740 kg/m^3 to 180 kg/m^3, thereby leading to instability. Across several proposed designs of SCWR (US, European and Japanese versions), the density change can be even more drastic, i.e., from about 777 kg/m^3 to 90 kg/m^3 (Ruspini et al., 2014). Therefore, it is logical to expect both static and dynamic instabilities inside the SCWR core. While the threshold of the former can be predicted from the steady-state versions of the conservation laws, the later must take into account different dynamic factors like the propagation time, inertia and compressibility. Therefore, the methodologies followed during heat transfer

scaling are inadequate to lead to identical stability behaviour and a separate treatment is essential.

Rohde, (2012) studied the potential of natural circulation and the stability of such a loop (three-pass core) an experimental facility, DeLight, was built at the Delft University of Technology. This facility is a scaled down version of the HPLWR using Freon R-23 as scaling fluid. Finally, it described the setup and some preliminary measurements of natural circulation. As part of the EU THINS project a new test section is being developed for DeLight in collaboration with NRG for detailed velocity measurements. Ambrosini and Sharabi (2008) proposed the dimensionless parameters in this paper for dealing with heated channels with supercritical fluids were devised as a rather straightforward extension of the classical formalism adopted for boiling channels. Proposed approach demonstrated in making curves of fluid density as a function of specific enthalpy to collapse into a single dimensionless one for each fluid seems to suggest an interesting generality. The comparison of stability predictions obtained by the simple linearized model with the results obtained by RELAP5/MOD3.3 calculations provided further confidence in the applicability of the proposed dimensionless parameters and in the approach here adopted for the analysis of instabilities in heated channels with supercritical fluids.

Marcel et al. (2009) did experimental investigation on the stability of supercritical reactors, a fluid-to-fluid downscaled facility was proposed. It is found that with an appropriate mixture of refrigerants R-125 and R-32, the dimensionless enthalpy and density of the supercritical water can be accurately matched for all relevant operational conditions of the reactor. As a result of the proposed downscaling, the operational pressure, temperature and power are considerably smaller than those of a water-based system, which in turn helps reducing the construction and operational costs of a test facility. Finally, it was found that the often used modelling fluid supercritical CO_2 cannot accurately represent supercritical water at reactor conditions. Rohde et al. (2011) propose a scaling procedure based on Freon R-23 as the

working fluid so that pressure, power and temperatures are significantly reduced and the physics determining the dynamics of the system are almost completely preserved. The scaling of the radial dimension can be uncoupled from the axial dimension as long as small perturbations are considered (such as in linear stability analysis) and the friction distribution is conserved. The scaling laws have been applied to the European design of a nuclear super-critical water reactor. The R-23 based, experimental facility will be used for a fundamental study of the system stability of the reactor. The facility can be used for more detailed studies regarding turbulence and heat transfer as well. The scaling laws seem to be applicable for a large range of super-critical pressures, as some fluid properties match rather well.

T'Joen and Rohde (2012) explored the stability of a natural circulation HPLWR considering the thermo-hydraulic–neutronic feedback. This was done through a unique experimental facility, DeLight, which was a scaled model of the HPLWR using Freon R-23 as a scaling fluid. An artificial neutronics feedback was incorporated into the system based on the average measured density. To model the heat transfer dynamics in the rods, a simple first order model was used with a fixed time constant of 6s. The results include the measurements of the varying decay ratio (DR) and frequency over a wide range of operating conditions. A clear instability zone was found within the stability plane, which seems to be similar to that of a BWR. He also suggests that these data could serve as an important benchmark tool for existing codes and models.

Zahlan et al. (2014) reviewed two recent sets of fluid-to-fluid scaling laws for supercritical heat transfer and a discussion of their possible limitations, they had proposed two additional sets of scaling laws, which take into account empirically adjustable versions of the Dittus–Boelter correlation and which was applicable to both the supercritical and the high subcritical flow regions. They had compiled a database of heat transfer measurements in carbon dioxide flowing upwards in vertical heated tubes that are free of deterioration or enhancement. They then applied the four sets of scaling laws to these data to compute values of the water-equivalent heat transfer coefficient and

compared these values to predictions of a transcritical look-up table, which was earlier shown to represent well a large compilation of measurements in water at supercritical and high subcritical pressures. It was shown that the two earlier methods systematically overestimated the heat transfer coefficient in water and introduced significant imprecision. In contrast, the two proposed methods of scaling introduce no bias and have lower precision uncertainties than those of the previous scaling methods.

Roberto et al. (2016) performed experiments using water under supercritical conditions were limited by technical and financial difficulties. These difficulties can be overcome by using model fluids that were characterized by feasible supercritical conditions, that was, lower critical pressure and critical temperature. Experimental investigations were normally used to determine the conditions under which model fluids reliably represent supercritical fluids under steady-state conditions. A fluid-to-fluid scaling approach has been proposed to determine the model fluids that represent supercritical fluids in a transient state. Recently, a similar technique known as fractional scaling analysis was developed to establish the conditions under which experiments can be performed using models that represent transients in prototypes.

Pucciarelli and Ambrosini (2016) developed a methodology for fluid-to-fluid scaling for predicted heat transfer phenomena with supercritical pressure fluids with the aid of RANS calculations. The proposed approach rephrases and further develops a previous attempt, whose preliminary validation was limited by the considerable inaccuracy of the adopted turbulence models when applied to deteriorated heat transfer. A recent improvement in the accuracy of heat transfer predictions allowed this further step, also based on the broader experience gained in the mean time in the prediction of experimental data.

Shi et al. (2015) developed frequency domain linear stability analysis code for SCWR under the USDOE Generation IV Initiative. Based on single-channel coolant and water rod models, a thermal-nuclear coupled SCWR stability analysis code named SCWRSA was previously developed and applied to

preliminary stability analyses of a U.S. Generation IV SCWR reference concept. In this work, a multi-channel thermal-hydraulics analysis capability has been developed and implemented into SCWRSA. An iterative solution scheme was developed to calculate the steady state flow distribution among parallel thermal-hydraulics channels under a fixed total flow rate and the equal pressure drop boundary condition. This scheme determines the coolant and water-rod flow rates simultaneously by taking into account the heat transfer between coolant and water rod. For linear stability analysis, perturbation calculation models for flow redistribution among parallel channels were developed along with an efficient scheme to solve the resulting system of linear equations. The functionality of the modified SCWRSA code was confirmed by reproducing the previous single-channel analysis results. It was also observed that the effects of the inlet boundary condition are not monotonic; compared to the constant mixed-mean enthalpy approximation, the instantaneous mixing approximation produces smaller decay ratios for the Dittus-Boelter correlation but larger decay ratios for the Jackson correlation, although the difference is not so significant. The decay ratio for thermal-nuclear coupled stability estimated with two-channel models was less than 0.17, which is well below the limit (0.25) traditionally imposed for BWR stability.

Pioro and Duffey (2005) showed that the majority of experimental data were obtained in vertical tubes, some data in horizontal tubes and just a few in other flow geometries including bundles. They conclude after survey that in general, the experiments showed that there are three heat transfer modes in fluids at supercritical pressures: (1) normal heat transfer, (2) deteriorated heat transfer with lower values of the heat transfer coefficient (HTC) and hence higher values of wall temperature within some part of a test section compared to those of normal heat transfer and (3) improved heat transfer with higher values of the HTC and hence lower values of wall temperature within some part of a test section compared to those of normal heat transfer. The deteriorated heat transfer usually appears at high heat fluxes and lower mass

fluxes. Also, a peak in HTC near the critical and pseudo-critical points was recorded.

Yoshikawa et al. (2005) developed a closed-loop circulation system for supercritical fluids that operates on the principle of density differences induced by a heating and a cooling source. Performance of the system was determined by measuring average flow velocities for CO_2 over a range of conditions from 7.8 to 15 MPa and from 15 to 55°C for the given initial loading densities, ρ_{in}, of 550–800 kg/m^3 and density differences, ρ_{eff} between heating and cooling sources of the loop of 62–121 kg/m^3. One-dimensional finite-difference simulation could predict the velocities at most conditions to within 35%. The flow rates achieved in the system could be correlated in terms of Grashof and Prandtl numbers and a dimensionless effective density difference between heating and cooling sources to within 25% and by an empirical equation in terms of the system pressure, loaded density, heating, and cooling source average density difference to within 10%. Average flow velocities as high as 4 m/min could be obtained with heating and cooling source (wall) temperature differences of 3–8 °C.

Ambrosini (2008) was showed that presently available powerful computational resources, in addition to provide a means to tackle huge engineering problems that were out of reach for any simple theoretical analysis, can be profitably used as tools to improve physical understanding of phenomena. The products of this effort, mainly oriented to understand key phenomena, was in particular: (i) A better awareness in the use of system codes, in relation to the effects of numerical schemes; (ii) the availability of flexible tools for assessing stability in quite different flow systems, on the basis of a unified approach; (iii) A survey of similarity and differences between phenomena in heated channels with boiling fluids and with fluids at super-critical pressure; (iv) revealing suggestions and clear phenomena interpretation about heat transfer mechanisms, stimulating further experimental investigation.

Licht (2009) did FLUENT simulations, which were used to produce radial profiles of the fluid properties. Changes in the integrated effect of the specific heat were used to explain changes in the heat transfer coefficient due to changes in the applied heat flux. Measurements of mean axial velocity profiles and axial wall temperature distributions show similar deterioration profiles regardless of whether the wall temperature exceeds the pseudocritical temperature or not. Detailed mean and turbulent velocity measurements show that the turbulence, diffusivity of momentum, and likely the diffusivity of heat are reduced during deterioration at a radial position equivalent to what is the law of the wall region for isothermal flow.

Sharabi and Ambrosini (2009) discussed heat transfer enhancement and deterioration phenomena observed in experimental data for fluids at supercritical pressure. The results obtained by the application of various CFD turbulence models in the prediction of experimental data for water and carbon dioxide flowing in circular tubes are firstly described. On this basis, the capabilities of the addressed models in predicting the observed phenomena are shortly discussed. Then, the analysis focuses on further results obtained by a low-Reynolds number k– ε model addressing one of the considered experimental apparatuses by changing the operating conditions. The obtained results, supported by considerations drawn from experimental information, allow comparing the trends observed for heat transfer deterioration at supercritical pressure with those typical of the thermal crisis in boiling systems, clarifying old concepts of similarity among them. The analysis performed to explore the heat transfer behaviour at imposed wall temperature boundary conditions provided confirmation of the basic mechanisms credited to cause heat transfer enhancement and deterioration.

Jäger et al. (2011) summarized the activities of the TRACE code validation at the Institute for Neutron Physics and Reactor Technology related to supercritical water conditions. In particular, the providing of the thermos-physical properties and its appropriate use in the wall-to-fluid heat transfer models in the frame of the TRACE code is the object of this investigation. In a

first step, the thermos-physical properties of the original TRACE code were modified in order to account for supercritical conditions. In a second step, existing Nusselt correlations were reviewed and implemented into TRACE and available experiments were simulated to identify the most suitable Nusselt correlation.

Kurganov et al. (2012) briefly analysed experimental studies on heat transfer of turbulent flows of SCP fluids in tubes when heating. Specific features of typical heat transfer modes (normal, deteriorated, and improved) are pointed out. The existing concepts concerning the nature of heat transfer deterioration are discussed. A simple classification of heat transfer regimes under high heat loads is proposed, which makes it possible to determine the reasons for and assess the degree of danger of heat transfer deterioration.

Fu et al. (2012) studied the loss of coolant accident (LOCA) of supercritical water cooled reactor (SCWR), the pressure in the reactor system will undergo a rapid decrease from supercritical to subcritical condition. This process is called trans-critical transients, which is of crucial importance for the LOCA analysis of SCWR Using the current version of system code (e.g. ATHLET, REALP). To solve this problem, a pseudo two-phase method is proposed by introducing a fictitious region of latent heat (enthalpy of vaporization h_{fg}) at pseudo-critical temperatures. A smooth transition of void fraction can be realized by using liquid-field conservation equations at temperatures lower than the pseudo-critical temperature, and vapor-field conservation equations at temperatures higher than the pseudo-critical temperature. Adopting this method, the system code ATHLET is modified to ATHLET-SC mod 2 on the basic of the previous version ATHLET-SC mod 1 modified by Shanghai Jiao Tong University. When the fictitious region of latent heat is kept as a small region, the code can achieve an acceptable accuracy. Moreover, the ATHLET-SC mod 2 code is applied to simulate the blow down process of a simplified model. The results achieved so far indicate a good applicability of the new modified code for the trans-critical transient.

Schmitt et al. (2012) identified a transcritical range which corresponds to cases where the pressure was above the critical point, but the injection temperature was below the critical value. This situation is of special interest because it raises fundamental issues, which have technological relevance in the analysis of flows in liquid rocket engines. This situation was here envisaged by analysing the behaviour of a nitrogen shear coaxial jet comprising an inner stream injected at temperatures close to the critical temperature and a coaxial flow at a higher temperature. This behaviour was more pronounced when the jet is placed at the location of maximum transverse velocity fluctuations. Experiments were carried out both in the absence of external modulation and by imposing a large amplitude transverse acoustic field. Real gas large eddy simulations are performed for selected experiments. The combination of experiments and calculations were used to evaluate effects of injector geometry and operating parameters.

2.4 Mathematical modelling

Zuber (1966) proposed the drift flux model in which a combined momentum balance is written for the two-phase mixture, and the slip between the phases is accounted for by additional relations. Lewins (1961) proposed point neutron kinetic equations (two ODEs, if one group of delayed neutron precursors is modelled) represent the neutron kinetics in the simplest form. Because of their simplicity, point kinetics equations have been widely used to study instabilities in BWRs. Many numerical codes also use point neutron kinetics.

Zhao et al., (2006), simulated supercritical water flow in the core using a three-region model: a heavy fluid with constant density, a mixture of heavy fluid and light fluid and light fluid that behaves like an ideal gas or superheated steam. Two important non-dimensional numbers, namely, a pseudo-sub cooling number and expansion number has been identified for supercritical region, and then stability map in the supercritical region is also plotted in the plane made of these two number.

Zhao et al. (2007) used the Three-region supercritical water flow model, the core-wide in–phase stability of U.S. reference SCWR design is investigated. It was found that U.S. reference SCWR design is sensitive to the flow restrictions in the hot fluid or the steam line. As long as the restriction in the steam line is small, the design will be stable. Zhao et al. (2006) analysed Coupled neutronicthermal-hydraulic out-of-phase and compared with that of BWR. The out-of-phase oscillation of SCWR is found to be dominated by the reactor thermal-hydraulic, whereas the BWR is more sensitive to the coolant density reactivity coefficient because of much stronger neutronics coupling. A stability model for BWR in addition with the already-developed model for the SCWR is comparison of its stability features, and it is found that SCWR is less sensitive to the coolant density neutronics reactivity coefficient then the typical BWR. Pandey and Kumar (2007) presented analysis was done to study channel thermal-hydraulic instabilities for SCWR, hence, a constant heat flux is assumed. Linear stability analysis and transient simulations was carried out with this model. In order to study instabilities due to neutronics thermal-hydraulic coupling, neutron kinetics and fuel rod dynamics have to be included in the mathematical model.

Meloni and Polidori (2007) presented a preliminary study performed with the RELAP5/PARCS code on the dynamic behaviour of such a system in order to demonstrate the code capability to support the design of the experiment and the safety analysis. The specific code version used joins the well-known capability of RELAP5 to treat light water reactors with the potentiality of PARCS modified by ENEA to simulate the three-dimensional neutronic of sub-critical systems, i.e. to treat external neutron sources. A quite detailed model for the coupled code is developed in order to realistically evaluate the thermal feedback effects, the control rod action and the external source strength changes. Pandey and Kumar (2007) proposed simple nonlinear lumped parameter dynamic model of supercritical water-cooled reactor has been developed. Stability analysis and transient simulations have been done without and with the effect of coupled neutronic. The stability analysis with

neutronic was found to be more conservative. Transient simulations without neutronic indicate a supercritical bifurcation and the existence of a stable limit cycles in the unstable region. The analysis with neutronic was more conservative and shows that the system can be unstable for large perturbations, even if it was stable for small. These findings could not have been obtained with linear stability analysis only. Thus, it was necessary to carry out nonlinear stability analysis in order to determine the conditions under which the reactor perturbations. Reiss et al. (2008) developed at Budapest University of Technology a coupled neutronic-thermal-hydraulics program system, which was capable of determining the steady-state equilibrium parameters and calculating the related power, temperature, etc. distributions for the above-mentioned reactor. The program system can be used to optimize the axial enrichment profile of the fuel rods. In the paper, the developed program system and its features are presented. Parametric studies for different operating conditions were carried out and the obtained results are discussed.

Shan et al. (2009) developed a sub channel code (ATHAS) for preliminary analyses of flow and enthalpy distributions and cladding temperatures at supercritical water conditions. The code was applicable for transient and steady state calculations. A number of heat-transfer correlations, frictional resistance correlations, and mixing models have been implemented into the code as options for sensitivity analyses. In addition, a 3D heat conduction model has been introduced to establish the cladding temperature. The results show that (1) a CANFLEX bundle is appropriate for use in the CANDU supercritical water-cooled reactor (SCWR) based on heat transfer analysis, (2) the selection of heat transfer, friction, and mixing correlations had a significant impact on the prediction of the maximum cladding-surface temperature, and (3) the inclusion of the 3Dheat conduction in the calculation had provided a more realistic prediction of the maximum cladding-surface temperature than assuming a uniform cladding temperature due to the heterogeneous characteristic of rods

Yang et al. (2010) studied, the 3D flow and heat transfer characteristics in rod bundle channels of the super critical water-cooled reactor were numerically investigated using CFX codes. Different turbulent models were evaluated and the flow and heat transfer characteristics in different typical channels were obtained. The effect of pitch-to-diameter (P/D) ratio on the distributions of surface temperature and heat transfer coefficient (HTC) was analyses. For typical quadrilateral channel, it was found that HTC increases with P/D first and then decreases significantly when P/Dis <1.4. There exists a "flat region" at the maximum value when P/Dis 1.4. If P/Dis larger than 1.4, heat transfer deterioration (HTD) occurs as main stream enthalpy is quite small. Furthermore, the HTD under low mass flow rate and the non-uniformity of circumferential temperature were also discussed.

Shang and Lo (2010) studied horizontal rods and rod bundles at SCWR conditions. Special STAR-CD subroutines were developed by the authors to correctly represent the dramatic change in physical properties of the supercritical water with temperature. In the rod bundle simulations, it is found that the geometry and orientation of the rod bundle have strong effects on the wall temperature distributions and heat transfers. In one orientation the square bundle has a higher wall temperature difference than other bundles. However, when the bundles are rotated by 90◦the highest wall temperature difference is found in the hexagon bundle. Similar analysis could be useful in design and safety studies to obtain optimum fuel rod arrangement in a SCWR.

Merroun et al. (2009) presented a new procedure, which can be used during code and solution verification activities of thermal-hydraulic tools based on sub-channel approach. The technique of verification proposed was based mainly on the combination of the method of manufactured solution and the order of accuracy test. The verification of SACATRI code allowed the elaboration of exact analytical benchmarks that can be used to assess the mathematical correctness of the numerical solution to the elaborated model

Zhao et al. (2011) studied a response matrix method, which directly solves the linearized differential equations in the matrix form without Laplace transformation, was introduced for the supercritical fluids flow instability analysis. The model is developed and applied to the single channel or parallel channel type instability analyses of a typical proposed Supercritical Water Reactor (SCWR) design. A uniform axial heat flux is assumed, and the dynamics of the fuel rods and water rods are not considered in this paper. The sensitivity of the decay ratio (DR) to the axial mesh size was analysed and found that the DR was not sensitive to mesh size once sufficient number of axial nodes was applied. The sensitivity of the stability to inlet orifice coefficient was conducted for the hot channel and found that a higher inlet orifice coefficient will make the system more stable. It was found that the SCWR stability sensitivity feature could be improved by carefully choosing the inlet orifice coefficients and operating parameters. Finally, the manufacturing feasibility of the inlet orifices for both the hot channel and average channel was studied and found to be favourable.

Joen et al. (2011) studied the effect of these property uncertainties and system uncertainties on numerically determined stability boundaries. These boundaries were determined through an eigenvalue analysis of the linearized set of equations. The results show that the impact of the density and viscosity tolerance individually as well as that of the uncertainty of the imposed pressure drop are negligible. The results also showed that the stability boundary was linked to the friction distribution rather than its average value, and that different correlations result in strong changes of the predicted boundary. This emphasizes the need for an accurate friction correlation for supercritical fluids. These findings were important to assess the design of experimental facilities which use scaling fluids.

Kotlyar et al. (2011) analysed the BG Core reactor system recently developed at Ben-Gurion University for calculating in-core fuel composition and spent fuel emissions following discharge. It couples the Monte Carlo transport code MCNP with an independently developed burn up and decay module SARAF.

Recently, a simplified thermal hydraulic (TH) feedback module, THERMO, was developed and integrated into the BG core system. To demonstrate the capabilities of the upgraded BG core system, a coupled neutronics TH analysis of a full PWR core was performed. The BG core results were compared with those of the state of the art 3D deterministic nodal diffusion code DYN3D. Very good agreement in major core operational parameters including k-eff eigenvalue, axial and radial power profiles, and temperature distributions between the BG core and DYN3D results was observed. This agreement confirms the consistency of the implementation of the TH feedback module although the upgraded BG core system was capable of performing both, depletion and TH analyses; the calculations in this study were performed for the beginning of cycle state with pre-generated fuel compositions.

Monti et al. (2011) studied the initially neutronic and thermal-hydraulic full core calculations for iterated until a consistent solution was found to determine the steady state full power condition of the HPLWR core. Results of few group neutronic analyses might be less reliable in case of HPLWR3-pass core than for conventional LWRs because of considerable changes of the neutron spectrum within the core. The obtained results represent a new quality in core analyses, which takes into full consideration the coupling between neutronic and thermal-hydraulics as well as the spatial effects of the fuel assembly heterogeneity in determining the local pin-power and the associated maximum clad temperature.

Tian et al. (2012) studied instability for supercritical water-cooled reactor CSR1000 based on frequency domain method in this paper. A code named FREDO-CSR1000 (Frequency Domain Analysis of CSR1000) has been developed. The analysis of flow instability for CSR1000 both in average channel and hot channel within rated power and flow has been performed with the FREDO-CSR1000 code. The key parameters including decay ratio, the maximum cladding surface temperature and the proper orifice pressure drop coefficient were obtained as well. The calculation results indicated that the decay ratio of the first flow path varies with power and flow monotonically.

However, the decay ratio of the second flow path ascends first and then descends, the trend of which is fluctuant because of the simultaneous influence of a multitude of variables. Barragán-Martínez et al. (2013) developed a model for the HPLWR fuel with HELIOS-2, and to subsequently compare the results against the MCNPX, in order to use the HELIOS-2 for performing further reactor physics studies given that although MCNPX is better HELIOS-2 is faster. According to results, the HELIOS-2 code is good enough to be used in neutronic simulations of a HPLWR. Hence, they conclude that HELIOS-2 can be used for making HPLWR analysis faster than MCNPX.

Based on the field of application, various numerical codes have been classified as thermal hydraulic system codes (THSC), neutron kinetics codes (NKC), severe accident analysis codes (SAAC), etc. Some of these codes with brief description are listed in Table 2-1 and Table 2-2 (Prasad et al., 2007).

One of the first coupled neutronics– thermal hydraulics calculations for SCWRs was developed by (Yamaji et al., 2005). The SRAC code system was coupled with the single channel thermal hydraulics code SPROD to analyze the Japanese SCLWR-H concept. Also, burnup calculations were included with few group macroscopic cross sections prepared in advance. Further MCNP and STAFAS used to examine the assembly of the European HPLWR concept. STAFAS is a sub-channel code based on the COBRA code with some modifications specifically made for the HPLWR. With this approach local behaviour of various parameters of the fuel assembly were analysed. The calculations were carried out in steady state, for the heat transfer between the fuel rods and the coolant Bishop's correlation was used, and the fuel temperature was calculated with a one-dimensional heat conduction model. Validation was done using the KIKO3D-ATHLET code system. For the burnup calculations, cross sections were prepared in advance using average technological parameters for the assemblies with and without absorber. At certain burnup steps branch calculations were performed for a wide parameter range. This method was rigorously tested. In (HPLWR_01), Monti

used the ERANOS/TRACE coupled code system to examine the HPLWR core. ERANOS is a package of various neutronics codes with a common interface originally developed for fast reactors. Nevertheless, it was successfully used for LWR applications. TRACE is a best-estimate thermal hydraulics system code, which also includes 3-dimensional models. After convergence was achieved for the core, a burnup analysis was carried out, but without any thermal hydraulic feedback (Monti et al., 2011).

Table 2-1: 3D neutron kinetic Code

Code	Description	Features
DYN3D	Based on nodal expansion method for solving.	Burn-up Calculation
NEM	Multigroup Nodes.	Option of 3D Cartesian modelling, cylindrical and hexagonal geometries
PARCS	Code applicable to both PWR and BWR cores.	Coupled with TRAC-M and RELAP5
NESTLE	Multidimensional equations in Cartesian or hexagonal geometries.	Several different core symmetry options are available including quarter, half and full core options for Cartesian geometry.
SIMULA	3D neutron kinetics with one, two or six groups. Solves the neutron diffusion equations in one or two groups, on 3D coarse-mesh nodes (quarter or full fuel assemblies) using a linear-discontinuous finite difference scheme.	Coupled with thermal hydraulic code COBRAIIIC/MIT2.

Table 2-2: Severe accident analysis codes

Code	Description	Features
VICTORIA	Developed to analyse fission product behaviour within the reactor coolant system (RCS) during severe accident situation.	Features burn-up calculation. Option of external coupling with thermal hydraulic code ATHLET. Option for modelling 3D Cartesian, cylindrical and hexagonal geometries coupled with TRACPFI thermal hydraulic code. It can predict in detail, the release of radionuclides and radioactive materials from fuel and transport in the RCS during core degradation.
SCDAP	Models the core behaviour during a severe accident. It works in combination with RELAP5/MOD3 to describe the overall RCS thermal hydraulic response, core damage progression, and fission product release and transport during severe accidents.	It uses the detailed fission product code VICTORIA to describe the fission product release and transport during severe accidents. The code includes many generic component models from which the general systems can be simulated.
MELCOR	A fully integrated code that models all phases of the	Models have been coded with optional adjustable parameters to facilitate

progression of severe accidents in LWRs	uncertainty analysis and sensitivity studies.

The severe accident analysis codes (SAAC) are developed to model the reactor transients during severe accidents. Accidents occur due to various chemical and physical processes during reactor operation. These include core uncovering (loss of coolant), fuel heat up, cladding oxidation, fuel degradation (loss of rod geometry), core-concrete attack and ensuing aerosol generation, in-vessel and ex-vessel hydrogen production, transport, and combustion, fission product release (aerosol and vapour) its transport and deposition, etc. (Prasad et al., 2007).

2.5 Seismic effect on flow instability

Although, very few literatures are available on the seismic effect on the thermalhydraulic of the reactor and none of them are on the SCWR. Few of the literature is reviewed here.

Hirano and Tamakoshi, (1996) analysed on the excitation of instability in BWRs due to seismically induced resonance, within the scope of a point kinetics model. For this purpose, the TRAC-BVl code has been modified to take into account the external acceleration in addition to gravity. As a result of this analysis, it was shown that reactivity insertion can occur accompanied by in-surge of the coolant into the core resulting from excitation. It was also shown that the amount of reactivity inserted largely depends on the degree of stability of the initial state and the amplitude of the seismic wave, whose frequency was the same as the characteristic frequency of the instability. Satou et al. (2011), studied on BWR subjected to an earthquake, the oscillating acceleration attribute to the seismic wave may cause the variation of the coolant flow rate and void fraction in the core, which might result in the core instability due to the void-reactivity feedback. Therefore, it was important to properly evaluate the effect of the seismic acceleration on the core stability from a viewpoint of plant integrity estimation. Therefore, they studied the numerical code analysing the behaviour of nuclear power plant under the seismic acceleration was developed based on the three-dimensional

neutron-coupled thermal hydraulic code, TRAC-BF1/SKETCH-INS. The coolant flow in the core is simulated with introducing the oscillating acceleration attributed to the earthquake motion into the motion equation of the two-phase flow as external force terms. The analyses were performed on a real BWR4-type nuclear power plant (Peach Bottom #2) with the sinusoidal acceleration and the acceleration obtained from the response analysis to the El Centro seismic wave of Imperial Valley earthquake. The behaviours of the core and coolant were calculated in the various parameters of acceleration. The effects of the frequency, amplitude and direction of the oscillating acceleration were discussed.

Rofooei et al. (2001) generalized nonstationary Kanai–Tajimi model which was used to describe and simulate the ground motion time histories. Both amplitude and frequency non-stationarities were incorporated in the model. The moving time-window technique was used to evaluate the time varying parameters of the model using actual earthquake records. Application of the model for several Iranian earthquakes Naghan (1977), Tabas (1978) and Manjil (1990) were presented. It was shown that the model and identification algorithms were able to accurately capture the nonstationary features of these earthquake accelerograms. The statistical characteristics of the spectral response curves of the simulated accelerograms were compared with those for the actual records to demonstrate the effectiveness of the model.

Suárez and Montejo (2005), presented a wavelet-based procedure to generate an accelerograms whose response spectrum was compatible with a target spectrum. The acceleration time history of a recorded ground motion was decomposed into a number of component time histories. Next, each of the time histories is appropriately scaled so that its response spectrum matches a specified design spectrum at selected periods. The modified components are used to reconstruct an updated accelerograms, its spectrum was compared with the target spectrum and the process was repeated until a reasonable match was obtained. To achieve this goal, a new wavelet, based on the impulse response function of an underdamped oscillator was proposed. The proposed

procedure was illustrated by modifying five recorded accelerograms with different characteristics so that their spectra match a seismic design spectrum prescribed in the 1997 Uniform Building Code for a seismic zone 3 and soil type SB (rock). Finally, Abram and Ion (2008) has been considerably more difficult to achieve a seismically safe plant design.

2.6 Observation from literature survey

1. Extensive research has been done on linear analysis of instabilities in natural circulation boiling systems but due to lack of experimental studies with super-critical fluids in a natural circulation loop, presently there are not enough experimental data available to benchmark numerical findings. A computer code SUCLIN using supercritical water properties has been developed to carry out the steady state and linear stability analysis of a SCW natural circulation loop. But again, the experimental data particularly for forced flow system must be needed at this point for the benchmarking and validation of the several existing stability analysis codes.
2. There are large numbers of work have been done in numerical analysis of the flow stability, a system response matrix method, which directly solves the linearized differential equations in the matrix form without Laplace transformation, is introduced for the supercritical fluids flow instability analysis. The model is developed and applied to the single channel or parallel channel type instability analyses of a typical proposed (SCWR) design, but it is failed to numerical predict for other types of flow such as annuals, sub-channel etc. Therefore, there must be a unified code, which can be able to bridge the gaps between, superficial to the detailed system analysis.
3. The researchers make use of features presently available in CFD models, in the aim to move step-by-step from simple channel cases towards the analysis of more realistic fuel bundle sub-channels. Both static and dynamic instabilities are observed and studied, which provide promising features of CFD codes for such applications but these

are computationally expansive. Therefore, for getting a qualitative as well as quantitative idea a less expansive and computational fast model is required which can able to tackle more complicated problems as well.

4. A closed-loop circulation system for supercritical fluids that operates on the principle of density differences induced by a heating and a cooling source has been developed. The one-dimensional two-phase thermal hydraulics solution of APROS (Advanced Process Simulator) process simulation software was developed to function at the supercritical pressure region, FLUENT simulations were used to produce radial profiles of the fluid properties, A simple classification of heat transfer regimes under high heat loads is proposed, which makes it possible to determine the reasons for and assess the degree of danger of heat transfer deterioration. To solve the accident of LOCA in SCWR, a pseudo two-phase method is proposed by introducing a fictitious region of latent heat (enthalpy of vaporization h_{fg}) at pseudo-critical temperatures. Despite of the above facts, there is a simplified simulator/program is required which quickly captured the above phenomena.
5. Experiment were performed, to find instable zone within the stable plane, which seems to be similar to that of a BWR by a mixture of R-125 and R-32. But the disadvantage of this mixture, however, is that R-32 is highly flammable. Moreover, thermal stability of R-32 is questionable for temperatures above 300 ^{0}C. A scaled down version of the HPLWR using Freon R23 as scaling fluid, DeLight, was built at the Delft University of Technology. After experiment, they concluded that due to large density changes in R23, instability is more, which finally difficult to capture. So, a better fluid is required for the scaling of SCWR to study the instability effects on both natural and forced circulating system with a unified scaling method.
6. Many experimental and analytical studies have been carried out to ensure the integrity of nuclear power plants during earthquakes mainly in the area of structural safety. In the area of thermal hydraulics,

seismically induced sloshing of fluid with a free surface is one of the important research themes. A similar technique has been applied to the thermal hydraulic analysis of reactors. Due to very few literatures available on the seismic effect on the thermal hydraulic of reactor and none of them on SCWR. Therefore, a preliminary work is required for the study of instabilities by artificial seismic waves.

Chapter 3 MATHEMATICAL MODELLING

3.1 Introduction

Study of the dynamic behaviour of SCWR involves several interrelated steps. These include the selection of a pertinent set of state variables capable of characterizing the neutronics and thermal-hydraulic processes, the formulation of time-dependent equations that establishes the coupling between and the solution through analytical and numerical techniques. Different mathematical modelling techniques are available in the literature as discussed in the previous chapter.

A lumped parameter model is considered in the present analysis, which is derived from the basic governing equations. The primary governing equations, which are PDEs, can be transformed into an equivalent nonlinear system of ODEs by nodalization and spatial integration. It has been a standard approach for studying the stability and nonlinear dynamics of the system. The general transient equations are complicated to solve because of the coupling between the momentum and energy equations and their nonlinear nature. It is possible to simplify these equations in two ways; by decoupling the momentum and energy equations using an approximate velocity distribution in the channel or by transforming the PDEs to ODEs, which can be solved separately in the time- and space-domain. The latter approach is the foundation of the method of characteristics. In the channel integral (CI) method, the mass, momentum, and energy equations are integrated over the entire length of the channel. The present model adopts a two-zone LPM-based approach following a similar methodology. Channel as the whole is divided into two nodes, separated by a time-dependent boundary characterized by the pseudocritical point. For stability analysis, two different boundary conditions are taken into consideration, namely the constant pressure drop and constant mass flow rate. These can be viewed as the two extreme conditions of the pump characteristic curve. For analysing the behaviour of the system, two

separate studies, by considering these utmost conditions, are carried out. A forced flow channel is simulated in the present study, with uniform heat flux on the wall. The channel is subjected to either constant pressure drops or constant mass flow rate boundary condition. The one-dimensional conservation equations for mass, momentum, and energy are taken. For the sake of generalizations, governing equations are nondimensionalized using suitable dimensionless parameters. The equations for mass and energy are integrated over the first node, i.e., from the inlet till the appearance of the pseudocritical boundary. Correspondingly, two ODEs are obtained regarding the location of the pseudocritical boundary. Now, again integrating the conservation equations over the second node, from the pseudocritical boundary to the channel outlet, two ODEs are obtained regarding the outlet enthalpy. These four equations are sufficient for the mass flow rate boundary condition. However, for pressure-drop boundary condition, the equation for conservation of momentum is integrated separately over both the zones and added to represent the net pressure drop across the channel. The system of six ODEs is used for analysis, along with algebraic equations, which are obtained by equating the ODEs of mass and energy equations for the two zones, and the equation of state. To capture the sharp variation in thermophysical properties of supercritical water around the pseudo-critical point, the comparison of the state is replaced by fitting a separate rectangular hyperbola for each of the zones. After being heated through the core, the supercritical coolant flows directly to the turbine through the turbine control valve.

The numerical simulation is done using MATLAB ODEs function 15s algorithms. ODE 15s is a variable-step, variable-order (VSVO) solver based on the mathematical differentiation formulas (NDFs) of orders 1 to 5. Optionally, it can use the backward differentiation formulas (BDFs, also known as Gear's method) that are usually less efficient. Like ODE113, ODE15s is a multistep solver (Shampine and Reichelt, 1997).

Table 3-1 shows the values of US SCWR reference design, which is used in the stability analysis.

Table 3-1: Design parameters of the reference SCWR Core.

Parameter	Value
Core pressure (MPa)	25
Core thermal/electrical power (MW)	3576.64/1573.72
Average linear power density (kW/m)	19.0
Coolant inlet outlet (^{0}C)	280.0/508.0
Thermal efficiency (%)	44.0
Core flow rate (kg/s)	1843.0
Fuel pin heated length (m)	4.20/3.38
Average mass flux of the assemblies (kg/s/m^2)	903.14
Number of fuel assemblies	145
Number of fuel pin per assembly	300
Assembly hydraulic diameter (mm)	3.4
Target core pressure drop (MPa)	0.15

3.2 Lumped parameter model

In LPM, the matter is assumed to be lumped at some discrete points in space. Alternatively, space can be viewed to be divided into multiple cells, and the matter is supposed to be lumped at these cells. A single vertical channel with upward motion is considered here for analysis, and the same is divided into two nodes for simplicity. The nodes are differentiated by a time-dependent boundary, characterized by the appearance of the pseudocritical temperature (Figure 3-1). Axial enthalpy variation within each node is assumed to be linear, along with a constant friction factor during the transients.

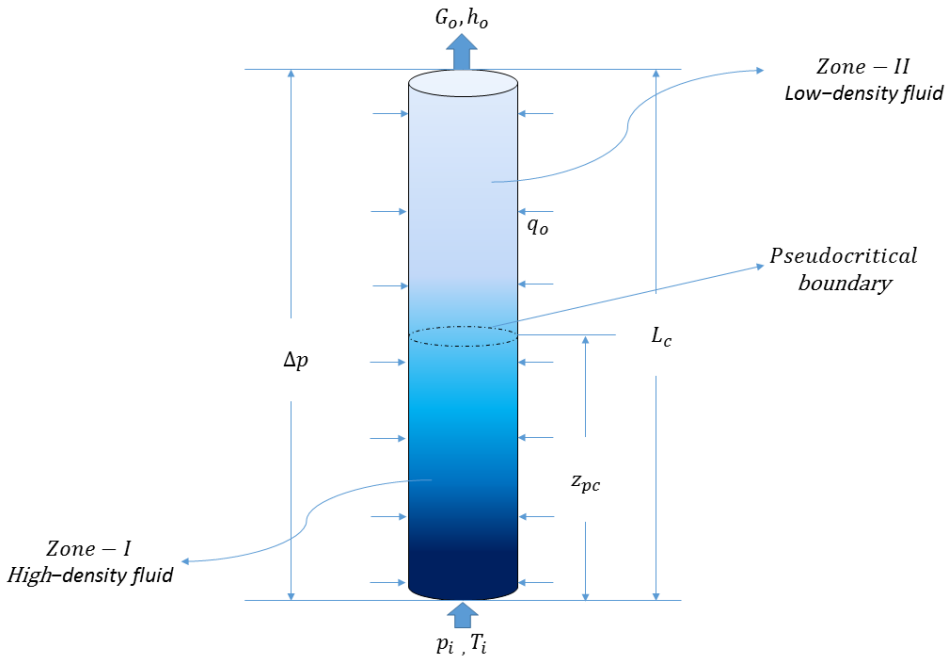

Figure 3-1: Schematic representation of the channel under consideration

In this context, a short discussion on the adoption of LPM is warranted. Such a reduced-order model allows the decoupling of momentum and energy equations, leading to a swift and consistent evaluation of both the temporal traces and static system characteristics. Therefore, it has historically been quite popular for stability appraisal of boiling channels (Guido et al., 1991; Paruya et al., 2012), and has subsequently found increased interest for supercritical flow systems as well. Nakatsuka et al. (1998) developed a dynamic model with fixed boundaries to test a once-through fast reactor against three kinds of perturbation, namely, the position of control rod, the feedwater flow rate and the turbine valve opening. That work was extended by Ishiwatari et al. (2003) to include the water rods. Sun et al. (2011) employed a three-region model with moving boundaries to predict the dynamic behaviour of CANDU-SCWR. A three-zone model for US reference design of SCWR with sliding pressure startup was also reported by Zhao et al. (2007). Excerpt from all such studies establishes LPM as a reliable tool for stability prediction of supercritical channels, commonly leading to a conservative estimate. Lumping of properties, of course, may lead to the loss of some localized information. However, the focus of the present study being on

developing the scaling methodology suitable for stability assessment, LPM is a more economical approach for testing its capabilities, compared to multi-dimensional CFD simulations. It is also much more comfortable to couple the effect of power dynamics and fuel rod dynamics with the thermal hydraulics in a simplified framework such as LPM, and hence the same is adopted in the present study.

The lumped parameter mathematical model can be divided into three parts: Thermal hydraulics, which models the fluid dynamics in the coolant channels; heater wall dynamics, which models the heat transfer from the fuel rod surface to the coolant, and power dynamics, which describes the dynamics of heat generation in fuel rod through nuclear fission.

3.2.1 Thermal-hydraulic modelling

A circular forced flow channel of uniform diameter is simulated in the present study, under uniform heat flux boundary condition imposed on the wall. The channel is subjected to constant pressure drop boundary condition under both steady and transient conditions. Accordingly, the one-dimensional conservation equations for mass, momentum and energy can be summarized as follow.

$$\frac{\partial \rho}{\partial t} + \frac{\partial G}{\partial z} = 0 \tag{3.1}$$

$$\frac{\partial G}{\partial t} + \frac{\partial}{\partial z}\left(\frac{G^2}{\rho}\right) = -\frac{\partial p}{\partial z} - \rho g - \left[\frac{f}{D_h} + 2K_i\delta(z) + 2K_o\delta(z-L)\right]\frac{G^2}{2\rho} \tag{3.2}$$

$$\frac{\partial}{\partial t}(\rho h) + \frac{\partial}{\partial z}(Gh) = \left(\frac{\pi_h}{A}\right) q''(t) \tag{3.3}$$

Heat loss to the surrounding is neglected here. For the sake of generalizations, governing equations are non-dimensionalized using the following definitions.

$$z^* = \frac{z}{L_c}, t^* = \frac{tG_c}{\rho_{pc}L_c}, G^* = \frac{G}{G_c}, \rho^* = \frac{\rho}{\rho_{pc}}, p^* = \frac{(p-p_r)\rho_{pc}}{G_c^2},$$
$$T^* = \frac{T-T_{pc}}{T_{pc}}, h^* = (h-h_{pc})\frac{\bar{\beta}_{pc}}{C_{p.pc}}, N_{Fr} = \frac{G_c^2}{\rho_{pc}^2 g L_c}, \quad 3.4$$
$$N_{TPC} = \frac{q_0''\pi_h L_c}{AG_c}\frac{\beta_{pc}}{C_{p.pc}}, N_{Eu} = \frac{fL_c}{2D_h}$$

Reference pressure (p_r) can be set to any suitable value, as the system thermal hydraulics is generally quite independent of pressure in the supercritical level. Hence, the outlet pressure is selected as the reference for the present work. Subsequently, the non-dimensional forms of governing equations can be presented as,

$$\frac{\partial \rho^*}{\partial t^*} + \frac{\partial G^*}{\partial z^*} = 0 \quad 3.5$$

$$\frac{\partial G^*}{\partial t^*} + \frac{\partial}{\partial z^*}\left(\frac{G^{*2}}{\rho^*}\right) = -\frac{\partial p^*}{\partial z^*} - \frac{\rho^*}{N_{Fr}} - [N_{Eu} + K_i\delta^*(z^*) + K_o\delta^*(z^*-1)]\frac{G^{*2}}{\rho^*} \quad 3.6$$

$$\frac{\partial}{\partial t^*}(\rho^* h^*) + \frac{\partial}{\partial z^*}(G^* h^*) = N_{TPC}\, f(t^*) \quad 3.7$$

Hereδ, dimensional Dirac delta functions (m^{-1}) at channel inlet and exit simulate the localized pressure losses at entry and exit respectively. Number of non-dimensional parameters and dimensionless groups (Eq. 3.4) are defined to transform the set of dimensional equations into a non-dimensional one for the sake of generalization.

Choice of the reference pressure (p_r) is quite arbitrary and hence the channel exit pressure is selected as the reference here, so that the pressure drop across the channel (Δp) can be equated to the inlet value alone in the non-dimensional scale. The boundary conditions can be specified in terms of two dimensionless numbers, namely, N_{TPC} and N_{SPC} $(= \beta_{pc}(h_{pc}-h_i)/C_{p.pc})$. While the former represents system power, the latter is proportional to $(h_{pc}-h_i)$ and

hence can be taken as a measure of the inlet temperature. While the former signifies the non-dimensional enthalpy differential between the inlet and the pseudocritical point, the latter corresponds to the power input to the channel. They can be viewed to be analogous respectively to the subcooling number and phase-change number for a boiling channel.

Here the definition of N_{TPC} corresponds to some reference power level q_0'' and the function $f(t^*)$ captures the transient variation in the power supply, which in turn is dependent on the neutronics.

3.2.2 Fuel dynamics

The heat transfer from the fuel rod to the coolant is defined by fuel dynamics. The internal thermal resistance of the fuel rod is assumed negligible compared to the external resistance to heat transfer between the heater and coolant. Hence, the temperature distribution inside the fuel rod is neglected, and it is considered as a body having a uniform temperature. The effects of heat conduction through the cladding, gap conductance, and heat diffusion through the fuel pellet have been neglected for simplicity, as it does not hamper the overall dynamics of the system (Regis et al., 2000; Yang and Zavaljevski, 2003). The purpose of ignoring the diffusion through the fuel element is to reduce the complexity. The primary goal of the analysis is to simulate the practical conditions simply and to provide the preliminary data for the more rigors analysis using this model. So that, the model can able to capture marginal stability boundary quickly and effectively. The fuel element chosen is Uranium dioxide having a heat capacity of 3.46 MJ/m^{3}K (Zhao et al., 2006).

Fuel rod dynamics is considered in the present model to study its effect on the stability of the system. The rate of heat transfer being proportional to the fuel-to-coolant temperature differential, it becomes imperative to consider temperature as a function of enthalpy, which has been designated as one of the primary variables in LPM. A single node for the fuel rod is found, assuming uniform temperature throughout, in conjunction with the two thermal

hydraulic nodes. Accordingly, the energy balance for the fuel rod, characterized by a constant steady-state power (P_{ss}), can be presented as,

$$C_f \frac{dT_f}{dt} = P_{ss} - \alpha_1 A_1 (T_f - T_1) - \alpha_2 A_2 (T_f - T_2) \quad 3.8$$

Here T_j, A_j and α_j respectively represents the average temperature, total peripheral area and convective heat transfer coefficient for the j^{th} fluid node, whereas T_f is the average temperature for the fuel rod. Average coolant temperature for each node is taken as the mean of the inlet and outlet values for that particular node. Since enthalpy is selected as the primary variable in the present analysis, temperature is considered as a piecewise quadratic polynomial function of enthalpy.

With the incorporation of the lumped fuel rod model, the energy equation for the j^{th} coolant node (Eq. (3.8)) needs to be modified as,

$$\frac{\partial}{\partial t}(\rho h)_j + \frac{\partial}{\partial z}(Gh)_j = \left(\frac{\pi_h}{A}\right) n_f \alpha_j (T_f - T_j) \quad 3.9$$

where A refers to the cross-sectional area of the channel and n_f is the number of fuel rods involved. Using the non-dimensional definitions proposed in Eq. (3.4), dimensionless forms of the above two equations can be given as:

$$\tau \frac{dT_f^*}{dt^*} = 1 - H_1 z_{pc}^* (T_f^* - T_1^*) - H_2 (1 - z_{pc}^*)(T_f^* - T_2^*) \quad 3.10$$

$$\frac{\partial}{\partial t^*}(\rho^* h^*)_j + \frac{\partial}{\partial z}(G^* h^*)_j = N_j' (T_f^* - T_j^*) \quad 3.11$$

where, $\tau = \dfrac{C_f G_c T_{pc}}{\rho_{pc} L_c P_{ss}}$ $\quad H_j = \dfrac{\alpha_j (n_f \pi_h L_c) T_{pc}}{P_{ss}}$ $\quad N_j' = \dfrac{P_{ss} H_j \beta_{pc}}{A G_c C_{p.pc}}$

3.2.3 Power dynamics

In nuclear reactors, the heat is generated due to fission. The theory behind this is the Neutron transport theory (Henry, 1975). It is used to explain the time-dependent behavior of neutron population in the reactor. This theory

allows for a precise representation of neutron interactions. The resulting equations are, however, mathematically complex due to their explicit dependence on neutron energy, the direction of motion, and position, and time. If equations depend on time then it would easily be handled. Under certain conditions, it is possible and widely useful to suitably integrate or average out energy, direction and position variables from the time-dependent transport theory equations, resulting in a set of ordinary differential equations with respect to time, in which the delayed neutrons can be retained if desired (Pandey, 1996).

It is recognized by different researchers that the delayed neutron emitters have the widely different decay constant and are better represented by six group of delayed neutron precursors. It is convenient and satisfactory (and most widely used in lumped parameter models) to treat the delayed neutron precursors using one precursor group model. This simplifies the equations by representing all the delayed neutrons as though they had a single mean lifetime or decay constant. Point reactor kinetics model with one group of delayed neutrons (Park et al., 1986; Theler and Bonetto, 2010; Pandey and Singh, 2016; Prasad et al., 2007), is widely used in linear and nonlinear analysis of nuclear-coupled thermal-hydraulic analysis, and as stated earlier the main objective of the model is to qualitative study with reasonable accuracy, hence by using the 6-groupes of delayed neutron. The mathematical model become more complicated nonlinear equations, which does not gives more advantage on the qualitative basis. Hence, the choice of one group of delayed neutron is justified. Finally, the resultant point reactor kinetics equations are coupled with the suitably reduced-order thermal-hydraulic model of the reactor core, with appropriate reactivity feedback mechanism, to yield a lumped parameter model. Point neutron kinetics with a single group of delayed neutrons is also incorporated in the developed model to embrace the effect of power dynamics. The constant steady-state power P_{ss} mentioned in the previous discussion is subsequently replaced by a time-varying

quantity. Transient variation in power and precursor density can be presented as,

$$\frac{dP}{dt} = \frac{k-\beta}{\gamma}P + \sigma C \tag{3.12}$$

$$\frac{dC}{dt} = \frac{\beta}{\gamma}P - \sigma C \tag{3.13}$$

Setting the steady-state reactivity to zero and neglecting the time-dependence, the feedback reactivity can be correlated to the fuel rod temperature and coolant enthalpy as,

$$k(t) = \mu_f\left(T_f(t) - T_{f,ss}\right) + \mu_{h1}\left(h_1(t) - h_{1,ss}\right) + \mu_{h2}\left(h_2(t) - h_{2,ss}\right) \tag{3.14}$$

where μ_f is the temperature coefficient of reactivity and μ_{hj} is the enthalpy coefficient of reactivity for the j^{th} fluid node. Here the feedback at any time instant is considered to correspond to the average fuel rod temperature and average coolant enthalpies at each node at that particular instant. The variables related to power dynamics can be non-dimensionalized using the concerned steady-state values as,

$$P^* = \frac{P}{P_{ss}}, \qquad C^* = \frac{C}{C_{ss}} \tag{3.15}$$

Consequently, the dimensionless versions of Eq. (3.12) and (3.13) can be presented as,

$$\frac{dP^*}{dt^*} = \frac{k-\beta}{\gamma}P^* + \sigma C^* \tag{3.16}$$

$$\frac{dC^*}{dt^*} = \frac{\beta}{\gamma}P^* - \sigma C^* \tag{3.17}$$

Variation in the non-dimensional power P^* determines the nature of Eq. 3.17, thereby providing the coupling between the neutronics and thermal hydraulic components. The reference power can be defined as, $P_{ss} = q_0''\pi_h L_c$. Magnitudes of the neutronics constants are taken from BWR designs, since all light water

reactors are typically characterized by similar numbers. Values for both the coefficients are taken from the work of Yang (2010).

3.3 Steady-state equations

The steady equations are obtained by putting the temporal derivatives zero in Eq. 3.5-3.7, 3.10, 3.16 and Eq. 3.17.

$$\frac{\partial G^*}{\partial z^*} = 0 \tag{3.18}$$

$$\frac{\partial}{\partial z^*}\left(\frac{G^{*2}}{\rho^*}\right) = -\frac{\partial p^*}{\partial z^*} - \frac{\rho^*}{N_{Fr}} - [N_{Eu} + K_i\delta^*(z^*) + K_o\delta^*(z^* - 1)]\frac{G^{*2}}{\rho^*} \tag{3.19}$$

$$\frac{\partial}{\partial z^*}(G^*h^*) = N_{TPC} \tag{3.20}$$

$$1 - H_1 z_{pc}^*\left(T_f^* - T_1^*\right) - H_2\left(1 - z_{pc}^*\right)\left(T_f^* - T_2^*\right) = 0 \tag{3.21}$$

$$\frac{k - \beta}{\gamma}P^* + \sigma C^* = 0 \tag{3.22}$$

$$\frac{\beta}{\gamma}P^* - \sigma C^* = 0 \tag{3.23}$$

Eq. 3.18-3.23, shows the steady state equations of the five state variables namely, z_{pc}^* h_o^* T_f^* P^* C^* . Eq. 3.18 is the equation of mass flux at steady state. There are two equations (Eq. 3.19-3.20) which captures the thermohydraulic aspects of the system. Moreover, one equation (Eq. 3.21) is coming from the fuel dynamics of the system, which gives the steady state value of average fuel rod temperature, finally the last two equations (Eq. 3.22-3.23) is provides the information of the power dynamics of the system.

The above equations, in addition to the equation of state, are solved by using MATLAB ODE function 15s, which is an in-built ordinary differential equation solver in MATLAB, when all the inlet field variables, i.e., pseudocritical length, enthalpy, fuel rod temperature, power and precursor density are specified. The results obtained from the steady state model are used as the initial condition for the transient simulation.

3.3.1 Comparison of steady state results

The results from LPM are compared with the 1-D models proposed by Ambrosini and Sharabi (2008). In their model, different inlet and exit orifice pressure drop coefficients were used to match the steady state axial pressure distribution obtained by them. The comparison of the steady state result at a power input of 25 kW/m obtained by LPM with those from the Ambrosini and Sharabi (2008) model is shown in Figure 3-2 and Figure 3-3. The geometrical and operating parameters of the problem under consideration are given in Table 3-2.

Table 3-2: Geometrical and operating parameters of the single channel (Ambrosini and Sharabi, 2008)

Geometrical parameters	
Length	4.2672 m
Hydraulic diameter	3.4 mm
Coolant flow area	$5.4972 \times 10{-}5\ m^2$
Operating parameters	
Inlet temperature	280◦C
Inlet pressure	25.14 MPa
Exit pressure	25.00 MPa

Based on the above observations, it has been concluded that the LPM steady-state results are matches well, which is within the acceptable limits.

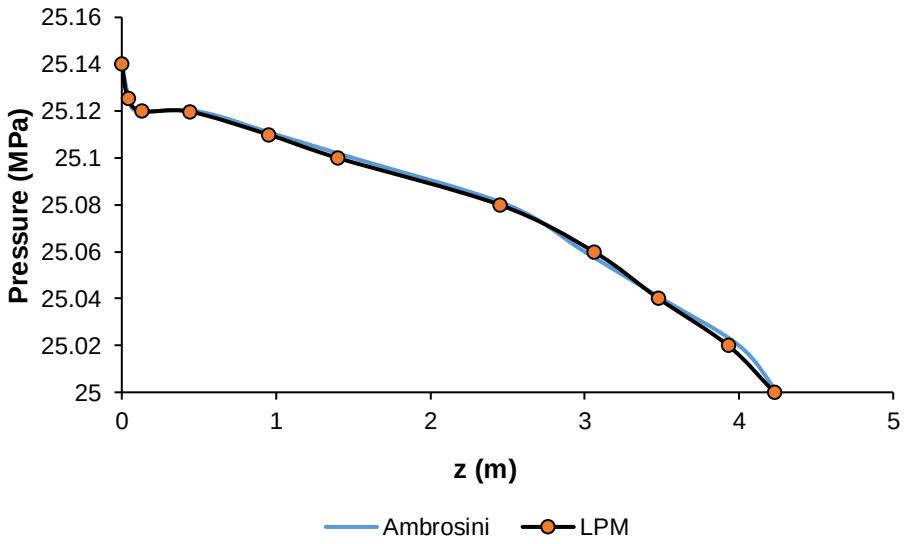

Figure 3-2: Comparison of the steady state pressure distribution along the channel for the single channel obtained by LPM with Ambrosini and Sharabi (2008)

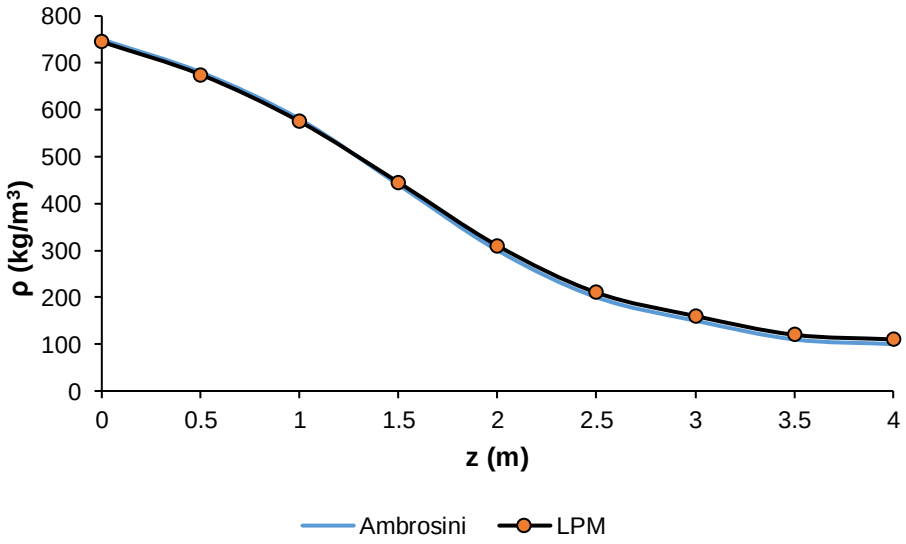

Figure 3-3: Comparison of the steady state density distribution along the channel for the single channel obtained by LPM with Ambrosini and Sharabi (2008)

Finally, from these calculations, results in reasonable agreement with the data reported in the mentioned reference.

3.4 Transient equations

The general transient equations are complicated to solve because of the coupling between the momentum and energy equations. Due to their nonlinear nature, It is possible to simplify these equations in two ways; by

decoupling the momentum and energy equations using an approximate velocity distribution in the channel, or by transforming the PDEs to ODEs, which can be solved separately in the time- and space-domain. The latter approach is the foundation of the method of characteristics. In the channel integral (CI) method detailed by Todreas and Kazimi (2001), the mass, momentum and energy equations are integrated over the entire length of the channel. The present model adopts a two-zone LPM-based approach following the similar methodology. Two different types of boundary conditions are studied separately, which are the constant pressure drop and constant mass flow rate respectively, along with specified coolant inlet temperature.

3.4.1 Pressure drop boundary condition

The non-dimensional governing equations are integrated over the first and second node respectively. In the first node the mass and energy equations are integrated separately from inlet until the appearance of the pseudocritical point, following two ODEs can be obtained.

$$B_2 \frac{dz_{pc}^*}{dt^*} = \left(G_{pc}^* - G_i^*\right) \tag{3.24}$$

$$B_1 \frac{dz_{pc}^*}{dt^*} = \left(N_{TPC} z_{pc}^* + N_{SPC} G_i^*\right) \tag{3.25}$$

Where, $N_{TPC} = \frac{q_0'' \pi_h L_c}{A G_c} \frac{\beta_{pc}}{C_{p.pc}}$ and $N_{SPC} = \beta_{pc}\left(h_{pc} - h_i\right)/C_{p.pc}$. Above two ODEs can be combined to obtain the following algebraic equation of inlet mass flux.

$$B_3 G_i^* = B_1 G_{pc}^* - N_{TPC} B_2 z_{pc}^* \tag{3.26}$$

Again, Integrating the non-dimensional mass and energy conservation equations over the second node, from the pseudocritical point to the channel outlet, two ODEs are achieved in terms of h_o^*.

$$h_o^* \frac{dh_o^*}{dt^*} = \frac{\left(G_o^* - G_{pc}^*\right) + (1 - B_4)\frac{dz_{pc}^*}{dt^*}}{(B_4 - B_5)(1 - z_{pc}^*)} \tag{3.27}$$

$$h_o^* \frac{dh_o^*}{dt^*} = \frac{N_{TPC}(1 - z_{pc}^*) - G_o^* h_o^* - (1 - B_4)\frac{dz_{pc}^*}{dt^*}}{(B_4 - B_5)(1 - z_{pc}^*)} \quad 3.28$$

Similar to the first node, the above two ODEs can also be combined in a single equation as,

$$G_{pc}^* = G_o^*(h_o^* - 1) - N_{TPC}(1 - z_{pc}^*) - 2(1 - B_4)\frac{dz_{pc}^*}{dt^*} \quad 3.29$$

Finally, the equation for conservation of momentum is integrated separately over both the zones and added to represent the net pressure drop across the channel as,

$$\Delta p^* = \frac{1}{2}\left(\frac{dG_i^*}{dt^*} + \frac{dG_o^*}{dt^*}\right) + \Delta p_f^* + \Delta p_g^* + \Delta p_a^* + \Delta p_{L,i}^* + \Delta p_{L,o}^* \quad 3.30$$

where, $\Delta p_f^* = \frac{G_{pc}^{*2} N_{Eu}}{2}\left[1 + \frac{1}{2\,N_{SPC}}\ln(1 + 2\,N_{SPC})\right] z_{pc}^* + \frac{G_o^{*2} N_{Eu}}{2}(2 + h_o^*)(1 - z_{pc}^*)$

$$\Delta p_g^* = \left[(1 - B_2) z_{pc}^* + B_4(1 - z_{pc}^*)\right] {N_{Fr}}^{-1}$$

$$\Delta p_a^* = G_o^{*2}(1 + h_o^*) - \frac{G_i^{*2}}{\rho_i^*} \qquad \Delta p_{L,i}^* = \frac{K_i}{2\rho_i^*} G_i^{*2} \qquad \Delta p_{L,o}^* = \frac{K_o}{2} G_o^{*2}(1 + h_o^*)$$

As the system under consideration is subjected to the specified pressure drop boundary condition, Eq. (3.21) is coupled with the differentiated form of Eq. (3.22) to provide an equation of outlet mass flux as

$$\frac{dG_o^*}{dt^*} = \left[2\Delta p_{Inertial}^* - \left\{G_i^* - G_o^* - N_{TPC}\frac{B_2}{B_3} z_{pc}^*\right\}\frac{dz_{pc}^*}{dt^*} - \left\{1 + \frac{B_1}{B_3} z_{pc}^*\right\}\frac{dG_{pc}^*}{dt^*}\right](1 - z_{pc}^*)^{-1} \quad 3.31$$

where, $B_1 = \frac{\ln(1 + N_{SPC})}{N_{SPC}} - (1 + N_{SPC})$ $\qquad B_2 = \frac{\ln(1 + N_{SPC})}{N_{SPC}} - 1$ $\qquad B_3 = B_1 + B_2 N_{SPC}$

$$B_4 = \frac{1}{h_o^*}\ln(1 + h_o^*) \qquad B_5 = \frac{1}{1 + h_o^*}$$

Therefore, the initial system of PDEs is converted to a set of algebraic equations and ODEs, with dimensionless time (t^*) as the sole independent variable. That eliminates the complexity associated with solving a system of PDEs and eradicates the huge computational resource requirement for finite difference simulation. In order to capture the sharp variation in thermophysical properties of supercritical water around the pseudocritical point, the equation of state is replaced by fitting a separate rectangular hyperbola for each of the zones (Figure 3-4) given as (Pandey and Kumar, 2007),

$$\rho^* = \frac{1 - 2h^*}{1 - h^*} \; for \; -1.58 \le h^* \le 0$$

$$\rho^* = \frac{1}{1 + h^*} \; for \; 0 \le h^* \le 1.74 \qquad 3.32$$

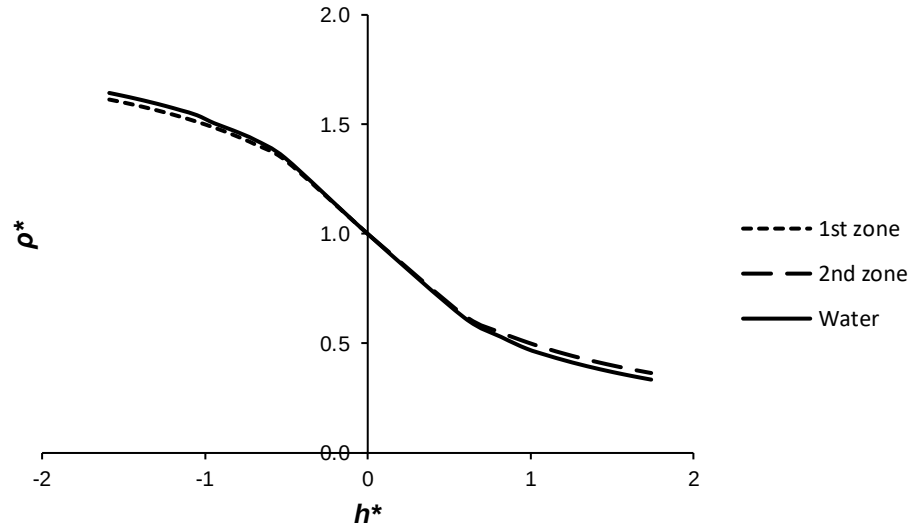

Figure 3-4: Polynomial fitting of IAPWS data for water at 25 MPa

3.4.2 Mass flow rate boundary condition

For considering mass flow rate boundary condition, the same procedure is applied as mentioned in Section 3.3.1, integrating the dimensionless

governing equations for mass and energy over the first node, the following two ODEs is obtained.

$$B_2 \frac{dz_{pc}^*}{dt^*} = \left(G_{pc}^* - G_i^*\right) \tag{3.33}$$

$$B_1 \frac{dz_{pc}^*}{dt^*} = \left(N_{TPC} z_{pc}^* + N_{SPC} G_i^*\right) \tag{3.34}$$

where, $N_{SPC} = \dfrac{\bar{\beta}_{pc}(h_{pc} - h_i)}{C_{p,pc}}$

The above two ODEs can be combined to obtain the following algebraic equation of inlet mass flux.

$$B_1 G_{pc}^* = B_3 G_i^* + N_{TPC} B_2 z_{pc}^* \tag{3.35}$$

Integrating the conservation equations over the second node, from the pseudocritical point to the channel outlet, two ODEs of h_o^* is obtained. After combining the ODEs of h_o^* equations, an algebraic equation of G_o^*, is obtained.

$$G_o^*(h_o^* - 1) = G_{pc}^* - N_{TPC}\left(1 - z_{pc}^*\right) - 2(1 - B_4)\frac{dz_{pc}^*}{dt^*} \tag{3.36}$$

The equation for conservation of momentum is not taken into considerations as the mass flow rate boundary condition is applied here.

where, $B_1 = \dfrac{\ln(1 + N_{SPC})}{N_{SPC}} - (1 + N_{SPC})$ $\quad B_2 = \dfrac{\ln(1 + N_{SPC})}{N_{SPC}} - 1$ $\quad B_3 = B_1 + B_2 N_{SPC}$

$$B_4 = \frac{1}{h_o^*}\ln(1 + h_o^*) \qquad B_5 = \frac{1}{1 + h_o^*}$$

3.5 RELAP model

RELAP5 is a highly generic code that, in addition to calculating the behaviour of a reactor coolant system during transients, can be used for simulation of a wide variety of hydraulic and thermal transients in both nuclear and non-nuclear systems. It is a sophisticated time-domain code based on two-fluid formulations, capable of simulating the flow at

supercritical pressures (Fu et al., 2012; Debrah et al., 2013). Present layout is visualized in RELAP5/MOD4.0 code as a single pipe, connected with inlet and outlet plenum (Figure 3 3). The single channel is modelled as a pipe component, containing 30 volumes, connected with junctions at the two ends. These junctions are further combined with time-dependent volume components to model the plenum. The heat supply to the active core is shaped using heat structures, which is subsequently divided into volumes similar to the active core and with constant power option. The heat structure is modelled as a material having high thermal conductivity and low heat capacity, to avoid distortions in the imposed thermal flux condition, and eliminating the effect of fuel dynamics. Accordingly, RELAP is employed to validate the thermal-hydraulic part of the present model solely.

To ascertain the stability behaviour of the RELAP model, simulations are initially performed at some guessed power level, often guided by the observations from the indigenous linear stability analysis. Generally, lower values of power are attempted with, to ensure a stable response, which can be concluded by following the resultant temporal variation in system variables. Subsequently, the power is gradually increased until the attainment of the marginally stable condition, signified by constant-amplitude fluctuations of the state variables. With the small rise in power level, the code returns diverging oscillations, indicating the unstable situation. Such hit-and-trial approach requires several simulations to identify the stability threshold and consequently to generate the stability map.

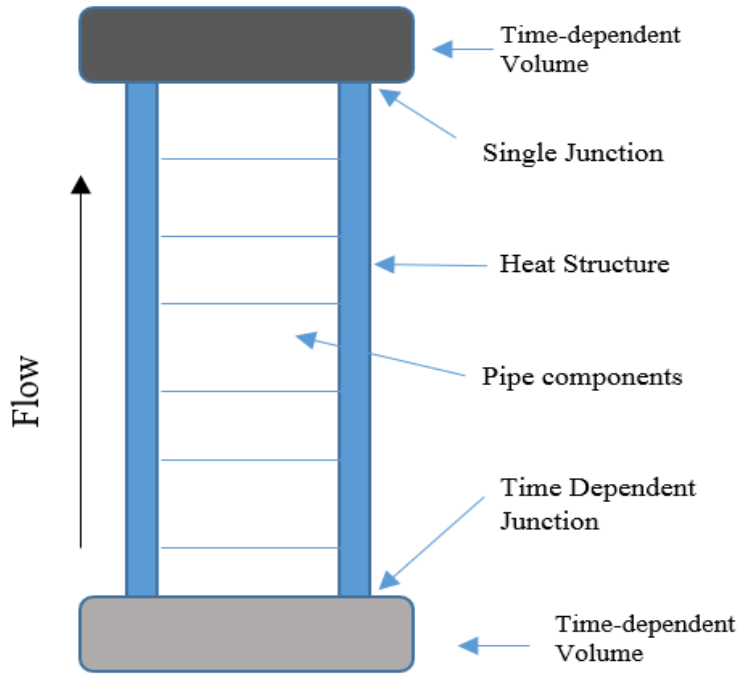

Figure 3-5: Nodalization diagram

3.5.1 Nodal sensitivity test

The influence of nodalization on the system stability has been investigated performing a sensitivity analysis on the RELAP model. The observations are made based on three different RELAP model having 10, 30 and 50 nodes respectively. Based on these observations, a stability map, Figure 3-6 has been plotted which shows the good agreement between models. Based on this study, the second model, which have 30 nodes, is selected for analysis in the present work.

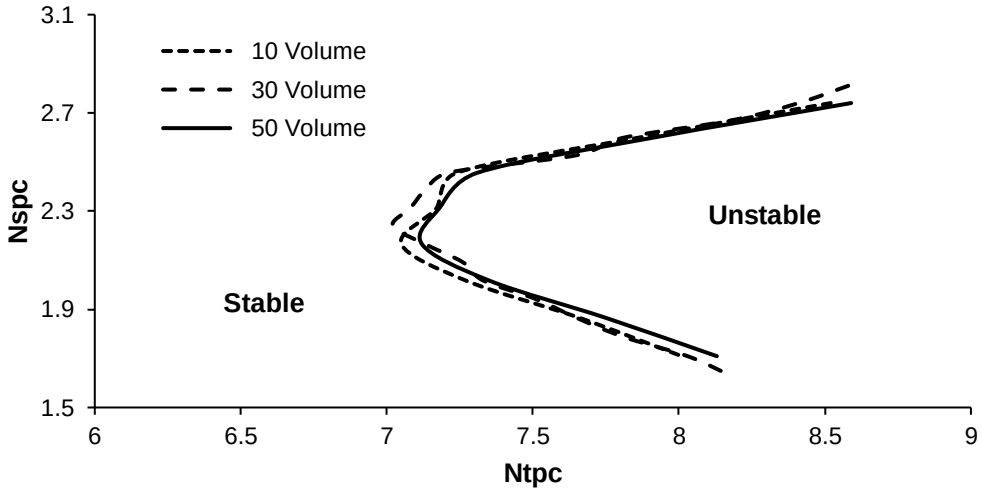

Figure 3-6: Nodal sensitivity for three different volumes

3.5.2 Comparison of LPM and RELAP5

Comparison of numerical results in terms of stability map is preliminary done with the RELAP5. This will give the initial idea about the dynamics of system. Also, RELAP is used by several researchers (Ambrosini and Sharabi, 2008; Colombo et al., 2012) for the validation of their code, hence it is useful as a first-hand toll for the beginning. The comparison with RELAP shows good consistency of the LPM model. Therefore, all the simulations are completed using LPM. RELAP5 transient simulations are carried out with various operating conditions, such as at 25 MPa pressure for finding the threshold of the stability. Here the single channel is modelled as a pipe component, with 30 volumes, connected with junctions at the two ends. These junctions are further connected with time dependent volume components to simulate the plena. The heat supply to the active core is simulated through heat structures, which is divided into the same number of volumes, as the active core. Corresponding nodalization diagram is shown in Figure 3-5.

Maintaining identical magnitudes of the initial and boundary conditions, simulations are performed with various sets of operating. Stability maps obtained with all the three tools employed here, namely linear stability analysis, transient simulation with LPM and RELAP5, are compared in Figure

3.7. All of them exhibit qualitatively similar profiles, as a progressive increase in heating power under a constant pressure drop across the channel eventually leads to instability. However, the LPM is found to yield a conservative estimate, with stability threshold corresponding to lower power values for any given inlet conditions. Prediction from the linear stability analysis matches exactly with transient simulations and that is only logical, as they employ the same set of mathematical equations. The disparity with RELAP5 can be ascribed to the lumped nature of fluid properties over both the zones. RELAP5 discretizes the channel in larger number of nodes, 30 in present model, compared to just two in LPM and hence in a better position to handle the rapid variation in properties around the pseudocritical point, although at the expense of significantly more computational resource obligation and substantial expertise requirement in handling the code.

The stability of the system is inferred from the nature of time evolutions of different variables like geometrical parameter, operating parameter and mass flow rate. The non-dimensional stability maps generated using LPM and RELAP5 are shown in Figure 3-7. It can be easily observed that the qualitative behaviour of both the maps is similar. The Stable region of the LPM is a subset of the stable region of RELAP5. Thus, despite many simplifying assumptions, the lumped parameter model is conservative

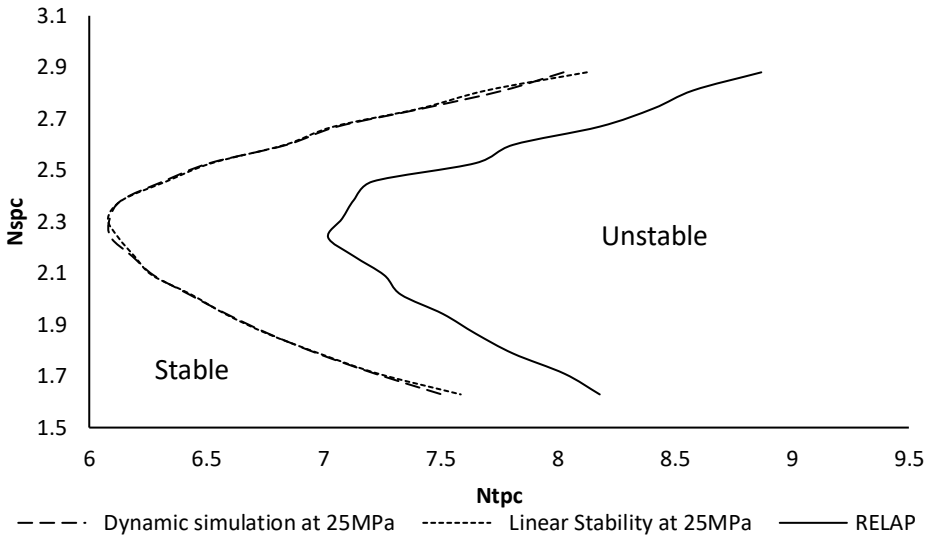

Figure 3-7: Comparisons of LPM with RELAP

3.6 Validation of LPM with the experimental result

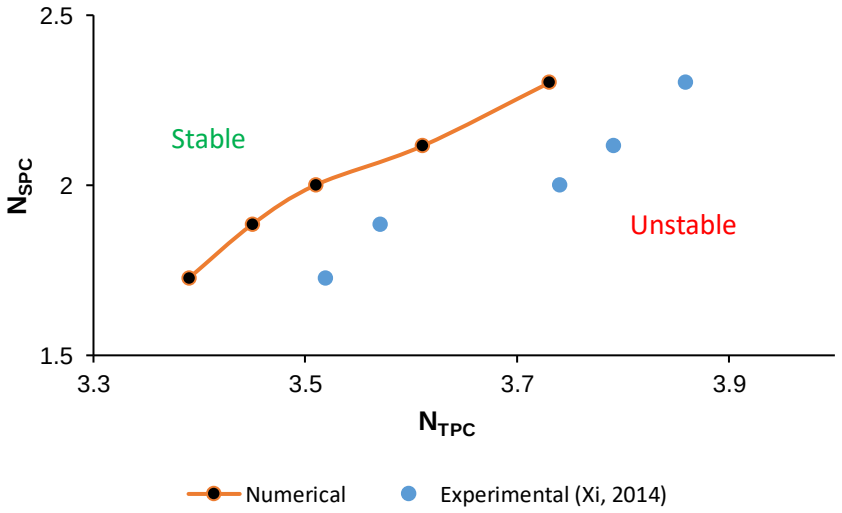

Figure 3-8: Validation of LPM with experimental data (Xi et al. (2014))

Limited number of papers available, which provide the experimental results based on the single channel, forced flow instability of SCWR. There are good numbers of paper available which uses RELAP5 for the validation purpose of their numerical works (Colombo et al., 2012; Kozmenkov et al., 2012; Mousavian et al., 2004; Papini et al., 2012).

Zhao et al. (2005) has used experimental (Khabensky and Gerliga, 1995) data for the validation of his single channel three zone supercritical LPM model. Due to the limited information available such as, no information regarding the inlet and outlet restrictions and many more important details of the experiment (Yu, 1965), and as this was the only set of relevant data they could find on the stability boundary at supercritical pressure, they were bound to use the same. Therfore, the predicted stability boundary agreed with the experimental stability boundary within ±30%.

In the flow instability experiment between two parallel channels with supercritical water, which was carried out by Xiong et al. (2012), according to his paper, due to the inadequacy of test section in the experiment, not so many results were obtained. The tube which were used for the experiment, INCONEL 625 pipes with inner diameter of 6 mm and outer diameter of 11 mm (Xiong et al., 2012), in which wall thickness of two tubes is just 2.5 mm, with which not sufficient experiment results could be obtained due to the limitation of pipe strength under high outlet temperature and pressure.

According to Xi et al., (2014a) the codes, which were used for comparing with the experiment, could not predict the oscillation period well, there was a considerable difference between numerical simulation and experiment.

Keeping these points into consideration the experimental validation has been done using Xi et al., (2014a) instead of Xiong et al. (2012) and others. Again, due to the scarcity of relevant articles on experimental study, few of the recent numerical works have also been compared and validated there numerical works (Li et al., 2018; Shitsi et al., 2018; Zhang et al., 2015) using the previous paper.

Figure 3-8 shows the comparison between the numerical and experimental data on the nondimensional plan; stability map having two axes as N_{TPC} and N_{SPC}. The stability map shows the similar trend, indicate that the numerical code is capable of predicting stability boundaries, as the relative errors are within ±7% range, which is the convincing range for validation.

Table 3-3: Comparison of experimental and predicted stability boundary

Pressure (MPa)	Inlet Enthalpy (kJ/kg)	Power/mass flow rate (kW/(kg/s))	Experimental N_{TPC}	Numerical N_{TPC}	Relative Error $\left\|\frac{N_{TPC,ex}-N_{TPC,nu}}{N_{TPC,ex}}\right\|$
23	795.63	2270	3.86	3.73	3.36 %
23	905.07	2230	3.79	3.61	4.74 %
23	972.02	2200	3.74	3.51	6.15 %
23	1040.2	2100	3.58	3.45	3.63 %
23	1133.4	2070	3.52	3.39	3.70 %

It is seen from the

Table 3-3, that most of the data points are within ±7% relative error range. The comparisons of numerical and experimental N_{TPC} shown in Figure 3-9 along with a linear trend line fit.

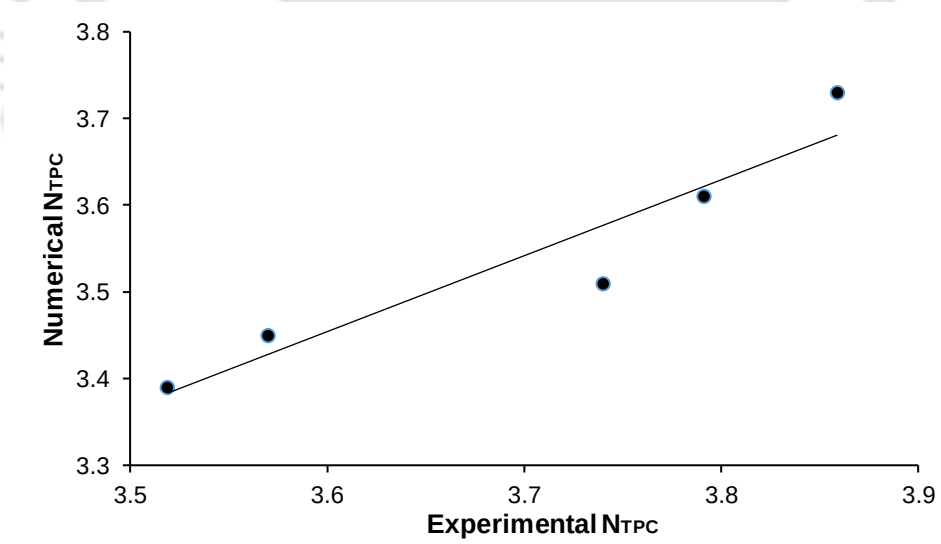

Figure 3-9: Comparison of experimental and numerical N_{TPC}

This section mainly added to the comparison of numerical results with the experiment (Xi et al., 2014b). The extractions of experimental data are based on the paper. Various system parameters including the system pressure, inlet temperature and total flow rate are tried to be set the same with the

experiments, to get MSB points obtained as the experiments shows. Then after changing the system power, further stability analysis has been performed. To illustrate the comparison in one two-dimensional plane, the system parameters are interpreted into dimensionless numbers N_{SPC} and N_{TPC}.

The results show a close match with Xi et al. (2014b) that of and the qualitative behaviour is also similar. It is observed that the plot shows small discrepancies between the numerical and the experimental result. The inconsistencies are due to the approximation in the equation of states and a few other assumptions which have been essential for a simpler model, also the primary objective of the current work. These discrepancies can be minimized by the use of better approximations. The reason behind assuming approximation is that in the present work, the emphasis is given on the qualitative behaviour of the fixed points. It can be noted that the more accurate model may be available and provide quite a good match with the experimental data would be possible, but that can be computationally expensive. The choice of the model used in the current work is based on its simplicity and reasonably accurate solutions. The simplicity of the model allows one to use this reduced order model (ROM) for more complicated, non-linear stability analysis.

The powers corresponding to MSB in calculations are all lower than those in experiments. This might be a good indication as the model once again proves itself as more conservative. The same thing happens during the comparison of the present model with RELAP (section 3.5.2). In case of RELAP and the current model, the trends are matching but with experimental validation of the model, the usual trend is missing. The reason is that RELAP is a transient code, which uses certain assumptions to solve the given sets of governing equations, but the actual experimental data could match within the specific ranges. Moreover, the tread may or may not be matches due to sever assumptions in the model.

Moreover, the less power corresponding to MSB as compared to the experimental result might be due to the several assumptions and equations

of state in the model. There are various other fundamental differences between the two; hence the comparisons will not be the same. Few significant differences are, in the experimental work shows only thermohydraulic results while the addition of neutronics makes system unpredictable, so from thermal hydraulics, the prediction of system stability is not fair. Another difference is that an experiment performed using the parallel channel, which shows some different dynamics as compared to the current single channel system.

As mention earlier in this section, due to several limitations and a very few numbers of articles available on experimental results, the need for more depth study is very much required for the validation of numerical results.

Overall, the purpose of the proposed model is to give the preliminary qualitative idea of the system behaviour by the simplified model, not the quantitively. For the latter part, the more rigorous study needs to be performed by other researchers.

3.7 Stability analysis

The term stability is generally associated with the temporal response of a dynamical system following an internal or external disturbance during its operation. There are in fact many different definitions of stability, among which the following are the most frequently encountered: stability according to Poisson, stability according to Lyapunov, and asymptotic stability. Depending on the temporal dynamics of the perturbation, the distinction of stability is done according to Lyapunov and asymptotic stability. Lyapunov stability is, if all trajectory that starts sufficiently close to fixed point remains close to it for all time. It is a very mild requirement on equilibrium points. In particular, it does not require that trajectories starting close to the origin tend to the origin asymptotically. Also, stability is defined at a time instant t_0 (Anishchenko et al., 2014).

3.7.1 Linear stability analysis

Linear stability analysis is typically the first step in the analysis of a nonlinear system and is widely used to determine the onset of instabilities

and system dynamic behaviour under small perturbations around a steady state (Appendix-A). This involves linearizing the nonlinear system around the steady state or equilibrium solution of interest and studying the characteristic roots of the linearized system.

SCWR being a complex nonlinear system, a rigorous stability analysis is possible only with some simplifying assumptions. That makes the use of a linearized model in time domain a necessity, particularly when identification of the stability boundary is of principal interest. Linear stability analysis is typically performed by linearizing the nonlinear equations around an equilibrium solution of interest and studying the characteristic roots of the linearized system. Dropping the nonlinear terms, a single vector equation of the following form can be obtained as,

Here $\mathbf{X} = \begin{bmatrix} z_{pc}^* & h_o^* & T_f^* & P^* & C^* \end{bmatrix}^T$ represents small perturbation around the steady state$\mathbf{X_0}$. The nature of the eigenvalues of the matrix $[A]$ determine the stability of the solution, as the presence of even a single root on the right-half plane of the state-space plot indicates an unstable system. In addition to this, the lumped parameter model (system of nonlinear ordinary differential equations) is linearized about its steady-state point and the eigenvalues of the matrix [A] are evaluated. The components of $[A]$ can be obtained from the lumped parameter equations, leading to stability characterization for any given set of boundary conditions (Appendix-A).

For performing the stability analysis, the governing equations resulting from the lumped parameter model are linearized about the steady state. The $[A]$ resulting from the linearized model is formed and the eigenvalues of this are evaluated at steady state. If the real parts of all the eigenvalues are negative, then the system is stable at that operating point. If any of the eigenvalues has a positive real part, then the system is unstable at that point. The stability boundary thus formed is the locus of points in the parameter plane for which the least stable eigenvalue lies on the imaginary axis. It is known from the Hopf bifurcation theory that the system can have oscillations if the

eigenvalues have a complex crossing. It is possible for the system to have different dynamic behaviour. In one case, if a pair of complex conjugate eigenvalues crosses the imaginary axis, then the system can have periodic oscillations. Such oscillations are known as stable limit cycles and the bifurcation is known as supercritical Hopf bifurcation. In the other case, the system can have oscillations in the stable region that get decayed for low perturbations but are amplified for large perturbations. This indicates the presence of an unstable limit cycle and such a bifurcation is called a sub critical Hopf bifurcation. This is dangerous from practical point of view, since the system will have diverging oscillations even though it is designed to operate in a stable region. The dynamic behavior of the state variables is obtained by integrating the governing equations in time domain.

3.7.2 Non-linear stability analysis

Linear stability analysis, however, fails to predict certain characteristics of nonlinear systems, such as the magnitude and frequency of possible limit cycle oscillations when the system is away from the marginal stability boundary in the parameter space. That can be ascertained through the dynamical simulation of the exact nonlinear equations in the time domain by perturbing any of the variables around a fixed point and subsequently observing the nature of temporal variations. Dynamics of the perturbed system may depend on the amplitude of imposed perturbation and several classes of periodic solutions are possible, (Lahey, 1986) for a boiling channel, which may happen in SCWR.

The linearly stable region continues to remain stable for small perturbations around the equilibrium in the presence of nonlinearities. However, the magnitude of these allowable perturbations depends on the nature of the bifurcation. For the case of a supercritical Hopf bifurcation, the equilibrium is globally stable in the linear stability regime and hence the stability of the solution is insensitive to the magnitude of the perturbation. In contrast, there are unstable limit cycles around the linearly stable equilibrium for a subcritical Hopf bifurcation and therefore the equilibrium is stable only to

perturbations smaller in magnitude than the amplitude of the unstable limit cycles. Larger perturbations tend to grow to large magnitudes even in the linearly stable regime. Therefore, a nonlinear analysis of the problem is required to ascertain the nature of the Hopf bifurcation. In addition, this analysis helps us in obtaining the amplitude of the limit cycles emanating from the Hopf point. This information is especially useful when the nature of the bifurcation is subcritical as it gives a rough estimate of the magnitude of perturbations for which the linearly stable equilibrium is nonlinearly stable as well (Lahey, 1986; Pandey and Singh, 2016; Wahi and Kumawat, 2011).

Chapter 4 SCALING METHODOLOGY FOR STABILITY APPRAISAL

4.1 Introduction

Considering the extreme operating conditions associated with the SCWR and possible consequences of any unforeseen event, it is essential to investigate all possible aspects of such a system at the laboratory scale, prior to its commercialization. Accordingly, researchers have shown general interest towards both the heat transfer and stability behaviour of supercritical flow systems since the inception of the present millennium. While the current trend of research is inclined towards numerical and computational (Cheng and Schulenberg, 2001) analyses, the role of experiments can never be undermined, particularly in the context of understanding new phenomena and exploring newer physics. Unfortunately, the associated volume of experimental literature is rather limited. The review work of Cheng and Schulenberg (2001) emphasizes on the scarcity of reliable experimental data in the typical parameter ranges for SCWR, which consequently presents a huge hurdle in accurate description and prediction of SCWR thermal hydraulics. That highlights the need of developing experimental facilities and subsequently necessitates phenomenological scaling, as it is impracticable to replicate the SCWR condition at lab-scale. Therefore, several attempts towards scaling of supercritical flow systems are available in open literature.

Considering the similarities between the boiling channels of BWR and heated supercritical channels, scaling principles are developed following similar approaches. (Marcel et al., 2009) developed scaling procedure to use a mixture of R-125 and R-32. With a system pressure of 6.2 MPa, it showed excellent similarities with SCW at 25 MPa. This mixture, however, has severe restrictions in terms of flammability limit and chemical stability and requires accurate monitoring of the mixture composition. Furthermore, they applied the same scaling rule to both the radial and axial directions, leading to rather

small radial dimension of the experimental facility, and hence resulting in undesirably large frictional pressure drop. Rhode et al. (2011) proposed an improved scaling procedure mainly for natural circulation systems based on R-23 as the model fluid. System pressure, power and temperature levels were significantly reduced, while preserving the dynamics of the system. Practical issues, such as the onset of heat transfer deterioration, was also touched upon in their work. They, however, introduced two multiplication factors for scaling for the flow rate and friction factor respectively, which require experiment-based empirical relations, and hence are not universal.

As none of the above-mentioned model fluids properly justifies the stability analysis due the property and some physical constrains. Therefore, the primary objectives of the study are to identify a less restrictive model fluid as compared to the other model fluids, which can properly mimic the SCW under the relevant scaled condition of an SCWR, and to define the scaling rules in a generalized way, to preserve the phenomenological physics. Focus is kept on uncoupling the radial scaling from the axial one, as only then a practicable combination of system dimensions can be proposed. US reference design of SCWR is considered as the prototype. Accordingly, the scaled dimensions of the lab-scale facility and corresponding operational settings in terms of power, flow rate and inlet temperature are proposed. The advantages of the proposed methodology over the existing ones have also been stressed upon, along with a discussion on the role of involved dimensionless groups.

4.2 Fluid-to-fluid scaling methodology

4.2.1 Conservation equations

The most important requirement of the fluid-to-fluid scaling is to determine the correspondence between the test facilities based on the model fluid to the prototypical parameter range. The general objective invariably is to develop a laboratory-scale test facility, which should behave identically to the prototype in terms of the phenomenon under consideration, and thereby easy extrapolation of the observations to the prototype-scale. Hence both the

model and prototype must be bound by the same set of conservation equations and maintain identical values of the characterizing dimensionless groups. Focus of the present study being the scaling of SCWR core to foretell the stability behaviour, a single heated channel of constant flow area is selected, with upward flow and uniform heat flux distribution (Figure 3-1). Corresponding 1-D equations for conservation of mass, momentum and energy, which is given in equations (3.1-3.3). Applying the above definitions, which gives the modified conservation equations (3.5-3.7). It is interesting to note that the absolute pressure can be freely chosen, since it is not a part of the balance equations, and hence system pressure is not expected to have any role on the scaling. A constant pressure drop boundary condition is employed for simulations with Δp = 0.15 MPa.

4.2.2 Scaling principles

As stated above, the scaling objective can be achieved by equating the characterizing dimensionless groups between the model and prototype. Other geometric and operating parameters need to be estimated based on the selection of the scaling fluid. Accordingly, the following factors are considered to proceed with the scaling.

(a) Nature of non-dimensional property variation of the prototype and model fluids needs to be identical over the entire range of operating parameters.

(b) From the conservation equations and associated boundary conditions, several dimensionless groups can be identified including N_{TPC}, N_{SPC}, N_{Fr} and N_{Eu}, which dominate the thermalhydraulic behavior and hence is expected to govern the stability. Their equality needs to be considered.

(c) There is a total of six parameters required to be scaled. Four of them can be adjusted independently during the design stage or experimental runs, namely, the tube diameter, length of heated channel, inlet temperature and heat flux. Inlet mass flux and pressure drop across the channel are coupled to each other and one of them can be derived from the imposed boundary

condition. As the present system is subjected to a constant pressure drop boundary condition, mass flux is a dependent variable here.

(d) Considering the drastic variation of all thermophysical properties of the supercritical fluid around the pseudocritical point, the same is selected as the reference point.

4.3 Selection of fluids

Considering the extreme operating conditions associated with SCWR, the focus of scaling fluid selection is on reducing the power, pressure and temperature levels of operation. As water experiences drastic variation in all thermophysical properties around the pseudocritical point, substantial change in density can be observed across the SCWR core, as SCW is heated from 280 to 530 °C. Since the scaling fluid must behave similarly over the entire operational range, selection of model fluid and its operating pressure is not straight-forward. To be more precise, the equation-of-state for the model fluid at the selected pressure level must resemble the same for the prototype fluid on the non-dimensional plane. An extensive comparative analysis is carried out as a part of the present study using REFPROP v9.1 as the database for thermophysical properties. As is shown in Figure 4-1, R134a at a pressure level of 6.2 MPa and CO_2 at 8 MPa can simulate water at 25 MPa with reasonable accuracy.

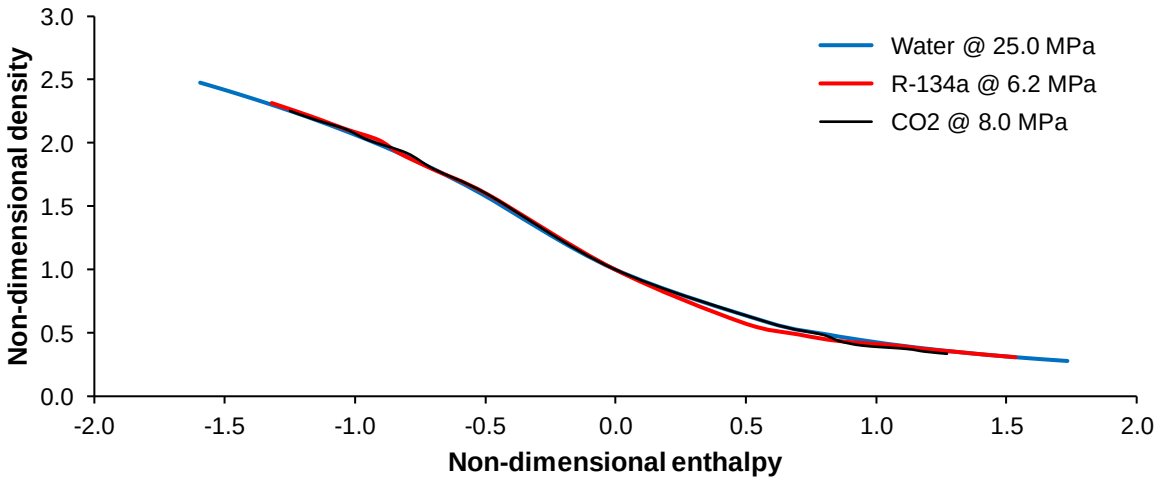

Figure 4-1: Non-dimensional property variation for three fluids at equivalent pressure levels

4.3.1 Scaling rules

While the operating pressure level for the model fluid can be selected by comparing the equation-of-state on $\rho^* - h^*$ plane, scaling rules need to be devised to identify other geometric and operating variables. That can be achieved by equating the dimensionless groups identified earlier.

4.3.2 Pressure

The role of pressure on system characterization is only through the similarity of the prototypical and model fluids on the $\rho^* - h^*$ plane and hence choice of a scale for pressure is quite independent. Accordingly, the scaling rule for pressure is defined as,

$$X_p = \frac{p_m}{p_p} \tag{4.1}$$

4.3.3 Length of the channel

The selected geometry being vertical, the length of the channel is related to the gravitational forces acting on the system and hence the same has been scaled by equating the Froude number between the model and prototype.

$$N_{Fr,m} = \left.\frac{G_c^2}{\rho_{pc} g L_c}\right|_m = \left.\frac{G_c^2}{\rho_{pc} g L_c}\right|_p = N_{Fr,p} \quad \Rightarrow X_L = \frac{L_{c,m}}{L_{c,p}} = \left[\frac{X_G}{X_\rho}\right]^2 \tag{4.2}$$

Here the density ratio corresponding to the pseudocritical value is defined as, $X_\rho = \rho_{pc,m}/\rho_{pc,p}$.

4.3.4 Mass flux

The objective of mass flux scaling is to ensure similar nature of heat transfer behaviour during normal heat transfer process. Present system being subjected to pressure drop boundary condition and mass flow rate being directly affected by the same, mass flux is scaled here using the non-dimensional pressure drop across the channel. It must be the same between model and prototype and hence,

$$p_m^* = \left.\frac{\Delta p\ \rho_{pc}}{G_c^2}\right|_m = \left.\frac{\Delta p\ \rho_{pc}}{G_c^2}\right|_p = p_p^* \ \Rightarrow\ X_G = \frac{G_{c,m}}{G_{c,p}} = \left[X_p\ X_\rho\right]^{0.5} \qquad 4.3$$

4.3.5 Hydraulic diameter

In an effort to differentiate axial and radial scaling, hydraulic diameter is scaled using the Euler number, as it is responsible for the scaling of dynamic behaviour of the flow system. Considering identical Euler number and friction factor between the model and prototype,

$$N_{Eu,m} = \left.\frac{f L_c}{D_h}\right|_m = \left.\frac{f L_c}{D_h}\right|_p = N_{Eu,p} \Rightarrow X_D = \frac{D_{h,m}}{D_{h,p}} = X_L \qquad 4.4$$

4.3.6 Power and inlet temperature

Channel power is scaled in terms of N_{TPC} as,

$$N_{TPC,m} = \left.\frac{q_0'' \pi_h L_c \beta_{pc}}{A G_c C_{p.pc}}\right|_m = \left.\frac{q_0'' \pi_h L_c \beta_{pc}}{A G_c C_{p.pc}}\right|_p = N_{TPC,p} \Rightarrow X_Q = \frac{X_G X_A}{X_D X_L}\frac{\beta_{pc,p} C_{p.pc,m}}{\beta_{pc,m} C_{p.pc,p}} \qquad 4.5$$

Similarly N_{SPC} can be equated to scale the inlet temperature as,

$$N_{SPC,m} = \left.\frac{\beta_{pc}(h_{pc} - h_i)}{C_{p.pc}}\right|_m = \left.\frac{\beta_{pc}(h_{pc} - h_i)}{C_{p.pc}}\right|_p = N_{SPC,p} \Rightarrow X_h$$
$$= \frac{(h_{pc} - h_i)|_m}{(h_{pc} - h_i)|_p} = \frac{X_{C_{p,pc}}}{X_{\beta_{pc}}} \qquad 4.6$$

The above similarity can be used to predict the h_{in} for the model fluid, which can further be combined with model pressure to get T_{in}.

Fuel rod dynamics is considered in the present model to study its effect on the stability of the system. The energy balance for the fuel rod, characterized by a constant steady-state power (P_{ss}), can be presented in equation (3.8). With the incorporation of the lumped fuel rod model, the energy equation for the j^{th} coolant node (Eq. (3.3)) needs to be modified as equation (3.9), where A refers to the cross-sectional area of the channel and n_f is the number of fuel rods involved. Using the non-dimensional definitions proposed in Eq. (3.4), dimensionless forms of the above two equations (3.10-3.11)

Point neutron kinetics with a single group of delayed neutrons is also incorporated in the developed model to embrace the effect of power dynamics. Transient variation in power and precursor density can be presented as equation (3.12-3.13), setting the steady-state reactivity to zero and neglecting the time-dependence, the feedback reactivity can be correlated to the fuel rod temperature and coolant enthalpy as equation (3.14). The variables related to power dynamics can be non-dimensionalized using the concerned steady-state values as equation (3.15), Consequently the dimensionless versions of equation (3.16-3.17) can be presented as, magnitudes of the neutronics constants are taken from BWR designs, since all light water reactors are typically characterized by similar numbers.

4.4 Results and discussion

Linear stability analysis is used as the tool for appraisal of stability threshold, which can typically be viewed as the first step in analysing a nonlinear system and is widely used to determine the onset of instabilities and system dynamic behaviour under small perturbations around a steady-state. This involves linearizing the nonlinear system around the steady-state or equilibrium solution of interest and studying the characteristic roots of the linearized systemA detailed methodology of stability analysis is discussed in Nayfeh and Balachandran (1992). Here the eigenvalues of the Jacobian matrix are calculated for a given set of parameters (N_{TPC} and N_{SPC}) using the in-house code and accordingly the stability map is developed to indicate the stability threshold, primarily for a vertical channel. The detail of this study has been given in Section 3.6.1.

Transient simulations are performed by progressively increasing the heating power, for a constant pressure drop across the channel, until the identification of instability. Such technique was found suitable for comparing the stability thresholds for boiling channels and heated channels with supercritical fluids (Ambrosini and Ferreri, 2006; Ambrosini et al., 2008).

4.4.1 Comparison with existing scaling method

The basic comparisons of the scaling criteria here is done by the Rhode et al. (2011), as this was the recent at the time of starting the work.

1. The scaling rule for the enthalpy and the density, which is a function of enthalpy can be derived from the preservation of the dimensionless equation of state by Rohde et al. (2011). In current approach more, practical way has been used which is equating N_{SPC} of both prototype and model.
2. The scaling rule for the hydraulic diameter is derived from the friction term. Applying the aforementioned rule, however, can lead to very small diameters inducing a too large frictional pressure drop. The latter becomes important when the available driving head (natural circulation) is limited (Rohde et al., 2011). In the current scaling rule more, practical Neu is used which have no such boundations and can be used for forced and natural circulating system.
3. The most fundamental way of scaling the flow area is to use the hydraulic diameter scaling criteria, as this comes directly from the conservation equations which preserves all the physical properties of the model, the same rule is applied in the current work. However, in the work of Rohde et al. (2011) some empirical based values have been taken, which seems intricate for general audience.

Table 4-1: Comparisons of present scaling method with Rhode et al. (2011)

Similarity Variables	HPLWR (R23) Rhode et al. (2011)	HPLWR R-134a (Present scaling method)	SCWR (R-134a) (Present scaling method)
Mass flux, X_G	0.74	0.41	0.55
Pressure, X_P	-	0.24	0.18
Density, $X\rho$	~1.70	1.41	1.72
Time, X_t	~0.44	0.58	0.43

Length, X_L	~0.20	0.10	0.14
Diameter, X_D	1.06	1.36	1.50
Area, X_A	~0.80	0.46	-
Power, X_Q	~0.08	0.14	0.10

Table 4-1 shows the comparison of two scaling methods. The first column shows the data of the similarity variables through the method proposed by Rhode et al. (2011). Next two column shows the values of the similarity variables data by the present method. Instead of R23, if R-134a is used then it could reduce the settling time, hydraulic diameter and power of the downscaled facilities significantly. On the other hand, at the approximately same power limit SCWR downscale using R-134a model fluid setup uses less mass flux and core length, which is ultimately more economical.

4.4.2 Comparison of different model fluids

Considering water at 25 MPa as the prototype fluid, scaling parameters are estimated for four possible model fluids and the same are listed in Table 4-2. As can clearly be seen, the pressure requirement for R134a is noticeably lesser than CO_2 and ammonia. The same is true for mass flux and power as well. Significant reduction in length scale can also be observed, albeit at the cost of increasing diameter. Overall it can be said that R134a is expected to lead to a more compact system with lesser pressure and power requirement.

Table 4-2: Scaling parameters for different model fluids with water at 25 MPa

Scaling Parameter	R134a at 6 MPa	CO_2 at 8 MPa	Ammonia at 15 MPa	R23 at 5.7 MPa
X_G	0.55	0.68	0.67	0.62
X_p	0.25	0.32	0.60	0.23
X_ρ	1.72	1.46	0.76	1.68
X_L	0.14	0.22	0.77	0.14
X_D	1.50	1.20	1.08	1.33
X_Q	0.10	0.13	0.53	0.13

R134a is a non-flammable refrigerant with insignificant ozone depletion potential. Ammonia is toxic in nature and also requires about 5.3-time larger power compared to R134a, along with substantially large pressure level and length scale. While pressure requirement for CO_2 is not severe, about 57% increase in system dimensions and 30% rise in power level can be noted. R23, of course, predicts values similar to R134a. It has already been tested as the model fluid in a scaled-down HPLWR, named DeLight, where large density variation across the code was observed, leading to instabilities. Accordingly, R134a can be suggested as the most suitable model fluid to simulate supercritical water among the four compared in the present study.

4.4.3 Generalized stability map

The general stability maps obtained through linear stability analysis for water, as well as for two different model fluids, namely, R134a and CO_2, are shown in Figure 4-2. All the curves nearly overlap with each other. As mentioned earlier, absolute pressure is, absent in the dimensionless version of the conservation equations and hence is not expected to play any role in determining the stability threshold. The same is apparent here for all the fluids considered from Figure 4-3. All the stability curves plotted here can be

correlated by the same mathematical relation. Integration of the stability threshold for three different fluids in a single relationship establishes the successful choice of the scaling rules adopted in the present analysis.

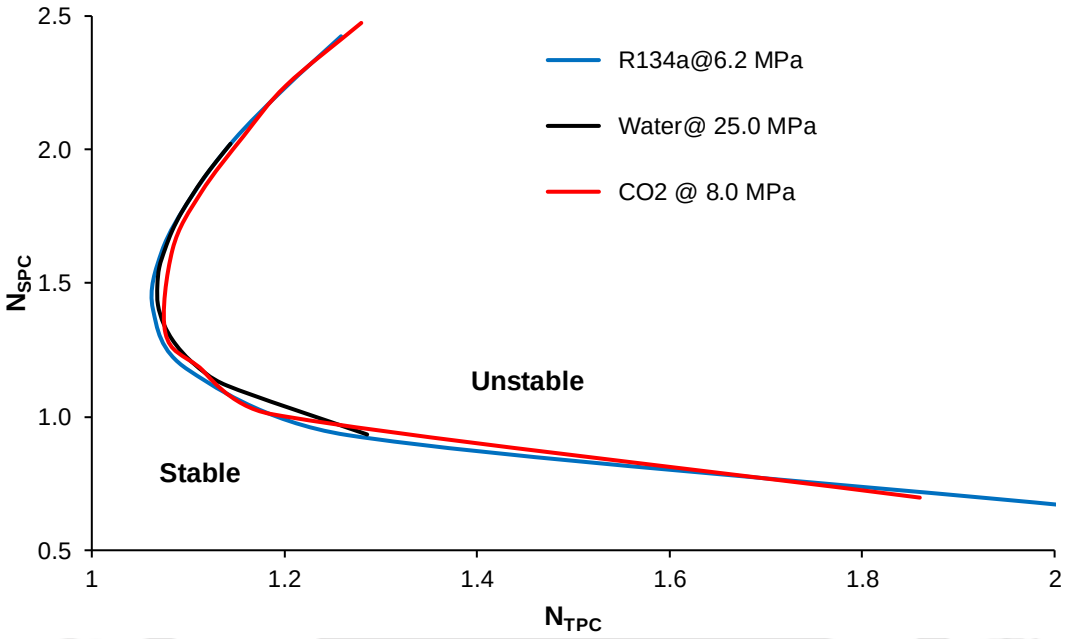

Figure 4-2: Stability map for three fluids following linear stability analysis

(a)

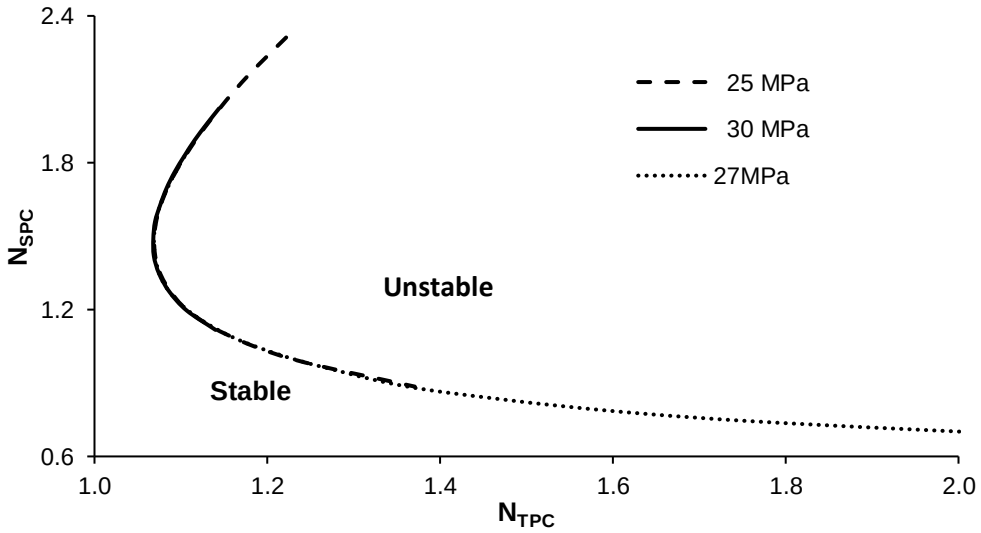

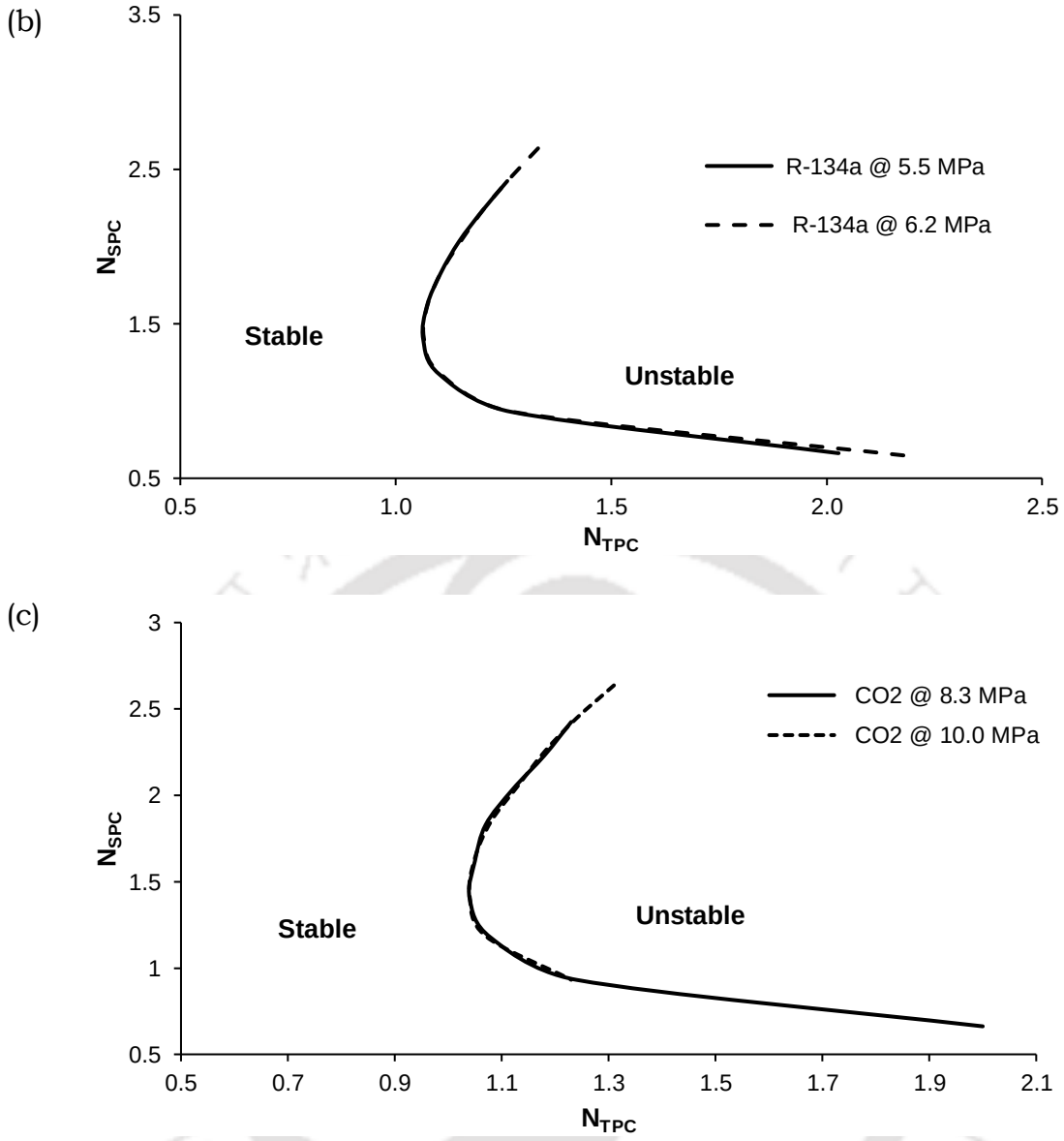

Figure 4-3: Effect of system pressure on the stability map for (a) water, (b) R134a and (c) CO_2

4.4.4 Transient analysis of R-134a

It is a tedious job to identify the stability threshold following transient analysis, as the nature of stability can be comprehended only after performing the simulation over a reasonable period and scrutinising the temporal variation thereof. Linear stability analysis, on the contrary, provides a direct measure of the neutrally stable point and hence can be employed as the guide for identifying simulation points for the transient analysis. Accordingly, transient analyses are performed with a few selected set of operating conditions, as is shown by two sample state points in Figure 4-4 for R134a.

Here the stability map is prepared following linear stability analysis. As described earlier, a small perturbation is imposed on inlet mass flow rate under steady-state, maintaining other parameters the same, and resultant variation in the state variables are followed. Oscillations subside quite early at point 'a' and the profiles continue with near-constant value (Figure 4-5). However, oscillations with growing amplitude can be observed at point 'b' (Figure 4-6). The portrait on the state-space plane exhibits a series of growing spirals, thereby diverging away from a stable fixed point.

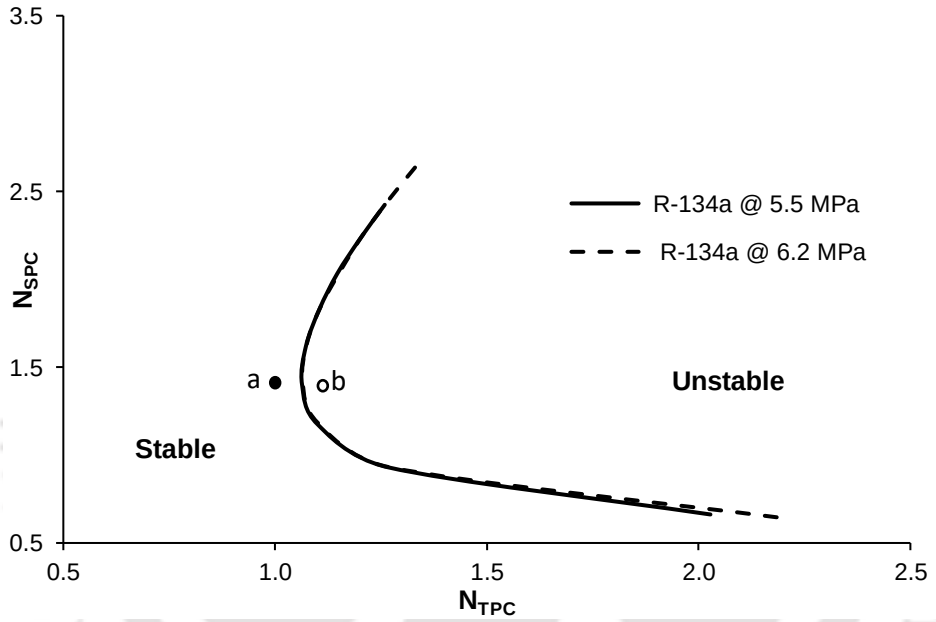

Figure 4-4: Linear stability map of R-134a corresponding to 25 and 30 MPa of water

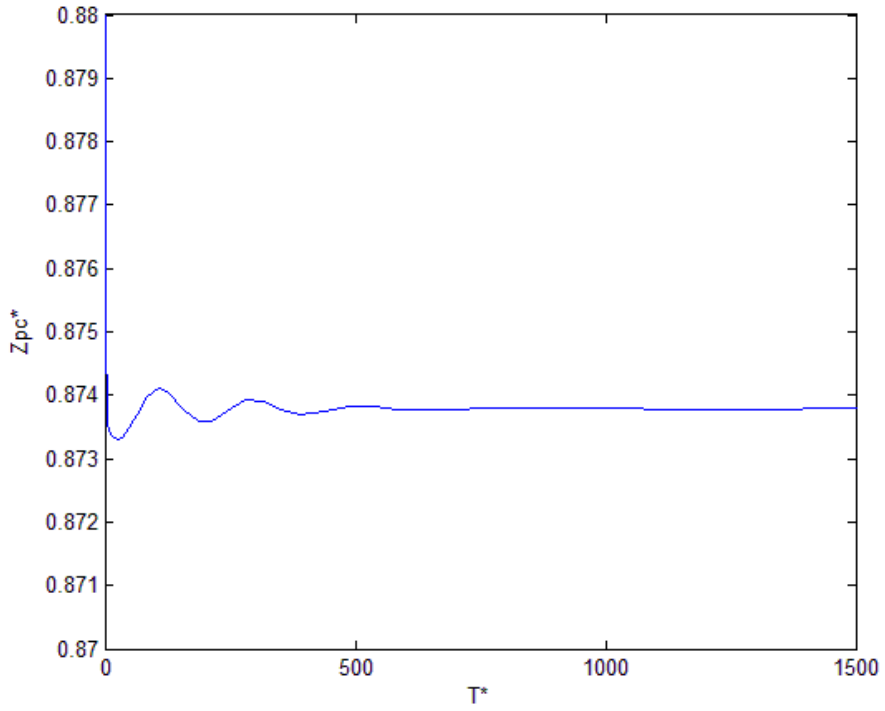

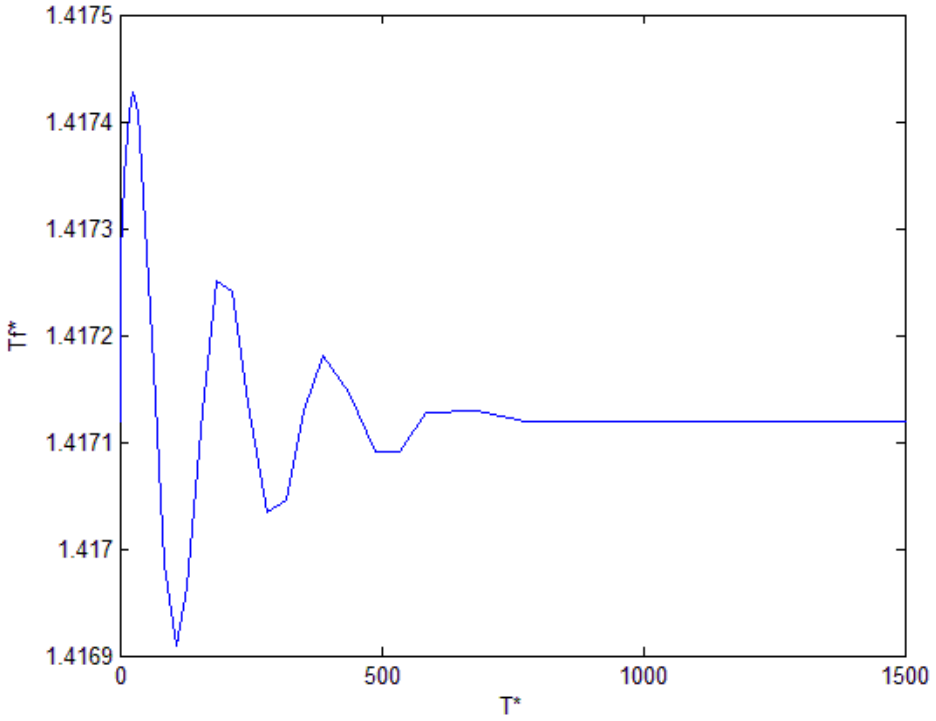

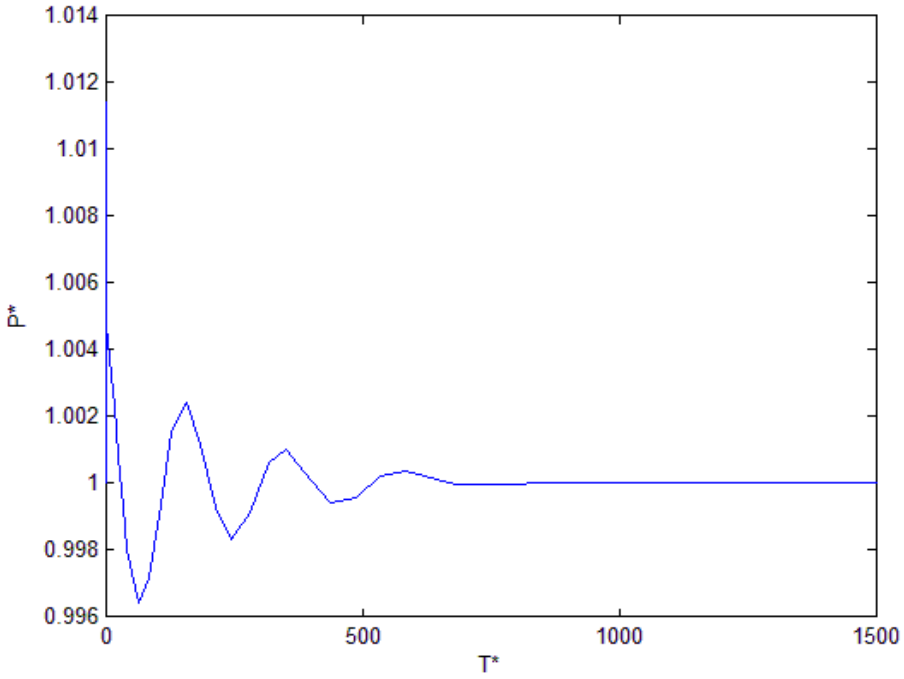

Figure 4-5: Stable response of SCWR corresponding to point 'a' in the stability map at 6.2 MPa system pressure, 800 kg/s mass flow rate and 241.8 MW input power

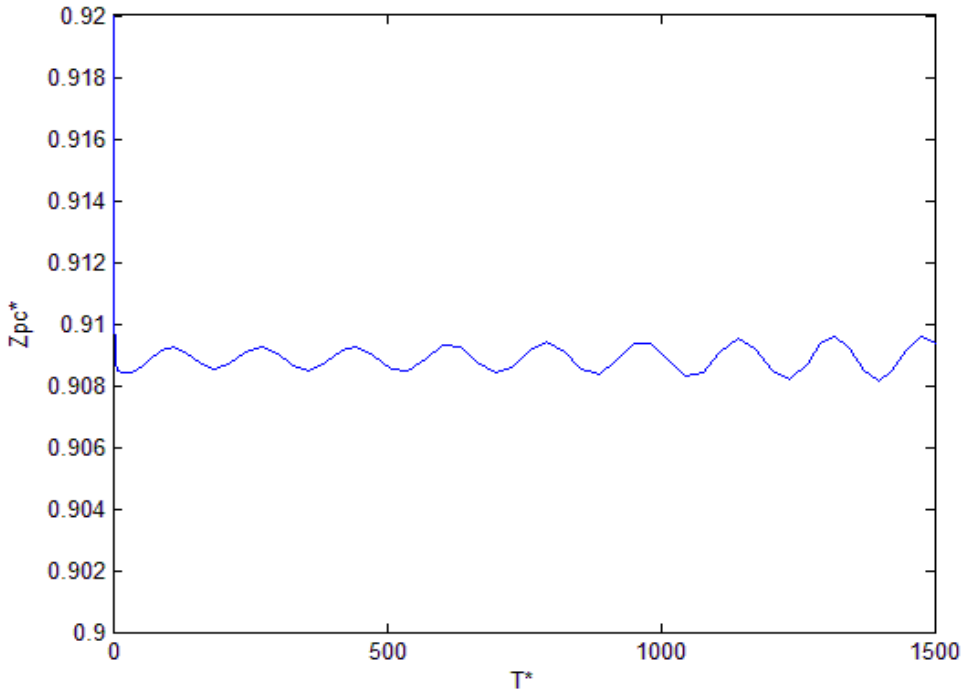

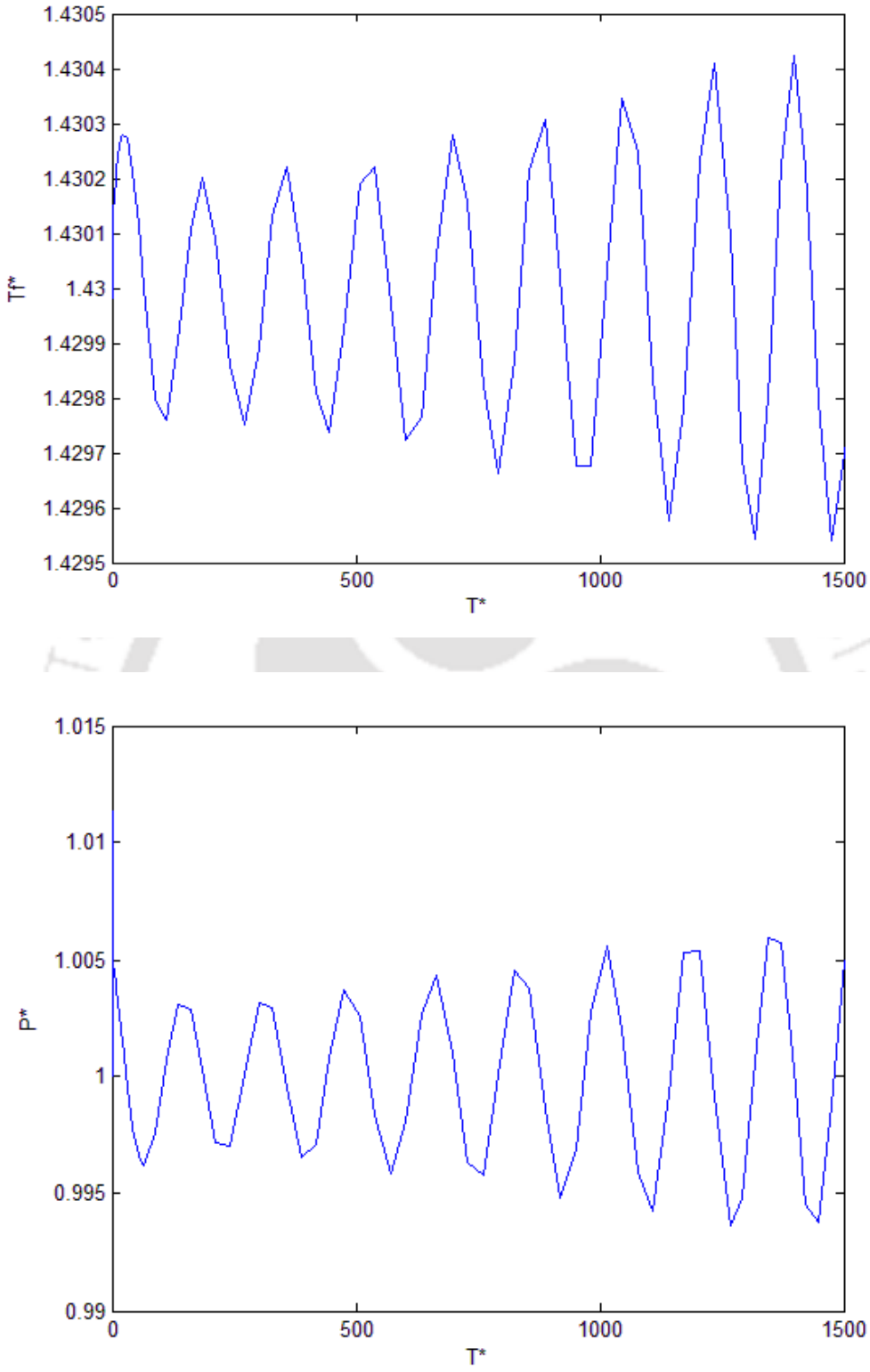

Figure 4-6: Unstable response of SCWR corresponding to point 'b' in the stability map at 6.2 MPa system pressure, 800 kg/s mass flow rate and 242 MW input power

4.5 Conclusions

The purpose of this study is to identify a model fluid, suitable for downscaling of the supercritical water system through a new scaling approach proposed exclusively for SCWRs. Starting from the basic conservation and balance equations, dimensionless forms for the thermal hydraulic, fuel dynamics and neutronics equations are developed. The following are the few important conclusions.

1. R134a is found to be the most suitable scaling fluid from temperature, pressure and power point of view. It also leads to more compact design and poses convenient chemical properties.
2. Four different fluids are compared by equating the important dimensionless groups, identified from the equations.
3. Stability behaviour of the prototype with water and model with R134a is compared using linear stability analysis. Stability map have been plotted to distinguish between stable and unstable zone for other model fluids.
4. R134a is a non-flammable refrigerant with insignificant ozone depletion potential. Ammonia is toxic in nature and also requires about 5.3-time larger power compared to R134a, along with substantially large pressure level and length scale.
5. Pressure requirement for CO_2 is not severe, about 57% increase in system dimensions and 30% rise in power level can be noted.
6. R23, of course, predicts values similar to R134a. It has already been tested as the model fluid in a scaled-down HPLWR, named DeLight, where large density variation across the code was observed, leading to instabilities. Hence, R134a finds its place for the same.
7. System pressure is found to have insignificant role from stability point of view. As absolute pressure is absent in the dimensionless version of the conservation equations and hence is not expected to play any role in determining the stability threshold.

8. For first-hand experience, RELAP5 is employed for comparison of the developed model and the present lumped approach, which is observed to produce conservative estimate of the stability threshold.

Chapter 5 PARAMETRIC EFFECTS ON STABILITY CHARACTERISTICS

5.1 Introduction

A supercritical fluid experiences drastic changes in thermodynamic and transport properties around the pseudocritical point. Accordingly the SCWR can exhibit large variation in density across the core, making it susceptible to density wave instability, quite similar to BWRs (Blázquez et al. 2013; Gajev et al. 2013; Peng et al., 1986), necessitating emphasis on passive safety design. Consequently, number of researchers have studied the stability response of supercritical flow systems in the recent past following diverse approaches, with more inclination towards the natural circulation loops.

It is evident from a scrupulous survey of relevant literature (Section 2.1) that, while the natural circulation-based systems have received reasonable attention, supercritical channels with forced flow generally experience a considerable amount of density variation across the core and hence are more susceptible towards thermohydraulic instabilities. However, there are limited number of studies on stability response of forced supercritical flow channels, particularly with two-phase-like property variation over a short distance around the pseudocritical point (Marcel et al. 2009; Sharabi et al. 2008; Sharma et al. 2010). Adoption of both linear and nonlinear approaches can be identified within the limited database available, with each having its pros and cons. While the linear stability analysis is quick and easy to compute, it can also predict the location of marginal stability based on the eigenvalues but fails to ascertain the nature of instability. The same can be obtained by transient simulation of conservation equations, but at the expense of substantial computational resource requirement. Both the methods can rather be viewed to complement each other for methodical stability appraisal. Present work, therefore, focuses on understanding the thermohydraulic and coupled neutronic-thermalhydraulic stability behaviour of a forced flow

heated channel carrying supercritical water and envisages the effect of associated system parameters on stability boundaries employing both linear stability analysis and dynamic simulation of the governing equations. While dealing with the complete set of conservation equations can be cumbersome, adoption of a reduced-order model by decoupling the momentum and energy equations can often provide a swift and reliable estimate. Such models are computationally less expensive compared to finite-difference-kind of approaches and hence are often preferred to obtain a first estimate. Accordingly, a lumped parameter based approach is followed, visualizing the channel to consist of two distinct zones, separated by the pseudocritical point. Integrating the conservation equations over each zone, a system of algebraic and ordinary differential equations (ODEs) is developed, which is subsequently employed for studying the parametric effects through both linear and transient analysis.

5.2 Mathematical modelling

A circular forced flow channel of uniform diameter is simulated in the present study, under uniform heat flux boundary condition imposed on the wall. The channel is subjected to constant pressure drop boundary condition (Section 3.4.1) under both steady and transient conditions (Figure 3-1). Accordingly, the one-dimensional conservation equations for mass, momentum and energy Eq. (3.1- 3.3). The non-dimensional parameter used for the getting dimensionless conservation equation is given by Eq. (3.4) and final non-dimensional equations are given by Eq. (3.5- 3.7).

In order to introduce the power dynamics into framework, mathematical model for point reactor kinetics and a lumped parameter representation of the energy balance across the fuel rod are taken into consideration. The heat generated through nuclear fission can be described by point reactor kinetics and the detailed modelling of this part is given in Section (3.2.1- 3.2.3). Finally, the set of governing equations are obtained by integrating these equations between two zones.

5.3 Results and discussion

Study of the dynamic behaviour of SCWR involves several interrelated steps. As explained, earlier that LPM is much simpler and computationally fast, that means, a greater number of simulations in less time. Considering this into the mind, number of stability maps have been plotted using maximum distinct locus point for the marginal stable boundary. The decision of the number of points is purely based on an individual choice, the number does not significantly affects the stability boundary (Ortega et al., 2008). More numbers of points means the MSB will be more smother; these points are required for getting the qualitative trends of the individual parameters on stability map, so there is nothing more serious except small deviation from their actual path, which is acceptable. An equivalent coolant channel of the US reference design of SCWR is taken for the references.

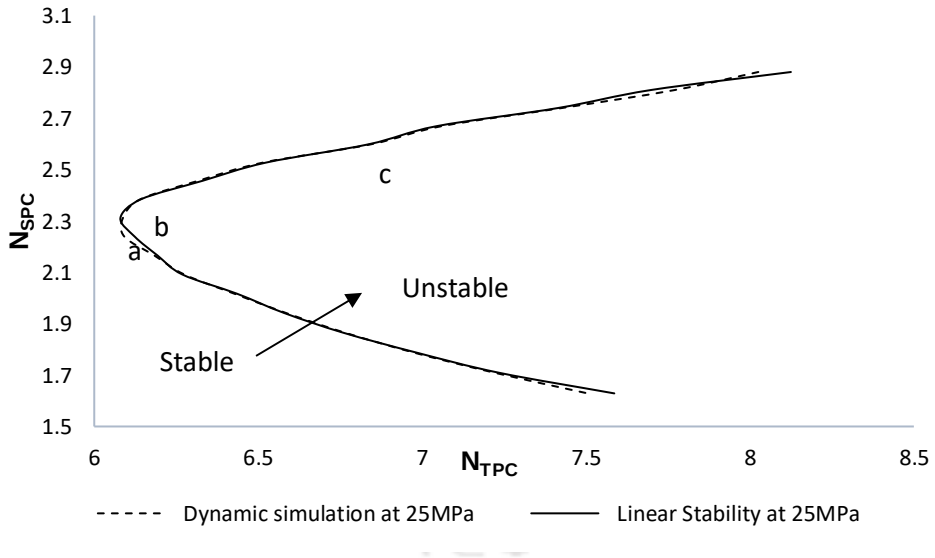

Figure 5-1: Stability map for water at 25 MPa system pressure

Stability maps following both linear stability and dynamic simulation at 25 MPa system pressure are compared in Figure 5-1. After getting the marginal stability boundary (MSB) from the linear stability analysis, the similar parametric condition is considered for the transient code, which gives the point corresponding to the given condition. By visual inspection it is predicted

that after some oscillations the system converges to its initial value, the corresponding value is marked as a point for MSB. Now, similar simulations are done for various inlet temperatures, the points obtained are then plotted as the MSB and termed as dynamic simulation. Both the maps exhibit amicable agreement. Figure 5-2 shows the comparison between two boundary conditions with identical inlet. The system behaviour is different in both the cases, which may be due to their different flow dynamics. However, the pressure drop boundary condition is considered in the present analysis because it is more realistic. For low levels of heater power, fluid temperature fails to attain the pseudocritical value within the channel exit, thereby ensuring a liquid-like representation of the fluid throughout the channel. As the entire channel resembles the node, 1 of LPM, all thermophysical properties exhibit small variations with temperature and hence the system behaves in a stable manner. However, for intermediate to high power levels, water crosses the pseudocritical point during its passage through the channel and therefore suffers a substantial reduction in its density and other transport properties Figure 5-2**.** Higher density and viscosity level in zone 1 results in significant frictional and gravitational pressure drop from the channel inlet to the pseudocritical point. However, both components are much smaller for the rest of the channel, with small increase in the acceleration part. Accordingly, the first zone has to bear the major share of the pressure drop imposed on the system. For low inlet temperatures, the pseudocritical boundary appears quite close to the exit plane.

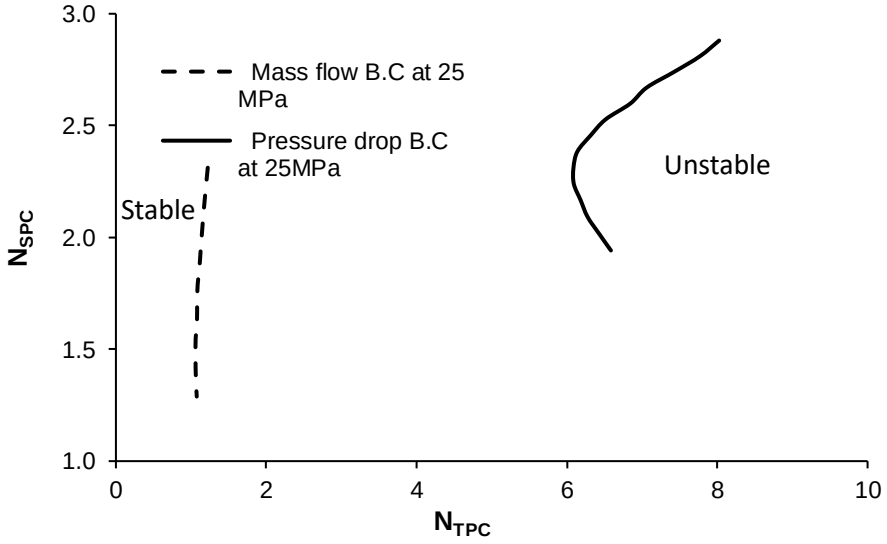

Figure 5-2: Comparisons of stability map at 25 MPa for thermal hydraulic in two different boundary conditions

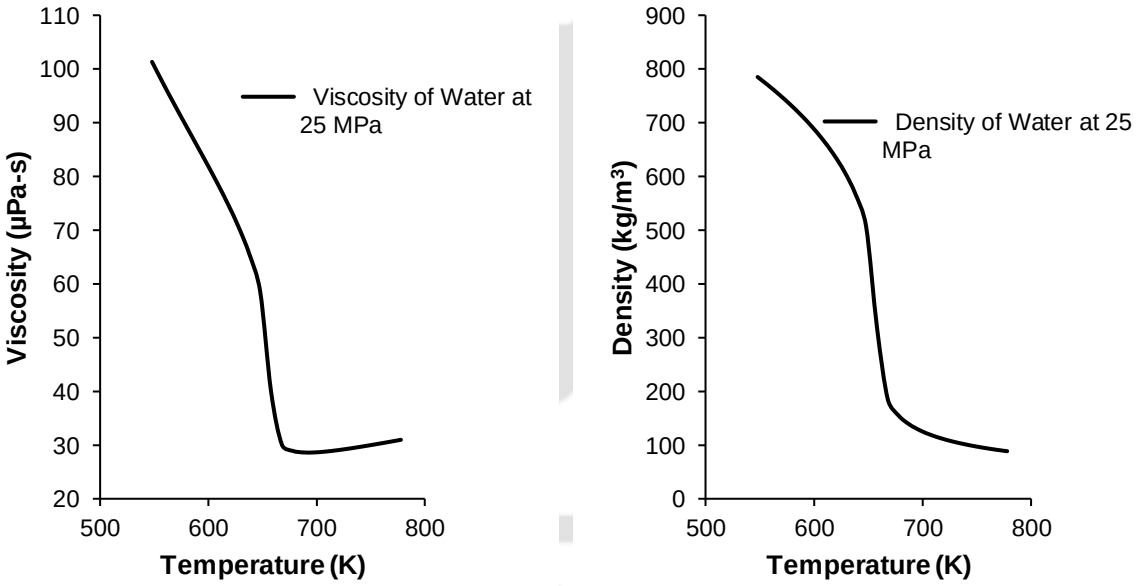

Figure 5-3: Variation of Viscosity and density with inlet temperature of water at 25 MPa

For any given heater power, as the inlet temperature increases, the pseudocritical boundary starts shifting towards inlet of channel. The system is stable for low and high inlet temperatures, when the pseudocritical boundary is close to the channel outlet and inlet, respectively. For intermediate inlet temperatures, when the pseudocritical boundary is in the

middle of the channel, the system exhibits flow instabilities. These instabilities are similar to density wave oscillations (DWO) in boiling channels, which is the most common type of instability (Prasad et al., 2007). They take place because of phase lag and feedback between flow rate, density, and pressure drop. The main cause of DWO is the wave resulting from perturbation in enthalpy, which travels at speed much lower than the speed of propagation of the pressure disturbances. A periodic disturbance of the inlet mass flow rate will lead to the oscillation of the pseudocritical boundary. The pressure drops in the first zone and second zone will then oscillate. These, along with mass flux oscillations, will lead to perturbations in density, which travel downstream at velocities that are approximately equal to the second zone fluid velocity. The pressure perturbation, however, travels much faster, at the velocity of sound. Phase lag will thus occur among the oscillating parameters, and these can lead to oscillations of the mass flow rate.

5.3.1 Transients simulations

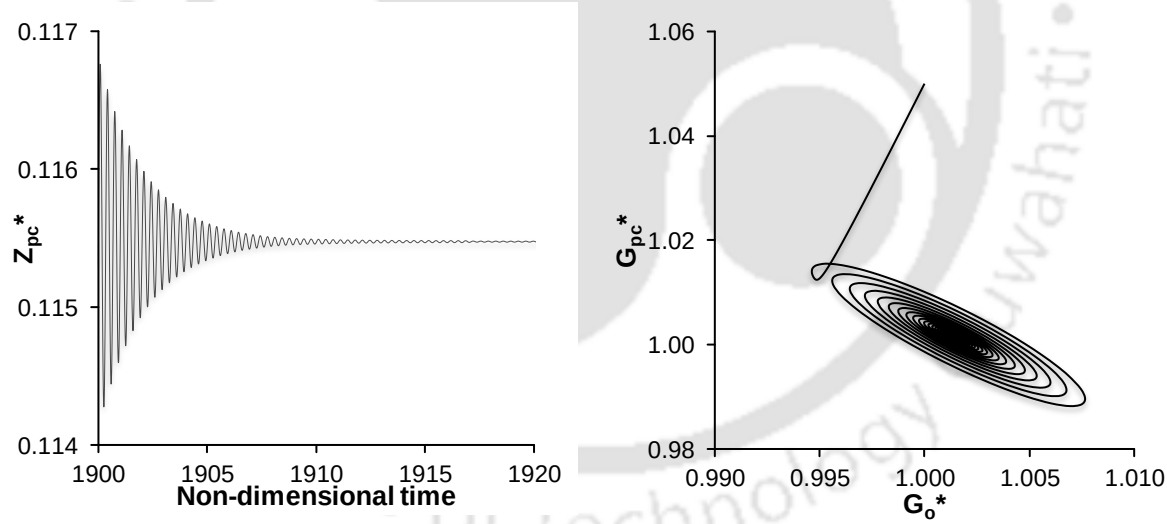

Figure 5-4: Stable response of SCWR corresponding to point 'a' in the stability map at 25 MPa system pressure, 1843 kg/s mass flow rate and 0.32 MW/Channel input power

The discussion in Section (3.7.1) substantiates the success of the linear stability analysis in predicting the stability threshold. However, to comprehend the nature of instability, transient simulations are performed at some selected operating conditions shown by three doted points named as a, b and c in Figure 5-1. A small perturbation is imposed on inlet mass flow

under constant channel pressure drop condition and corresponding temporal profiles of system variables are followed over a sufficiently long interval. The variation in z_{pc}^* for a typically stable system is presented in Figure 5-4, along with the concerned phase-portrait on $G_{pc}^* - z_{pc}^*$ plane; a point 'a' shows this. It is evident that the oscillations subside quite early and the profile continues with a near-constant value. Corresponding phase portrait exhibits converging spirals into a stable fixed point. Temporal development of z_{pc}^* for a system in vicinity of the marginal stable boundary, which is shown by point 'b' in Figure 5-5. Hardly any distinguishable change can be observed in the amplitude of oscillation over the considered time span. This indicates the stable limit cycle. Corresponding phase portrait assumes the shape of a near-perfect circle, beyond some period of initial development. At some point 'c' far from the limit cycle it's detected that, with small increase in the input power, oscillations with growing amplitude can be observed (Figure 5-6). The portrait on the state-space plane exhibits a spiral, diverging away from a stable fixed point for a typically unstable system.

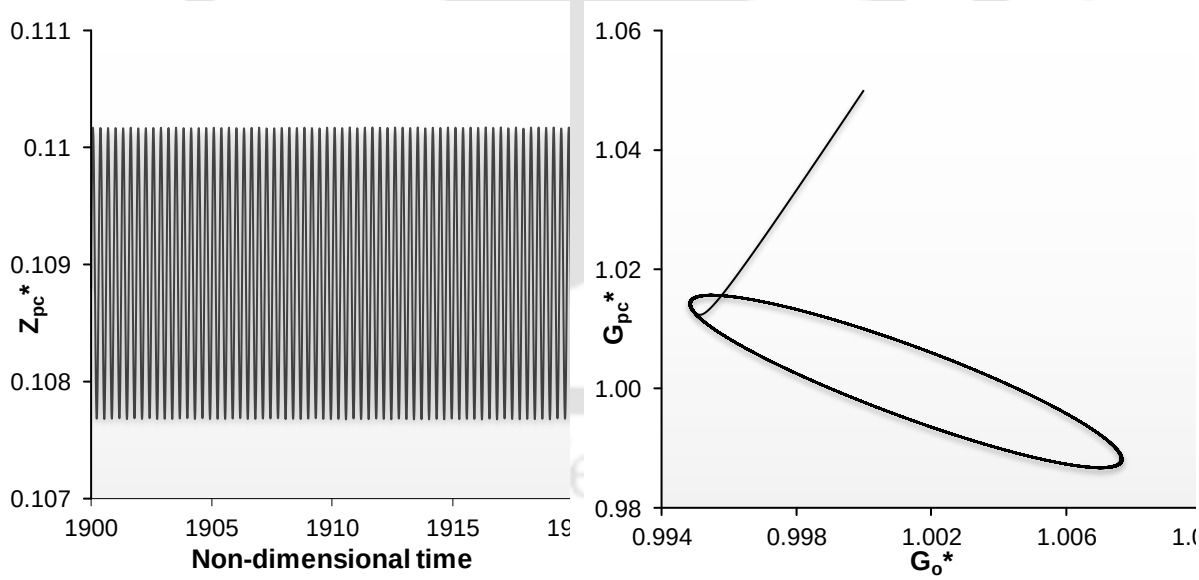

Figure 5-5: Neutrally stable response of SCWR corresponding to point 'b' in the stability map at 25 MPa system pressure, 1843 kg/s mass flow rate and 0.35 MW/Channel input power

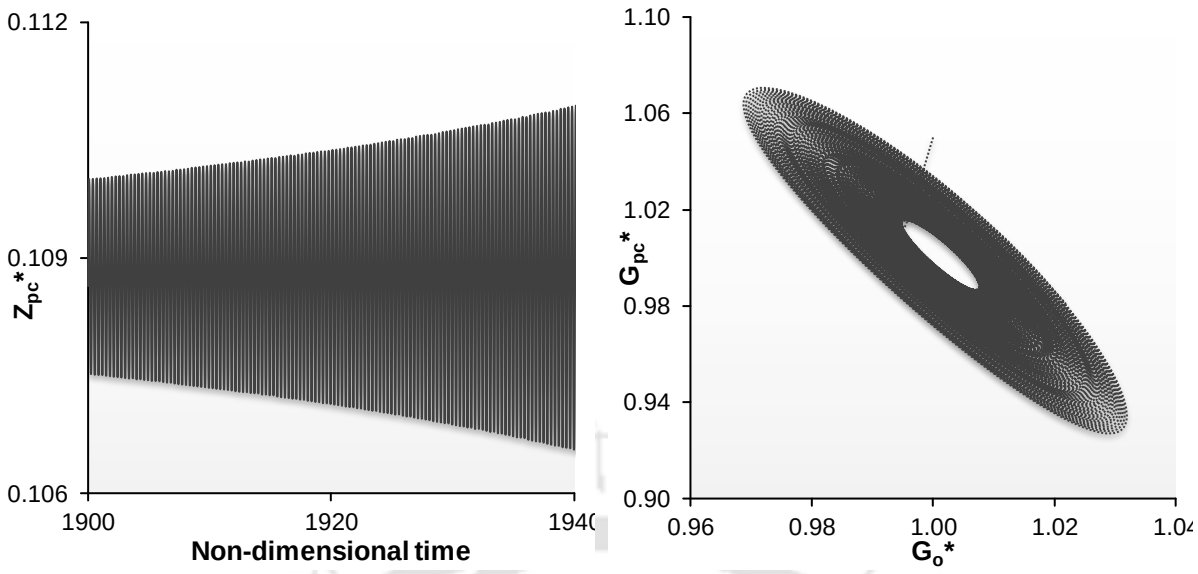

Figure 5-6: Unstable response of SCWR corresponding to point 'c' in the stability map at 25 MPa system pressure, 1843 kg/s mass flow rate and 3.16 MW/Channel input power

5.3.2 Parametric effects on pure thermal hydraulic stability

Stability behaviour of any flow system is strongly dependent on geometric and operating parameters and the same is applicable for supercritical channels as well. Therefore, the influence of various parameters on thermohydraulic stability needs to be investigated. Parametric analyses with the present lumped-parameter model is performed for 25 MPa system pressure, with inlet and outlet orifice coefficients of 115 and 10 respectively, unless stated otherwise. Few of the studies have been done without the orifice coefficient, i.e. the value of inlet and orifice coefficient are zero. It is found that the stability of U. S. reference SCWR design is sensitive to the flow restrictions in the hot fluid or the steam line. As long as the restriction at outlet in the steam line is small, the design will be stable. Few combination of orifice coefficient was suggested by other researcher (Su et al., 2013) for hot channel. At 115.0 orifice coefficient, the pressure drop through the hot channel was calculated to be 0.163 MPa, which is closer to the target pressure drop, 0.15 MPa. Corresponding to this the orifice diameter would be ~3.4 cm. There should be no difficulty in manufacturing such orifices (Zhao et al., 2006).

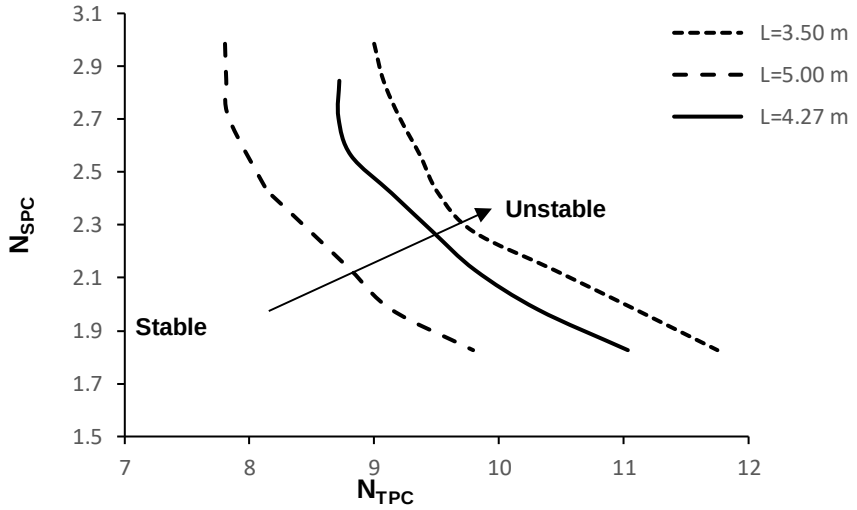

Figure 5-7: Effect of channel length on non-dimensional plain

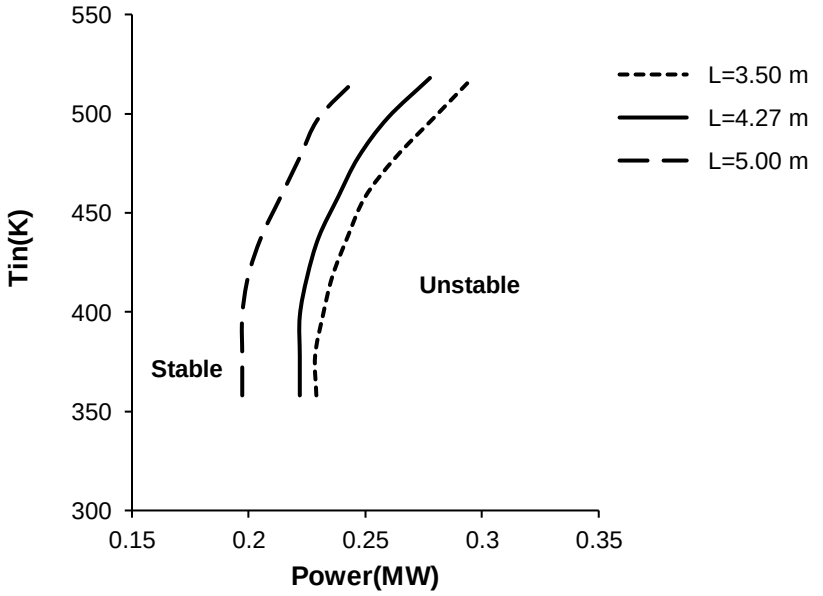

Figure 5-8: Effect of channel length, Inlet temperature verses power

5.3.2.1 Effect of length

The effect of channel length on the stability threshold is presented in Figure 5-7 and Figure 5-8. For a given inlet temperature, neutral stability curve shifts towards lower power level with increase in channel length. In Figure 5-7 and Figure 5-8, the neutral stability boundary is shown for various

heated lengths (L) in the stability map. Increasing the heated length creates a destabilizing effect (L= 3.50 m, L = 4.27 m and L = 5.00 m). This phenomenon can be explained based on the gravitational and frictional pressure drop in the momentum equation. It can be noticed that for a given inlet temperature and power for three different lengths, the frictional pressure drop decreases by 0.4 times while the increase in gravitational pressure drop is 1.8 times for L =3.50 m and L =4.27 m for the fixed mass flow rate. Due to increase in channel length, the mass flow rate reduced as pressure drop is a boundary condition. Consequently, the pseudocritical point shifted towards the inlet of the channel, hence the system is unstable (Zhao et al., 2006). On the other hand, increasing the length also extends the second zone, thereby causes an unstable effect.

5.3.2.2 Effect of hydraulic diameter

Furthermore, the effect of the hydraulic diameter (D_h) of the coolant channel on the margins for instability is analysed. Figure 5-9 and Figure 5-10 shows the neutral stability boundary for various hydraulic diameters in non-dimensional and in dimensional form, for D_h = 2.5, 3.4 and 4.0 mm. The corresponding neutral stability boundary with a hydraulic diameter for a fuel assembly of SCWR is given in solid line. Increasing the hydraulic diameter has a stabilizing effect. This same kind of nature has been observed by Ortega et al. (2008). It has to be noted that a typical fuel assembly of a supercritical US reference design of SCWR have a hydraulic diameter of D_h = 3.4 mm (Zhao et al., 2005).

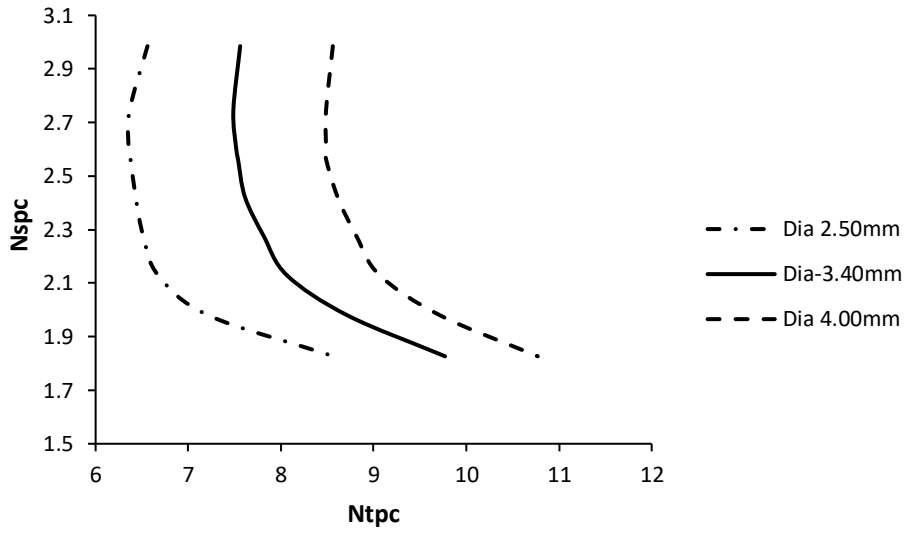

Figure 5-9: Effect of channel hydraulic diameter on non-dimensional plain without orifice coefficient

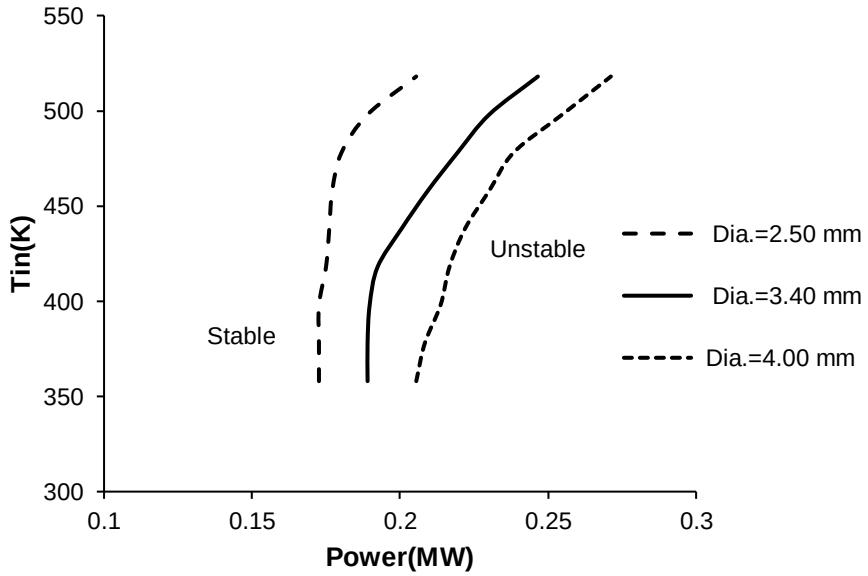

Figure 5-10: Effect of channel hydraulic diameter, Inlet temperature verses power plain

5.3.2.3 Effect of orifice coefficients

An inlet orifice coefficient always stabilized the system strongly, as Figure 5-11 and Figure 5-12 shows. This is similar to the phenomena in BWR. In the two-phase system the stability boundary depends on the pressure loss distribution in heavy fluid region (i.e. before the boiling boundary reached, or the subcooled liquid) and the region of lighter fluid which is above the boiling boundary on the other hand, for the super critical case, the subcooled liquid

region corresponds to the high-density region before the fluid is heated beyond the pseudo-critical point. Any device, which increases the pressure loss of the heavy liquid region, increases the so-called in-phase pressure loss. On the contrary, the effect of a flow resistance at the channel outlet (or also called out-of-phase pressure loss) is strongly destabilizing. Strong care must be taken with pressure losses at the outlet or the upper part of the coolant channel. Since an in-phase pressure loss is the most sensitive parameter for stabilizing a supercritical flow channel, inlet orifices coefficient can be customized to assure stable operation with respect to DWOs for otherwise unstable channels.

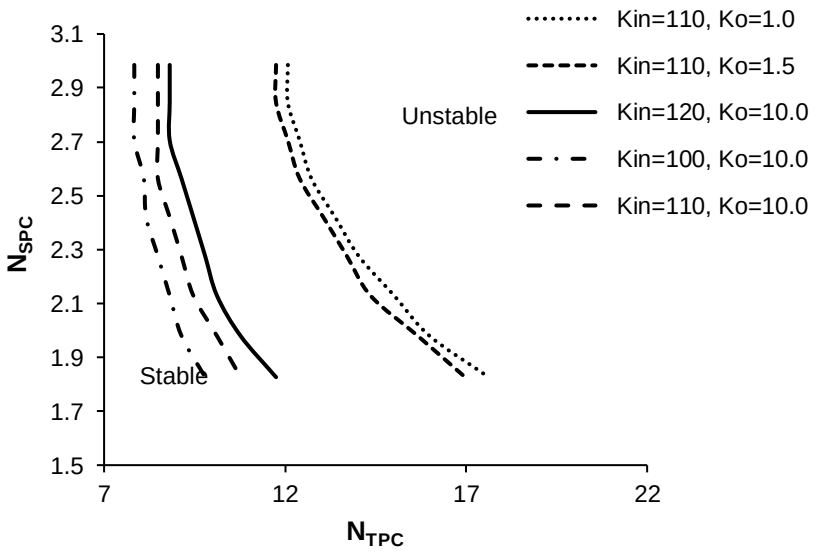

Figure 5-11: Effect of inlet and outlet orifice coefficient stability map

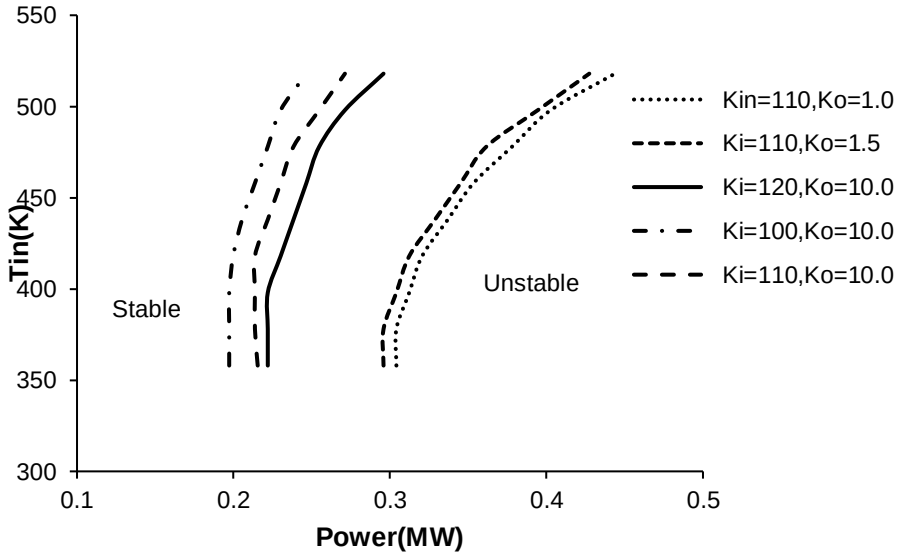

Figure 5-12: Effect of inlet and outlet orifice coefficient, Inlet temperature verses power

5.3.2.4 Effect of system pressure

The effect on stability of different system pressure of heated channels is studied in the N_{SPC} and N_{TPC} plane. The neutral stability boundary is given for a pressure of p = 25 MPa and p = 30 MPa along with the comparison of linear stability curve Figure 4.3 (a). Absolute pressure is, absent in the dimensionless version of the conservation equations and hence is not expected to play any role in determining the stability threshold. The curves are coincide with each other at all pressures.

5.3.3 Coupled neutronics-thermal hydraulic stability

In order to study the influence of the neutronics coupling on the stability of the system, coupled neutronics-thermal hydraulic performance has been evaluated. Typical values of the various reactivity feedback coefficients for the US reference design of SCWR are given by (Yang and Yang, 2005). The fuel time constant is varied from 2 s to 16 s, which is based on its estimated range of 2-8 s for the BWR fuel at the normal operating conditions. The enthalpy reactivity, density reactivity constant value is taken similar to that of U.S. SCWR (Yi et al., 2004; Zhao et al., 2007). However, all these parameters are likely to change with burn-up and operating conditions.

Further, in order to investigate their influence on the low frequency thermohydraulic oscillations, all these parameters have been varied to study their influence on the instability, similar to parametric studies on BWR (Nayak et al., 2000).

5.3.3.1 Effect of fuel time constant

The effect of fuel time constant on the stability of SCWR is shown Figure 5-13. The fuel time constant will vary depending on the fuel properties and operational conditions. Van der Hagen (1998) has shown that with the use of lumped parameter model it could be achievable. The fuel time constant, in the present analysis, has been varied over a wide range from its normal operating value to study its influence on the stability. The stability of the reactor decreases with increase in fuel time constant. Previous studies on BWR (March-Leuba and Rey, 1993; Nayak et al., 2000) have shown that changes in fuel time constant have both stabilising and destabilising effects. It was found that the stabilising effect is due to the inherent filtering of high frequency oscillations, and the destabilising effect is due to the phase delay to the feedback. For the moderate frequency thermohydraulic oscillations observed in the SCWR, the phase delay is more significant to destabilise the reactor for an increase in fuel time constant than the filtering effect (Chaudri et al., 2013; Zhao et al., 2006 a,b).

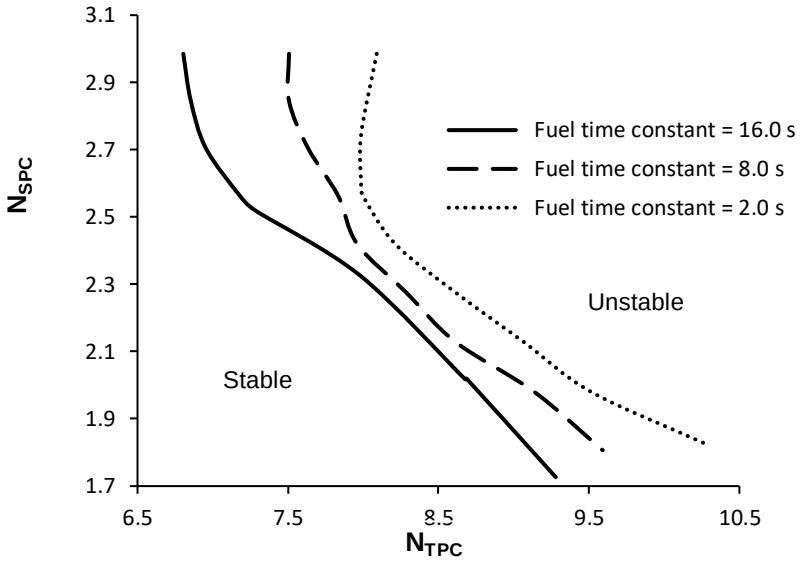

Figure 5-13: Effect of Fuel time constant at pressure 25MPa and enthalpy reactivity coefficient is –0.005

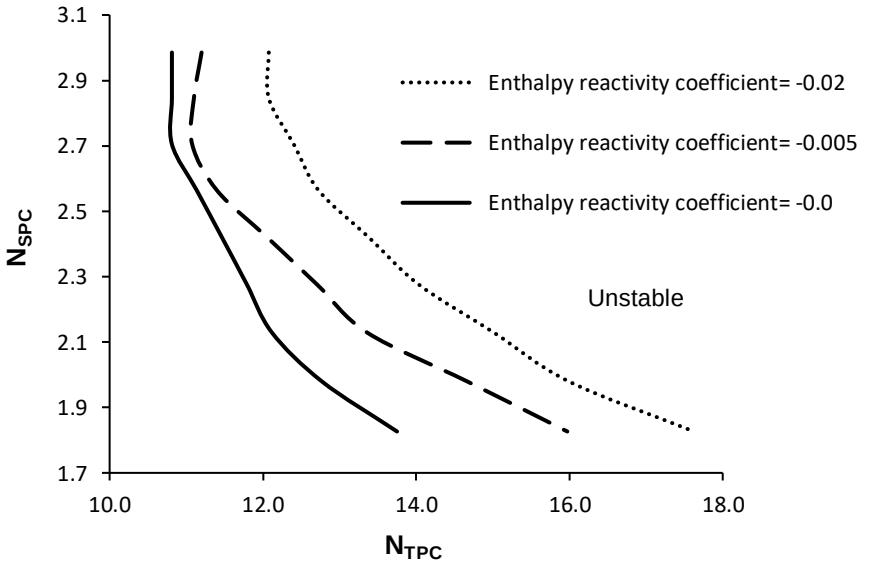

Figure 5-14: Effect of enthalpy Reactivity Coefficient at pressure 25MPa and fuel time constant 8 s.

5.3.3.2 Effect of enthalpy reactivity coefficient

The enthalpy reactivity coefficient depends on the core design, while the Doppler coefficient is almost constant (Yang and Yang, 2005). From the viewpoint of plant control, it should not be too large or too small. If it is too large, the SCWR is unstable and the controllability is worse because the power is more sensitive to the flow rate. On the other hand, if it is too small, the

controllability is also worse because the density feedback is smaller and then the main steam temperature is more sensitive to the flow rate (Ishiwatari et al., 2003). Figure 5-14, shows the effect of enthalpy reactivity coefficient on the threshold of stability for the SCWR reactor. The stability of the reactor is found to increase with an increase in the absolute value of the negative enthalpy reactivity coefficient. Results from previous investigations for vessel type BWRs have shown that the stability of the reactor decreases with increase in negative enthalpy reactivity coefficient due to the increase in gain of the void reactivity feedback loop (Uehiro et al., 1996; van Bragt and van der Hagen, 1998). (Nayak et al., 2000), observed that by addition of neutronics feedback at such low frequency of thermo- hydraulic oscillations (<0.07 Hz) which was studied by them for AHWR system, stabilises the reactor due to less phase lag between the fuel heat generation rate and channel thermohydraulic oscillations. The similar phenomena has been observed in SCWR.

5.4 Conclusions

The present study employs a simplified lumped parameter model (LPM) for stability evaluation of SCWR. Stability maps predicated by the transient simulation with LPM and linear stability analysis show excellent match, as expected. Further, there is qualitative match between the stability maps prepared using LPM and RELAP5. Parametric effects on the stability threshold have been investigated and major conclusions are the following.

a) Increasing the heated channel length has destabilizing effect on the system, which is quite common in boiling channels also.
b) Stabilizing effect on the system has been observed by increasing the hydraulic diameter with and without orifice coefficient.
c) Increase in inlet orifice coefficient has stabilizing effect whereas the reverse can be observed for the outlet orifice.
d) System pressure is found to have negligible effect on the non-dimensional stability threshold.

e) The stability of the reactor decreases with increase in fuel time constant.

f) The stability of the reactor is found to increase with an increase in negative enthalpy reactivity coefficient.

The results reported here predict the stability behaviour of the SCWR, considering thermal hydraulics, fuel rod dynamics, and power dynamics.

Chapter 6 STABILITY ANALYSIS OF SCWR USING THREE ZONE LPM

6.1 Introduction

Instability analysis is very important for the safely of the SCWR. To analysis these aspects, two zone LPM has been developed (section 3.2). As it is the simplified model, and gives the qualitative information about the system stability. Therefore, to know the extents of stability margin by increasing the numbers of nodes, the study has been done in this chapter using three zone model. The model has been developed using the same concept, which has been used in section (3.1). Moreover, using this model the instability has been characterized. Earlier, in order to characterize such instabilities, the concept of two-region model comprising of (i) a "liquid like region" and (ii) a "gas like region" is used (Zuber, 1966). The transition between the two regions was identified by the appearance of the pseudocritical point. An improvement on that in the form of a three-region model was later proposed, which was found to provide reasonably better prediction on the stability prediction of SCWR. Therefore, present study carries out a lumped parameter base stability analysis for a heated channel with supercritical fluid following three-region model. In the present model stability analysis has been done on three geometrical parameters and their detailed stability map has been plotted for locating the stable and unstable zones.

Zhang et al., (2015) proposed a three-region model to investigate the density wave instabilities of SCW in tubes, where a specific region of SCW was defined as "two-phase mixture", and the demarcation points of three regions were the pseudo critical point and a point with "latent heat" of 400 kJ/kg. The three region model was proved better than the two region one considering some limitations. Zhao et al., (2005) proposed another three-region model for the analyses of density wave instabilities of SCW in tubes, on the basis of the partition method different. A linear stability analysis code in the frequency

domain was developed by many researchers (Yi et al., 2004; Yoo et al., 2006) to study the thermal-hydraulic stability of the supercritical pressure light water reactor at constant supercritical pressure. Then, the thermal-hydraulic stability of super- critical pressure light water reactor for both full-power condition and partial-power condition was investigated. To carry out the steady state and linear stability analysis of a SCW natural circulation loop, (Sharma et al., 2013) proposed a computer code by using supercritical water properties. However, because of the complexity of the physical properties of SCW, there is still not a unified model for studying the instabilities of SCW flows in tubes. Concerning the previous studies as mentioned above, the three commonly used mathematical models for the study of density wave instabilities of SCW flows are carried out (Zhang et al., 2015; Zuber, 1966), which is based on frequency domain method. The three models are derived based on the different partition methods of SCW. Detailed information is shown in the following section.

Under subcritical pressures, the flow region in a tube was usually divided into three parts, i.e., the preheating region, the boiling region and the superheating region, for studying density wave instability. Considering the similar features of subcritical water and SCW, the models derived at the subcritical pressure may also be employed for the relevant study at the supercritical pressure, if the flow region in tubes at the supercritical pressure could be divided into three parts just like that at the subcritical pressure. Many efforts had been carried out in the recent decades (Zhang et al., 2015; Zuber, 1966) and different models were established for the study on density wave instability of SCW in tubes, based on the models used for subcritical conditions. The three commonly used mathematical models were from (Zhang et al., 2015; Zuber, 1966), respectively. The primary differences among the three models were the regional partitions of SCW. The different regional partitions in the three methods are simply expressed as follows, and are described using graphs in the same form to facilitate the comparisons. Zhang et al. (2015) compared the above three model and suggested some

improvements by increasing the second region area which reduced the relative error of the present model by 26%, while that of the other three models are all greater than 30%.

In the present analysis, the main focused is to analyses the thermal hydraulics parameter by using the improved three zone lumped parameter model (LPM) (Zhang et al., 2015). The parameters which have been varied for the study are channel length, hydraulic diameter and inlet and outlet orifice coefficients. Transient plot and stability map has been plotted for these parameters which further supports the stability analysis. However, the detailed analysis has been done by considering two different values of the geometrical parameter and three different values for orifice coefficient apart from the design values.

6.2 Mathematical modelling

The reactor core has been divided in three separated regions (Figure 6-1), namely, (1) liquid-like heavy fluid region with constant density, (2) mixture region of heavier and lighter fluid behaving similar to a homogeneous two-phase mixture and (3) gas-like lighter fluid with constant density. The basic dimensional conservation equations (3.1-3.3) are similar to the two zone model, finally using the nondimensional parameters equation (6.1) as in dimensional equations,

$$z^* = \frac{z}{L_c}, \quad t^* = \frac{tG_c}{\rho_{pc}L_c}, G^* = \frac{G}{G_c}, \rho^* = \frac{\rho - \rho_{pc}}{\rho_{pc}}, p^* = \frac{(p - p_r)\rho_{pc}}{G_c^2}, T^* = \frac{T - T_{pc}}{T_{pc}}, h^* = \frac{(h - h_{pc})}{h_{pc}}, N_{Fr} = \frac{G_c^2}{\rho_{pc}^2 g L_c}, N_{TPC} = \frac{q_0'' \pi_h L_c}{AG_c}\frac{\beta_{pc}}{C_{p.pc}}, N_{Eu} = \frac{fL_c}{2D_h} \quad 6.1$$

Which finally gives equations (6.2-6.4).

$$\frac{\partial \rho^*}{\partial t^*} + \frac{\partial G^*}{\partial z^*} = 0 \tag{6.2}$$

$$\frac{\partial G^*}{\partial t^*} + \frac{\partial}{\partial z^*}\left(\frac{G^{*2}}{\rho^*}\right) = -\frac{\partial p^*}{\partial z^*} - \frac{\rho^* - 1}{N_{Fr}} - [N_{Eu} + K_i \delta^*(z^*) + K_o \delta^*(z^* - 1)]\frac{G^{*2}}{\rho^*} \tag{6.3}$$

$$\frac{\partial}{\partial t^*}(\rho^* h^*) + \frac{\partial}{\partial z^*}(G^* h^*) = N_{TPC}\, f(t^*) \tag{6.4}$$

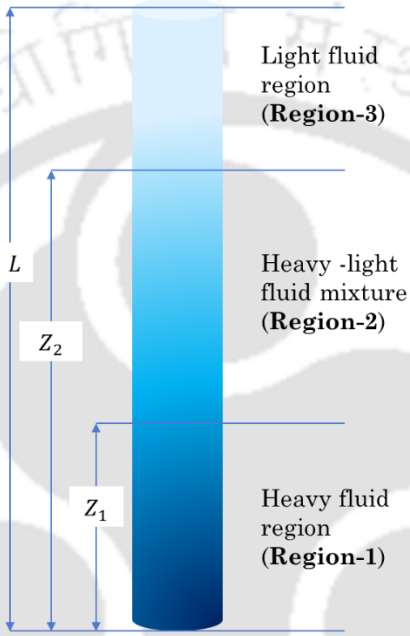

Figure 6-1: Schematic view of the heated channel following by three-region model

The above equations are then integrated separately over each of the regions, while incorporating suitable equation of state.

6.2.1 Equations of state (EOS)

Due to lots of anomalies between two-zone and three-zone model and that also on the cost of stability, is preliminary based on the EOS. However, observing the method by which Zhao et al., (2006) divided the model into three-zone, the following two major glitches have been observed. Firstly, T_{PSW} which is the temperature at the boundary of H-F and H-L-M is defined as a constant, equalling to 350 ^{o}C. It is obvious that near the small zone where the density varies sharply at different pressures does not have the same starting

point. It means that T_{PSW} changes with the pressure, and defining T_{PSW} as a constant is not so appropriate. Secondly, the temperature of the exit delineation between H-L-M and L-F is somewhat low, which is approximately 450 ^{o}C. In SCWR the exit, temperature is greater than 500 ^{o}C. So, a more practical method must have needed.

Hence, considering these gapes, a more general and resolute relations have been proposed. The relations levee the aforementioned breaks. These equations of state for each of the regions are obtained by fitting a piecewise linear function with IAPWS data of water at 25MPa (Figure 6-2), which is given as below.

$$\begin{aligned} \rho^* &= -2.21h^* + 0.49 && for \quad -0.6 < h^* \leq -0.3 \\ \rho^* &= -3.6683\, h^* && for \quad -0.3 \leq h^* \leq 0.05 \\ \rho^* &= -2.11h^* - 0.0363 && for \quad 0.05 \leq h^* \end{aligned} \qquad 6.5$$

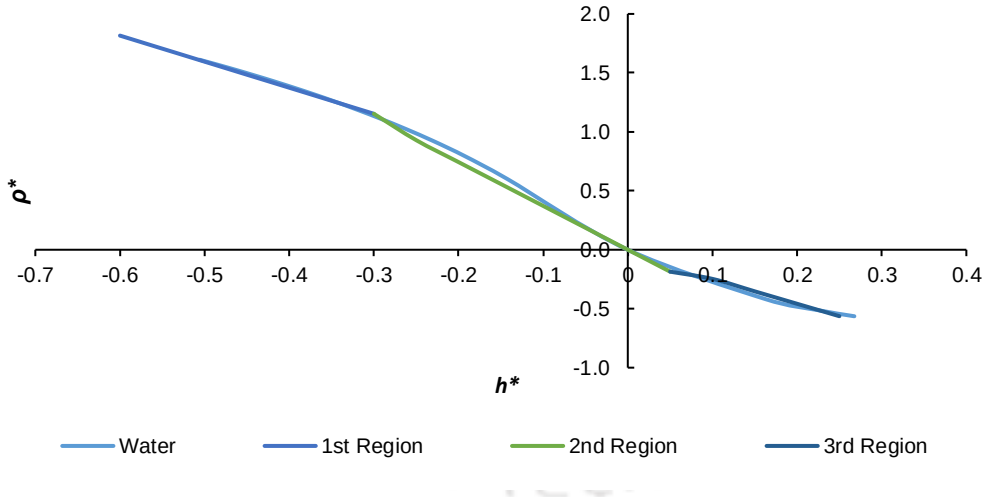

Figure 6-2: Fitting of equation of state with IAPWS data of water at 25 MPa.

6.2.2 Enthalpy profile and relation between ρ^* and h^*

Assuming a linear enthalpy variation with axial coordinate the following relations hold for the first, second and third node.

$$h^* = (h_1^* - h_i^*)\frac{z^*}{z_1^*} + h_i^*$$

$$h^* = \left[\frac{h_1^* - h_2^*}{z_1^* - z_2^*}\right](z^* - z_1^*) + h_1^* \qquad 6.6$$

$$h^* = \left[\frac{h_2^* - h_o^*}{z_2^* - 1}\right](z^* - 1) + h_o^*$$

Where h_1^* and h_2^* are the non-dimensional enthalpy at the boundaries of the two regions.

Using the property relations into the non-dimensional governing equations and integrating the equation for three different zone for the equation of state variables. The mass and energy equations are further integrated over region 1st from inlet to Z_1, which gives one ODEs and one algebraic equation.

$$\frac{dz_1^*}{dt^*} = \frac{G_i^* - G_1^*}{A_1}$$

$$G_1^* = \frac{N_{TPCM} z_1^* A_1 + G_i^* h_i^* A_1 - G_i^* B_1}{h_1^* - B_1} \qquad 6.7$$

Where, $A_1 = \frac{a_1(h_1^* - h_i^*)}{2} + (a_1 h_i^* + b_1) - (a_1 h_1^* + b_1)$

$$B_1 = a_1 h_i^*(h_1^* - h_i^*) + a_1 h_i^{*2} + \frac{b_1(h_1^* - h_i^*)}{2} + b_1 h_i^* - (a_1 h_1^* + b_1)h_1^*$$

$$C_1 = 1 + b_1$$

In the same way, mass and energy equations are integrating over region 2 i.e. from Z_1 to Z_2, which gives an ODEs and an algebraic equation

$$\frac{dz_2^*}{dt^*} = \frac{G_1^* - G_2^* - D_2\frac{dz_1^*}{dt^*}}{C_2}$$

$$G_2^* = \frac{N_{TPCM} C_2(z_2^* - z_1^*)C_1 - G_1^*(h_1^* C_2 - A_2) + (D_2 A_2 - B_2 C_2)\frac{dz_1^*}{dt^*}}{(h_2^* C_2 - A_2)} \qquad 6.8$$

Where, $A_2 = \left((a_2 h_1^{*2} + h_1^*) - (a_2 h_2^{*2} + h_2^*) + \left((2a_2 h_2^* + 1) A_{21} \left(G_2^* - z_1^* - \left(\left(\frac{G_2^*}{1.41} \right) - \left(\left(\frac{z_1^*}{1.41} \right) \right)^2 \right) (z_1^* - G_2^*)^{-1} \right) \right) + (A_{21}^2 a_2 (G_2^* - z_1^*)^2) - \left(2a_2 A_{21}^2 \frac{B_2}{z_1^* - G_2^*} \right) \right)$

$Where, A_{21}$=$((h_1^*$-$h_2^*)/(z_1^*$-$G_2^*))$

$$B_2 = \left((2h_1^* - h_2^*)\left(1 + a_2(2h_1^* - h_2^*)\right) - (a_2 h_1^{*2} + h_1^*) - a_2 A_{21}^2 (z_1^* - G_2^*)^2 + (2a_2 h_1^* + 1) A_{21} \left(z_1^* - G_2^* + \left(\left(\left(\frac{G_2^*}{1.41} \right) - \left(\frac{z_1^*}{1.41} \right) \right)^2 \right) (z_1^* - G_2^*)^{-1} \right) + \left(2a_2 A_{21}^2 \frac{B_2}{z_1^* - G_2^*} \right) \right)$$

$$C_2 = \left(-a_2 (h_1^* - h_2^*) - \left((0.5 G_2^{*2}) + (0.5 z_1^{*2}) - (z_1^* G_2^*) \right) a_2 \left((h_1^* - h_2^*)(z_1^* - G_2^*)^{-2} \right) - a_2 h_2^* \right);$$

$$D_2 = \left(a_2 (h_1^* - h_2^*) + \left((0.5 G_2^{*2}) + (0.5 z_1^{*2}) - (z_1^* * G_2^*) \right) a_2 \left((h_1^* - h_2^*) * (z_1^* - G_2^*)^{-2} \right) + a_1 h_1^* \right)$$

Finally, the same process is repeated for region 3 i.e. from Z_2 to L, which give the simile sets of equations.

$$\frac{dh_o^*}{dt^*} = \frac{G_2^* - G_o^* - A_3 \frac{dz_2^*}{dt^*}}{B_3} \qquad 6.9$$

$$G_O^* = \frac{(B_4 - h_2^* B_3) G_2^* + (B_3 A_4 - A_3 B_4) \frac{dz_2^*}{dt^*} - B_3 N_{TPCM} (1 - z_2^*)}{(B_4 - B_3 h_o^*)}$$

Where A_3, B_3, A_4, B_4 are combination of state variables and constants.

$$A_3 = \left(-a_3(h_2^* - h_o^*)\right) + \left((G_2^* - 0.5h_2^{*2} - 0.5)(h_2^* - h_o^*)(G_2^* - 1)^{-2}\right) + (a_3 h_o^* + b_3) + a_3 h_2^*$$

$$B_3 = \left(\left((G_2^* - 0.5G_2^{*2} - 0.5)(G_2^* - 1)^{-1}\right) + a_3\right)$$

$$A_4 = \left(-a_3(h_2^* - h_o^*)\right) + \left((G_2^* - 0.5G_2^{*2} - 0.5)(h_2^* - h_o^*)(G_2^* - 1)^{-2}\right) + (a_3 h_o^* + b_3) + a_3 h_2^*$$

$$B_4 = (2a_3(G_2^{*2} - G_2^{*3}0.33 - G_2^* + 0.33)(h_o^* - 1)(G_2^* - 1)^{-2}) + \left[2a_3\left\{h_o^*(G_2^* - 0.5G_2^{*2} - 0.5)((G_2^* - 1)^{-1}) + \frac{h_2^* - h_o^*}{G_2^* - 1}(G_2^* - 0.5h_2^{*2} - 0.5)\right\}\right] + 2a_3(i_1(h_o^* - G_2^*) + h_o^*(G_2^* - 0.5G_2^{*2} - 0.5)(h_2^* - h_o^*)(G_2^* - 1)^{-2}) - (a_3 h_o^{*2} - (c_3 + a_3 h_2^*)h_2^*)$$

For solving the transient equations, the initial condition for solving the system of ODEs is the steady state values of equations (6.3-6.5) for the state variables z_1^*, z_2^*, h_o^*. All the six equations are coupled with each other. The inlet operating parameters power, mass flux and inlet temperature are specified. The code first calculates the G_1^*, z_1^* then G_2^*, z_2^* and lastly G_o^*, h_o^*.

6.3 Results and discussion

SCWR as a prototype is selected for simulation in the present analysis. It is a direct cycle system with 25 MPa design pressure and core inlet and outlet temperatures of 280 and 500°C respectively (Zhao et al., 2006). Coolant density is allowed to decrease from about 780 kg/m^3 at the core inlet to about 90 kg/m^3, which raises concern over the possible appearance of instabilities and hence necessitates the stability appraisal. Both linear stability behaviour and dynamic simulation results are characterized in terms of sub-pseudocritical number (N_{SPC}) and trans-pseudocritical number (N_{TPC}).

With constant-pressure-drop boundary condition, for low levels of heater power, fluid temperature fails to attain the pseudocritical value within the channel exit, thereby ensuring a liquid-like representation of the fluid throughout the channel. As the entire channel resembles the node, 1 of LPM,

all thermophysical properties exhibit small variations with temperature and hence the system behaves in a stable manner. However, for intermediate to high power levels, water crosses the pseudocritical point during its passage through the channel and therefore suffers a substantial reduction in its density and other transport properties. Higher density and viscosity level in region 1 results in significant frictional and gravitational pressure drop from the channel inlet to the pseudocritical point. However, both components are much smaller for the rest of the channel, with small increase in the acceleration part. Accordingly, the first zone has to bear the major share of the pressure drop imposed on the system. For low inlet temperatures, the pseudocritical boundary appears quite close to the exit plane. For any given heater power, as the inlet temperature increases, the pseudocritical boundary starts shifting towards inlet of the channel. The system is stable for low and high inlet temperatures, when the pseudocritical boundary is reasonably close to the channel outlet and inlet, respectively. For intermediate inlet temperatures, however, when the pseudocritical boundary is in the middle of the channel, the system exhibits flow instabilities. These instabilities are similar to density wave oscillations (DWO) in boiling channels, which is the most common type of instability(Pandey and Kumar, 2007; Prasad et al., 2007). They take place because of phase lag and feedback between flow rate, density, and pressure drop. The main cause of DWO is the wave resulting from perturbation in enthalpy, which travels at speed much lower than the speed of propagation of the pressure disturbances. A periodic disturbance to the inlet mass flow rate will lead to the oscillation of the pseudocritical boundary, enforcing oscillations in the pressure drops in both the zones. These, along with mass flux oscillations, will lead to perturbations in density, which travel downstream at velocities approximately equal to the second zone fluid velocity. The pressure perturbation, however, travels much faster, at the velocity of sound. Phase lag will thus occur among the oscillating parameters, and these can lead to oscillations of the mass flow rate.

To comprehend the nature of instability, transient simulations are performed at some selected operating conditions shown by three doted colour points green, blue and red in Figure 6-6. A small perturbation is imposed on inlet mass flow under constant channel pressure drop condition and corresponding temporal profiles of system variables are followed over a sufficiently long interval. The variation in z_{pc}^{*} for a typically-stable system is presented in Figure 6-3, this is shown by a green point. It is evident that the oscillations subside quite early and the profile continues with a near-constant value. Corresponding phase portrait exhibits converging spirals into a stable fixed point. Temporal development of z_{pc}^{*} for a system in vicinity of the marginal stable boundary which is shown by blue point in Figure 6-6 is presented in Figure 6-4. Hardly any distinguishable change can be observed in the amplitude of oscillation over the considered time span. This indicates the stable limit cycle. Corresponding phase portrait assumes the shape of a near-perfect circle, beyond some period of initial development. At red point, with small increase in the input power from the stability threshold, oscillations with growing amplitude can be observed (Figure 6-5). The portrait on the state-space plane exhibits a spiral, diverging away from a stable fixed point for a typically unstable system.

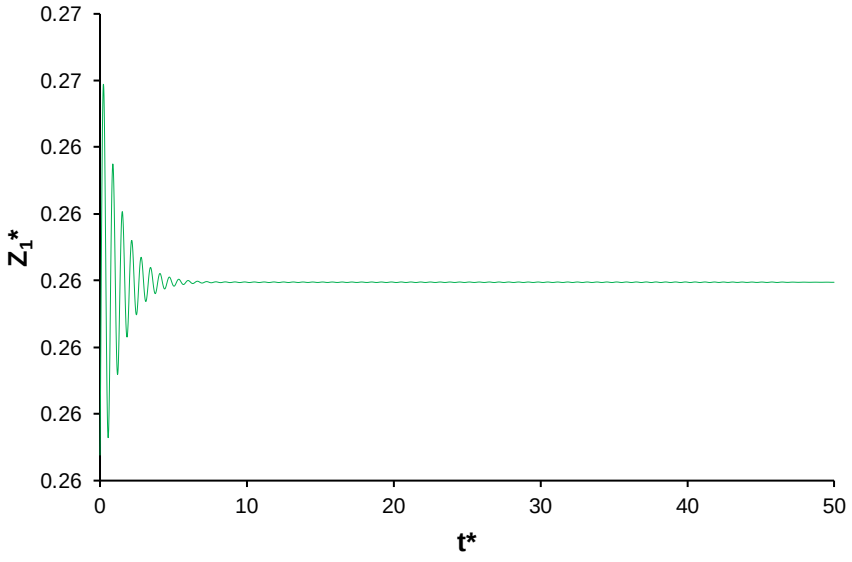

Figure 6-3: Transient variation of 1st zone boundary in stable region at Ntpc =6.0 and Nspc =2.24

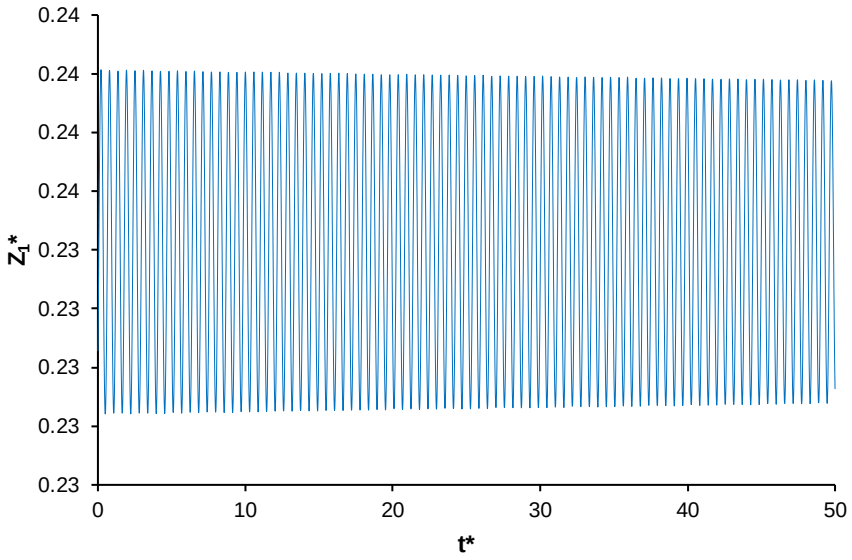

Figure 6-4: Transient variation of 1st zone boundary on marginal stable boundary Ntpc =6.13 and Nspc =2.24

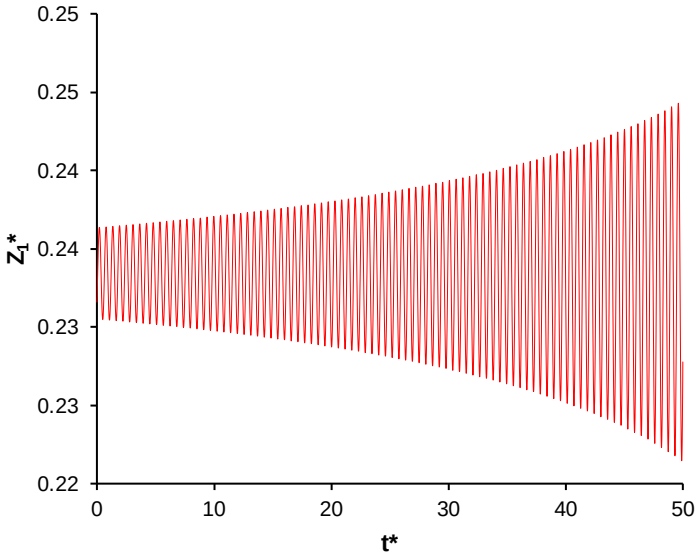

Figure 6-5: Transient variation of 1st zone boundary in unstable region at Ntpc =6.28 and Nspc =2.24

6.3.1 Effect of length

The effect of channel length on the stability threshold is presented in Figure 6-6. For a given inlet temperature, neutral stability curve shifts towards lower power level with increase in channel length. In Figure 6-6, the

neutral stability boundary is shown for various heated lengths (L) in the stability map. Increasing the heated length creates a destabilizing effect (L= 3.50 m, L = 4.27 m and L = 5.00 m). This phenomenon can be explained on the basis of the gravitational and frictional pressure drop in the momentum equation. It can be noticed that for a given inlet temperature and power for three different lengths, the frictional pressure drops decrease to 0.4 times, while the increase in gravitational pressure drop is 1.8 times for L =3.50 m and L =4.27 m for the fixed mass flow rate. Due to increase in the channel length, the mass flow rate reduces, as pressure drop across the channel is a predefined boundary condition. Consequently, the pseudocritical point shifts towards the inlet of the channel, thereby destabilizing the system (Zhao et al., 2006).

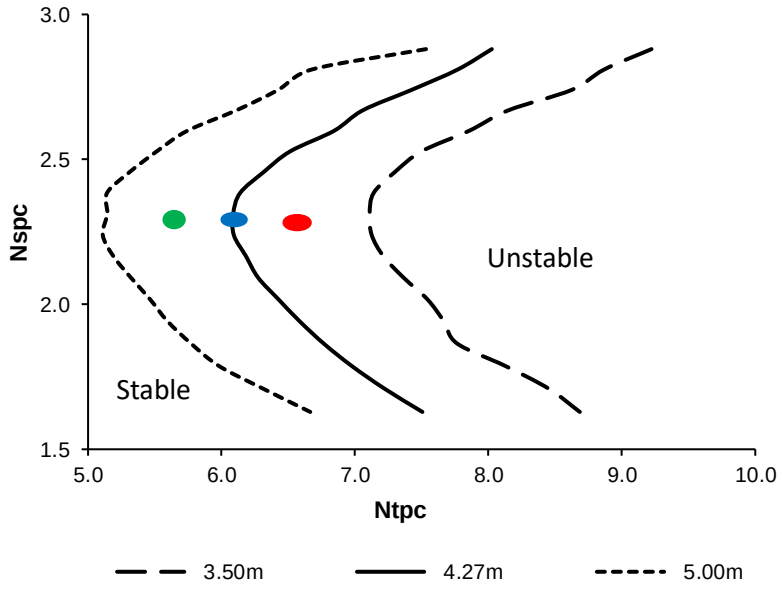

Figure 6-6: Stability map of three different channel length.

6.3.2 Effect of hydraulic diameter

Furthermore, the effect of the hydraulic diameter (D_h) of the coolant channel on the margins for instability is analysed. Figure 6-7 shows the neutral stability boundary for various hydraulic diameters in non-

dimensional and in dimensional form, for D_h = 2.5, 3.4 and 4.0 mm. The corresponding neutral stability boundary with a hydraulic diameter for a fuel assembly of SCWR is given in solid curve. Increasing the hydraulic diameter has a stabilizing effect. Few of the irregular shapes in stability map have been observed during the simulations, these are due to the change in the orifices coefficients as observes in the two-zone model. In all the MSB there is a sharp topological change which is only due to the change in the value of k_{in} and k_{out} at that particular point. Two times per stability map, these changes have been made. It has to be noted that a typical fuel assembly of a supercritical US reference design of SCWR have a hydraulic diameter of D_h = 3.4 mm.

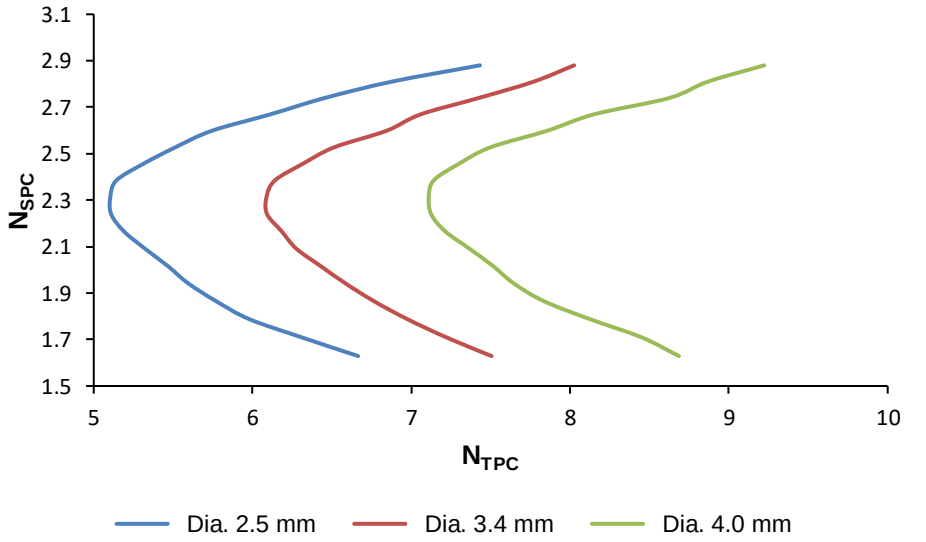

Figure 6-7: Stability map of three different channel hydraulic diameter.

6.3.3 Effects of orifice coefficients

An inlet orifice coefficient always stabilized the system strongly, as Figure 6-8 shows. This is similar to the phenomena in BWR. In the two-phase system the stability boundary depends on the pressure loss distribution in heavy fluid region (i.e. before the boiling boundary reached, or the subcooled liquid) and the region of lighter fluid which is above the boiling boundary on the other hand, for the super critical case, the subcooled liquid region corresponds to the high-density region before the fluid is heated beyond the pseudo-critical point. Any device, which increases the pressure loss of the heavy liquid region, increases the so-called in-phase pressure loss. On the

contrary, the effect of a flow resistance at the channel outlet (or also called out-of-phase pressure loss) is strongly destabilizing. Strong care must be taken with pressure losses at the outlet or the upper part of the coolant channel. Since an in-phase pressure loss is the most sensitive parameter for stabilizing a supercritical flow channel, inlet orifices coefficient can be customized to assure stable operation with respect to DWOs for otherwise unstable channels.

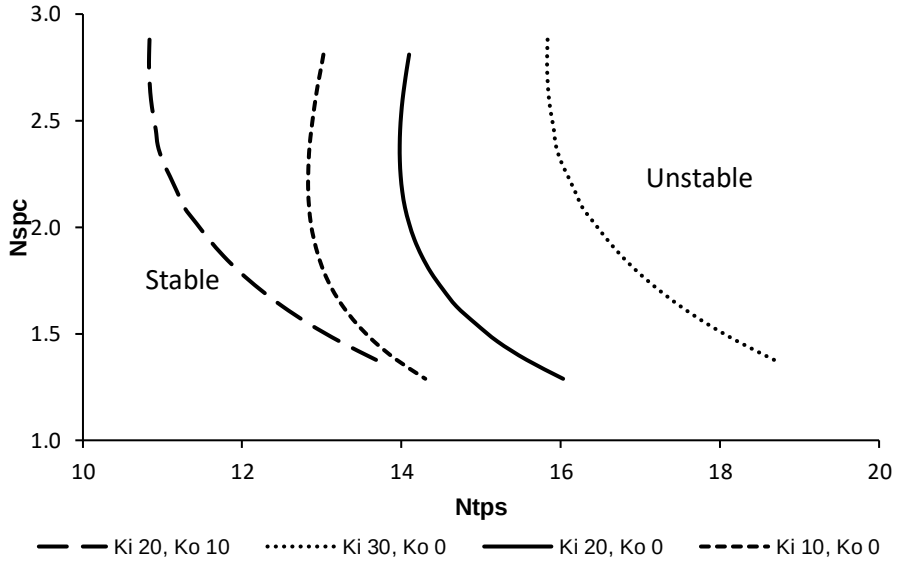

Figure 6-8: Stability map of four different sets of orifices coefficients

6.4 Comparisons of two-zone and three-zone model

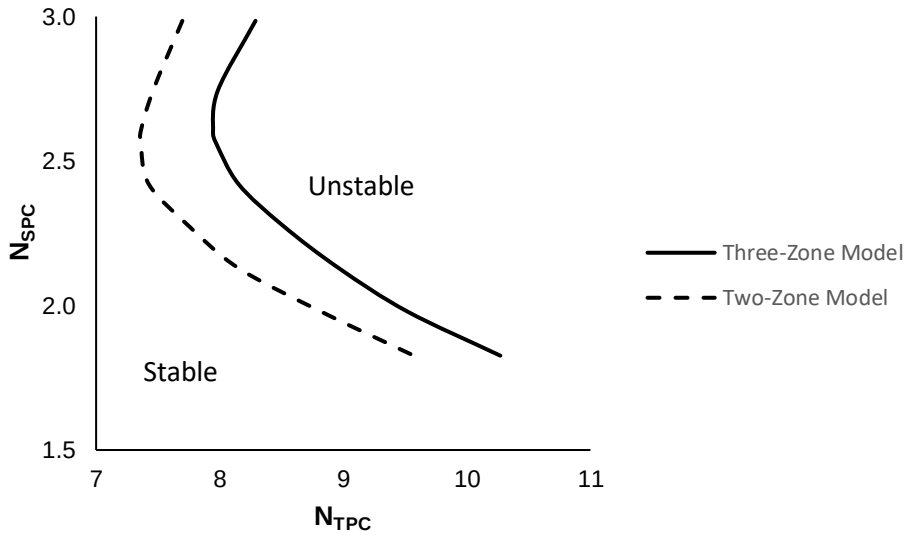

Figure 6-9: Stability map comparing two- zone and three-zone model.

In Figure 6-9 the stability maps have been compared between the two models of LPM. After rectifying few elementary problems in the earlier model (Zhao et al., 2006) which is given in Section 6.2.1, it has been found that two-zone LPM is more useful considering the prime objective of the current work.

As seen from the Figure 6-9, that the difference between two-zone and three-zone model stability maps are within the convincing range of ±10%. Hence considering the complexity and computation expanses of three-zone model, it is recommended that two zone LPM is more appropriate. The three-zone model used in this work is basically a grid impendency test, based on that a more real two-zone model is finally proposed for rest of the works. As the purpose of both the model is to give the qualitative information about the stability, therefor the two-zone LPM work more efficiently as compared to three-zone model.

6.5 Conclusions

A reduced-order model, also called lumped parameter model (LPM), with three zones is proposed in the present study to ascertain the stability characteristics of SCWR. Acknowledging the complexity associated with

handling the complete set of conservation equations and numerical models thereof, momentum and energy conservation equations are integrated following the CI method, converting the PDEs to a set of algebraic equations and ODEs. The resultant lumped parameter model is employed to envisage both the linear and transient stability behavior of a heated supercritical channel. Stability maps predicated by the transient simulation with LPM and linear stability analysis show excellent match, as expected. Parametric effects on the stability threshold have been investigated and major conclusions are the following.

a) Increasing the heated channel length has destabilizing effect on the system, which is quite common in boiling channels also.

b) Stabilizing effect on the system has been observed by increasing the hydraulic diameter.

c) Increase in inlet orifice coefficient has stabilizing effect whereas the reverse can be observed for the outlet orifice.

d) There is only ±10% enhancement in the MSB by using three-zone model as compared to the two- zone, hence later one is more suitable for further study.

The results reported here predict the stability behavior of the SCWR, considering three-zone LPM only.

Chapter 7 NONLINEAR DYNAMICS AND BIFURCATION ANALYSIS

7.1 Introduction

Supercritical water experiences effective changes in thermodynamically and transport properties nearby the pseudocritical boundary. Therefore, the SCWR will exhibit colossal variation in density across the core, creating it assailable to density wave instability, similar to BWRs (Blázquez et al. 2013; Gajev et al. 2013; Peng et al. 1986), compelling emphasis on passive safety design. Consequently, a number of researchers have studied the stability response of supercritical flow systems in the recent past following various approaches, with more preference towards natural circulation loops.

The linear stability analysis is computationally fast, which locates marginal stability boundary based on eigenvalue approach. Linear stability analysis characterizes the system behaviour for small perturbation about the steady state. In order to predict the nature of system transients following large perturbations, it is necessary to conduct nonlinear stability analysis or bifurcation analysis. While nonlinear stability analysis of boiling channels has been done by several researchers (Prasad and Pandey, 2007; Mishra and Singh, 2016), such analysis for SCWR is not found in the literature. This is important because a subcritical Hopf bifurcation lead to an unstable limit cycle, which is dangerous as it, makes the system unstable for large perturbations. The autonomous shooting technique can be used to find the exact location of an unstable limit cycle, as was done by (Durga Prasad and Pandey, 2008). However, most of the researchers (for example, Mishra and Singh, 2016) inferred the existence of an unstable limit cycle by simulating the transients for small and large perturbations, and did not locate it in the state space by the shooting method.

Present work, therefore, focuses on understanding the thermohydraulic, coupled neutronic-thermalhydraulic stability behaviour of a forced flow heated channel carrying supercritical water, and envisages the effect of associated system parameters on stability boundaries employing both linear and nonlinear stability analysis. Reduced order models are computationally less expensive compared to finite-difference-kind of approaches and hence are often preferred to obtain a first estimate. Accordingly, a lumped parameter-based approach is followed (Section 3.2), visualizing the channel to consist of two distinct zones, separated by the pseudocritical point

7.2 Mathematical modelling

A round forced flow channel of uniform diameter is simulated in the present study, under uniform heat flux imposed on the wall. The channel is subjected to constant mass flow rate boundary condition in both steady and transient conditions. Accordingly, the 1D conservation equations for mass, momentum and energy can be summarized by Eq. (3.5-3.7) and finally using equations from Section (3.4) for the transient study.

7.3 Results and discussion

In the present work, linear stability and nonlinear analysis (Section 3.6) are carried out using in-house code based on the MATLAB and a software MATCONT. The linear analysis provides the numbers of discreet points, which are the locus of MSB at a particular pressure, in this case at 25 MPa. The L-shaped stability map in the N_{TPC}-N_{SPC} space obtained from the analysis is shown in Figure 7-1. This result is used in the following sections for analysis of bifurcations, which lead to different types of dynamic behaviour of the system. In order to verify the predictions of linear stability analysis, numerical simulations of the system of ODEs (Eq. 3.1–3.3) are carried out for the design operating conditions, using the MATLAB ODE solver ODE15s (Mcevoy, 2009).

7.3.1 Identification of generalized Hopf (GH) points

In this study, the bifurcation analysis has been carried out by using MatCont (Dhooge et al. 2003; Mishra and Singh 2016; Meijer 2008). It

provides a continuation and bifurcation toolbox, which is compatible with the standard MATLAB ODEs representation of differential equations. The GH point obtained for the system under study is shown in Figure 7-1. Hence, it is predicted that the system will exhibit supercritical (soft and safe) and subcritical (hard and dangerous) Hopf bifurcations, respectively, below and above the GH point. This is verified by numerical simulations in the following sections.

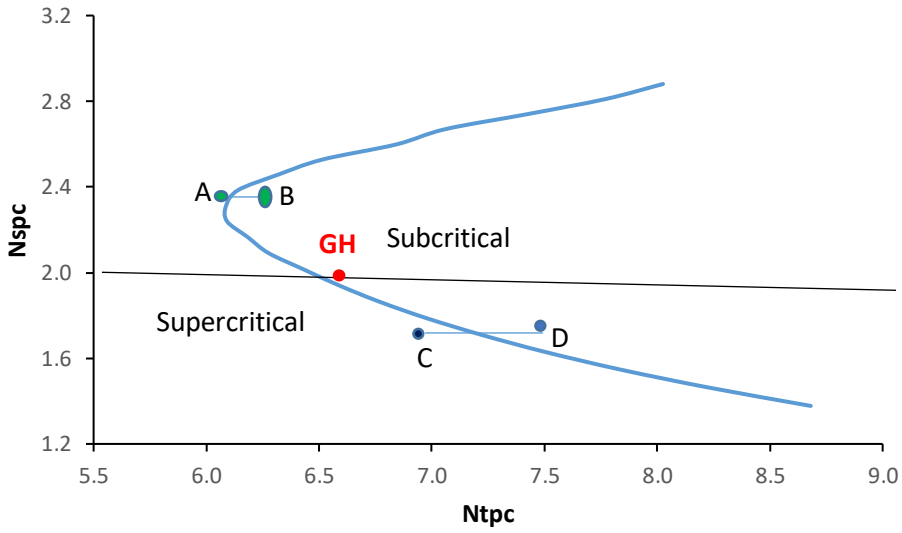

Figure 7-1: Stability map showing GH point on MSB

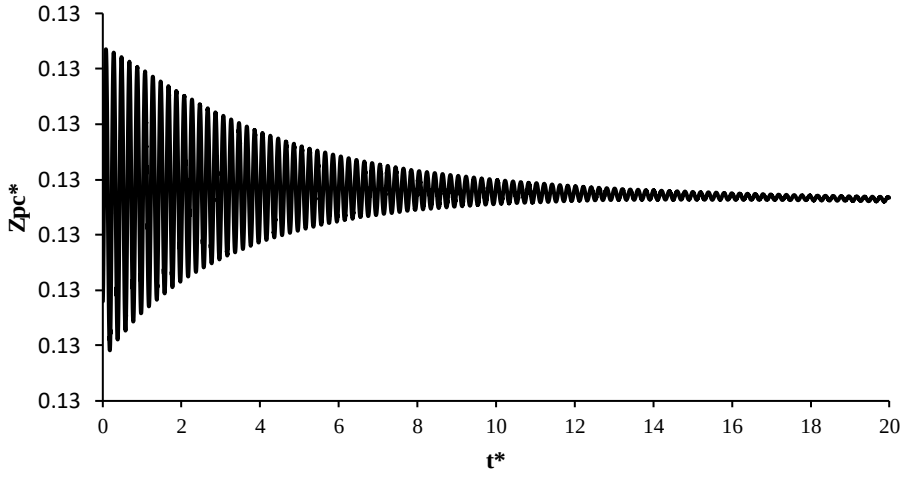

*Figure 7-2: Temporal variation of Zpc**

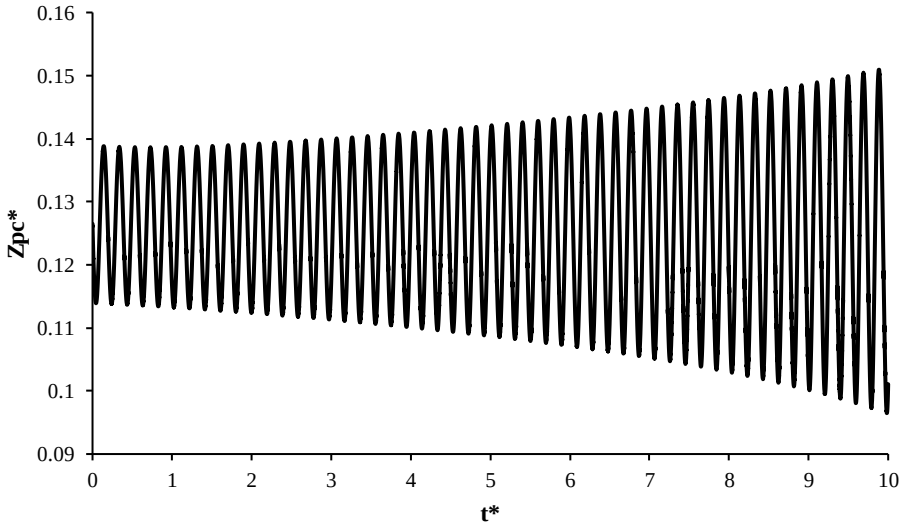

*Figure 7-3: Temporal variation of Zpc**

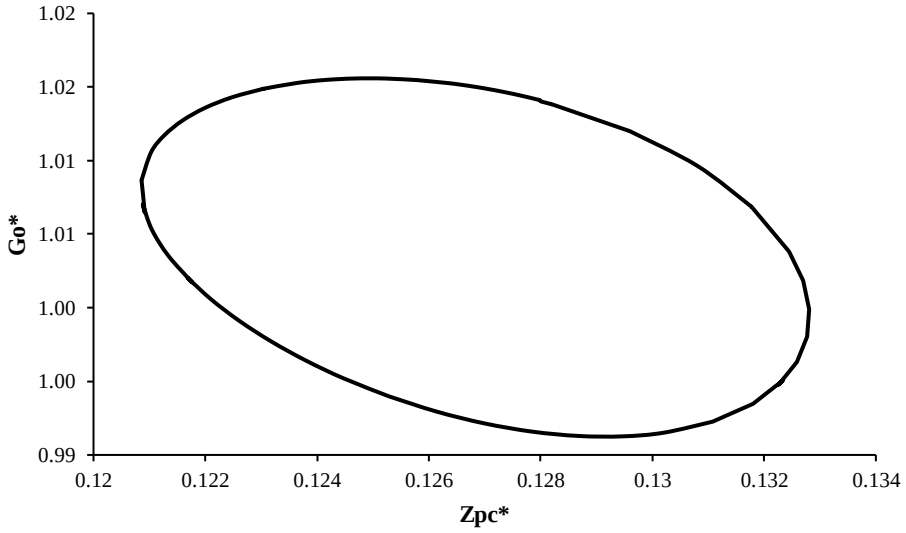

*Figure 7-4: Phase portrait of Go*and Zpc**

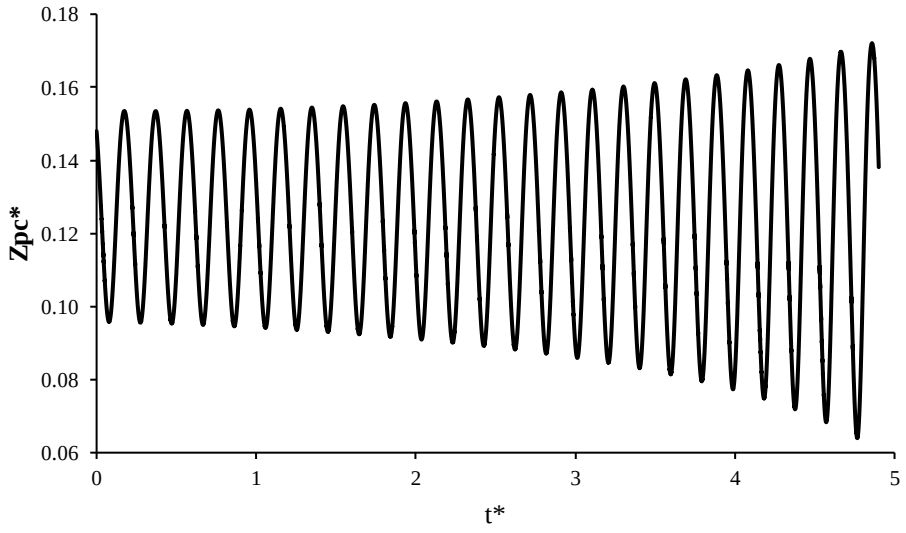

Figure 7-5: Unstable temporal variation of Zpc corresponding to point M*

7.3.2 Numerical simulation analysis in supercritical region

Figure 7-3 represents the time evolution of pseudocritical boundary of the coolant at parametric values corresponding to point D on Figure 7-1. These points are in the unstable side of MSB as delineated by the linear stability analysis. Therefore, for small perturbations, the oscillations are grow with time (Figure 7-3). However, since point D is in the supercritical region,

the oscillating trajectory ultimately follows a periodic orbit (Figure 7-4). This indicates the existence of a stable limit cycle in the unstable region (as predicted by linear stability analysis) which is the characteristic of a supercritical Hopf bifurcation

7.3.3 Numerical simulation analysis in subcritical region

Figure 7-2 represents the time evolution of pseudocritical boundary of the coolant for parametric values corresponding to point A on Figure 7-1. This point, although in the stable region, is also in the subcritical Hopf region of the stability map. Therefore, as expected, there is converging solution for a small perturbation (Figure 7-2) and diverging solution for comparably larger perturbations (Figure 7-5). This also shows that linear stability analysis is not sufficient for the complete understanding of the stability characteristic of the system, as it shows point A to be in the stable region.

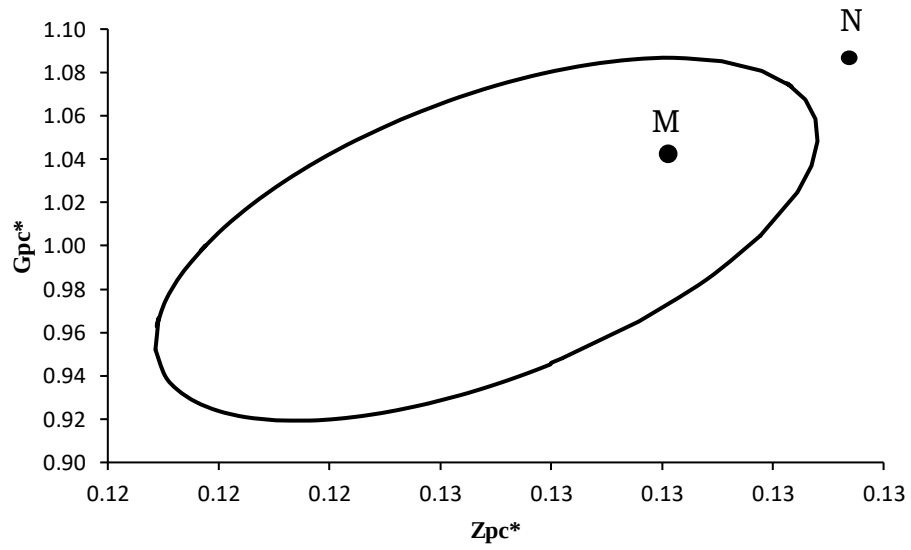

Figure 7-6: Phase portrait of Gpc and Zpc**

Unlike stable limit cycles, it is not possible to obtain the phase-portraits of unstable limit cycles by numerical integration, unless the initial point is exactly on the limit cycle. Therefore, a point on the unstable limit cycle is located, and its period estimated, by the autonomous shooting method (Park et al., 1987). This technique, based on the Newton–Raphson method and the orthogonality condition, locates a point on a periodic orbit of an autonomous

system and determines its period. Then its phase portrait (Figure 7-6) is obtained by numerical integration for one period, starting from the point found by shooting. Trajectories emanating from two initial conditions are shown in Figure 7-5 and Figure 7-2 corresponding to point N and M. The trajectory emerging from point N diverges out, whereas the trajectory from point M converges to the fixed point. This shows that the system can be unstable for large disturbances even though it is stable for small perturbations about its steady-state. Thus, relying only on linear stability analysis can have dangerous consequences if an unstable limit cycle happens to exist.

7.4 Analysis of neutronics and geometrical parameters

Stability in Ntpc–Nspc plane was studied by varying different parameters such as the fuel time constant, the density reactivity coefficient, the length-area ratio and the mass flow rate. The results are discussed below.

7.4.1 Effect of fuel time constant:

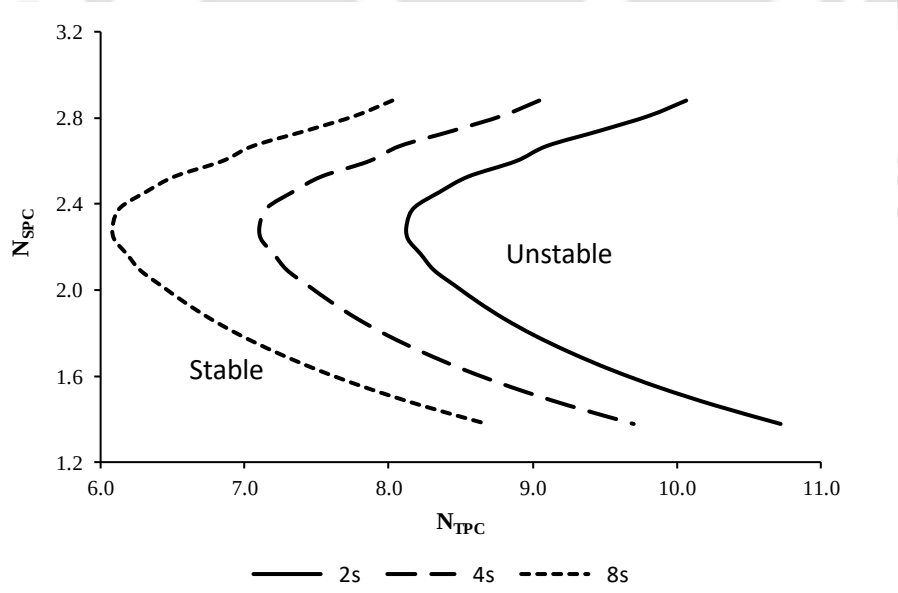

Figure 7-7: Stability map of Fuel time constant at 25MPa at density reactivity constant $10^{-5}/(kg/m^3)$

The fuel time constant will vary depending on the fuel properties, operational conditions and fuel burn-up. The fuel time constant in the present

analysis has been varied over a wide range from its normal operating value to study its influence on the stability of the system. The effect of fuel time constant on the stability of SCWR is shown in Figure 7-7. It can be observed from the figure that, with increase in fuel time constant, the threshold power for instability decreases. Hence, the stability of the reactor deteriorates with increase in fuel time constant. Previous studies have shown that changes in fuel time constant have both stabilising and destabilising effects on boiling channels (March-Leuba and Rey 1993; Durga Prasad and Pandey 2008). It is known that the stabilising effect is due to the inherent filtering of the oscillations having a frequency greater than 0.1 Hz and the destabilising effect is due to the phase delay to the feedback. For the moderate-to-low frequency thermohydraulic oscillations observed in SCWR, the effect of phase delay is more significant than the filtering effect, thus destabilising the reactor with increase in fuel time constant (T'Joen and Rohde, 2012).

7.4.2 Effect of the density reactivity constant:

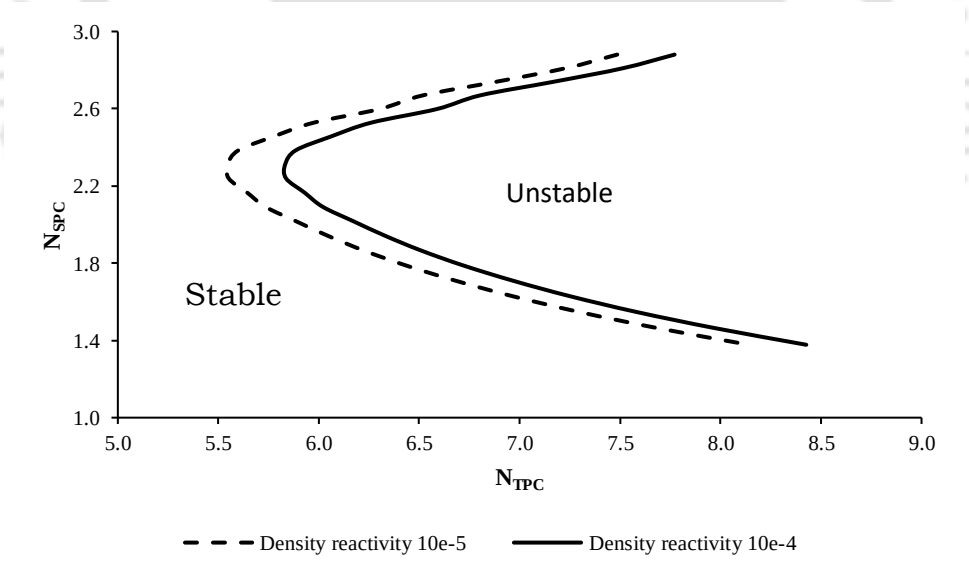

Figure 7-8: Stability map of density reactivity constant at 25 MPa and fuel time constant 2s.

From the two reactivity feedback coefficients, the density reactivity coefficient depends on the core design, while the Doppler coefficient is almost constant. The Doppler coefficient of the SCWR is comparable to that of the BWR. The SCWR density coefficient is much smaller compared to that of the

typical BWR because the water rods provide most of the moderation power. The coolant density coefficient of the SCWR is very small, only ~5% of that for a typical BWR. In the numerical simulations, the density reactivity coefficient was varied from 10^{-5}/(kg/m^3) to 10^{-4}/(kg/m^3) (Zhao et al. 2006b), in order to study its effect on the system stability. The analysis was done for a fixed value of the fuel time constant = 2.0 s. Results of the simulations are shown in Figure 7-8. It can be seen that the stability of SCWR improves slightly with 10 times increase in the density reactivity coefficient. Results from previous investigations for pressure vessel type BWRs have shown that the stability of the reactor decreases with increase in negative void reactivity constant due to the increase in gain of the reactivity constant feedback loop (Uehiro et al., 1996; Van Bragt and Van der Hagen, 1998). This is consistent with the known fact that SCWR is less sensitive to density reactivity coefficient than BWR. The reduced sensitivity of the SCWR is due to the fact that most of the moderation power is provided by the water rods, which have small or no density fluctuation (Zhao et al. 2006a).

7.4.3 Effect of the length area ratio:

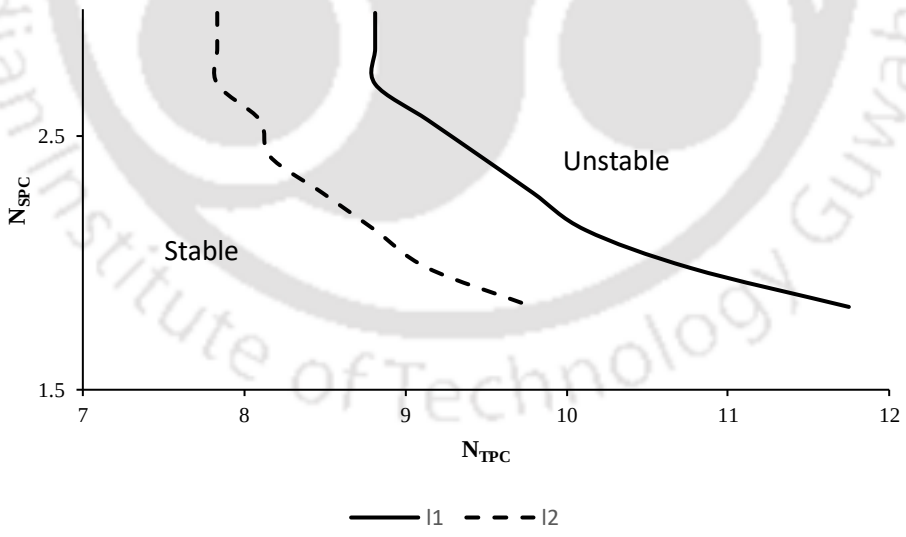

Figure 7-9: Stability map of L/A ratio of system at 25 MPa

In Figure 7-9, the MSB is shown for various values of heated channel length-to-area ratio (L/A) in the stability map. The onset of instability is at

lower Ntpc for smaller values of L/A. (Here, L1<L2, as the channel diameter is kept constant.) Increasing the ratio has a destabilizing effect. This is due to the fact that, as riser length increases, it exacerbates the "vapour like fluid" pressure drop. Similar effects in the context of BWR have been reported in the literature (Paul and Singh, 2014).

7.4.4 Effect of the mass flow rate:

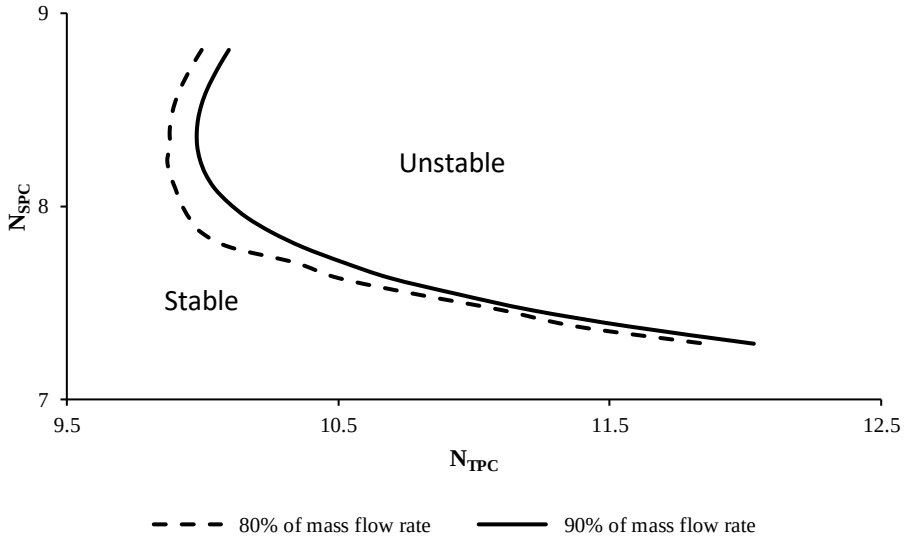

Figure 7-10: Comparisons of different mass flow at 25 MPa

Two different mass flow rates are chosen to study the effect of the mass flow rate on MSBs and the results are shown in Figure 7-10. Results demonstrate the monotonic enhancement of the MSB with the increase in the mass flow rate. It is because at a higher mass flow rate, more power is required to make the reactor unstable if the coolant has the same inlet enthalpy. The increase in the mass flow rate for the same power level increases the density and thereby, increases the gravitation pressure drop. The contributions of gravitational pressure drop are more as compared to the combined effect of other pressure drops, which makes the reactor more stable. Similar behaviour has been observed in CANDU (Dutta et al., 2015b).

7.5 Conclusions

In the present work, the linear as well non-linear stability analysis of SCWR has been carried out by employing the lumped parameter model (LPM).

The model is used to obtain the stability map in a nondimensional parameter plane. Stability maps obtained by the transient simulation with LPM and linear stability analysis show excellent match, as expected. Parametric effects on the stability threshold have been investigated and major findings are the following.

a. Nonlinear analysis is quite complicated for prototype due to the large perturbation. The same is studied here for SCWR numerically, which gives a qualitative idea of the system.
b. Effects of large perturbations have been studied on the thermal hydraulics coupled neutronics for SCWR using in-house MATLAB code and MatCont.
c. Generalized Hopf (GH) bifurcation is observed from non-linear analysis of the system. Which is use for separating the sub-to supercritical Hopf bifurcation region.
d. The range of unstable limit cycle is obtained by predicting its boundary through the shooting technique. This is important as it gives the range up to which the system is unstable in linear stable region.
e. The stability of the reactor deteriorates with increase in fuel time constant. The region is similar as described earlier.
f. The stability of the reactor is found to improve marginally with increase in density reactivity coefficient.
g. Increasing the heated channel length and area ratio has destabilizing effect on the system, which is quite common in boiling channels also.
h. Reduction in the mass flow rate has destabilizing effect on SCWR, similar to BWR and CANDU SCWR.

Based on the above observations it has been concluded that still the experimental study of large perturbation is difficult but on the same, it required for the validations for numerical works.

Chapter 8 NEUTRONICS-COUPLED THERMAL HYDRAULIC CALCULATION OF SCWR UNDER SEISMIC WAVE ACCELERATION

8.1 Introduction

Nuclear facilities are designed so that earthquakes and other external events will not expose the safety of the plant. In France, a nuclear plants are designed to withstand an earthquake twice as strong as the 1000-year event calculated for each site. It is estimated that, worldwide, 20% of nuclear reactors are operating in areas of significant seismic activity. The International Atomic Energy Agency (IAEA) has a Safety Guide on Seismic Risks for Nuclear Power Plants. Various systems are used in planning, including Probabilistic Seismic Hazard Assessment (PSHA), which is recommended by IAEA and widely accepted.

Peak Ground Acceleration (PGA) or Design Basis Earthquake Ground Motion (DBGM) is measured in Galileo units – Gal (cm/sec^2) or g – the force of gravity, one g being 980 Gal. PGA has long been considered an unsatisfactory indicator of damage to structures, and some seismologists are proposing to replace it with Cumulative Average Velocity (CAV) as a more useful measure since it brings in displacement and duration.

The logarithmic Richter magnitude scale (or more precisely the Moment Magnitude Scale more generally used today*) measures the overall energy released in an earthquake, and there is not always a good correlation between that and intensity (ground motion) in a particular place. Japan has a seismic intensity scale in shindo units 0 to 7, with weak/strong divisions at levels 5 & 6, hence ten levels. This describes the surface intensity at particular places, rather than the magnitude of the earthquake itself.

When a nuclear power plant is subjected to a huge earthquake, the seismic vibration propagates through the core internals and shakes the coolant water with measurable oscillating acceleration compared with the gravitational one. So far, the effects of seismic vibration on a nuclear power plant have been researched mainly on the viewpoint of the integrity of structure or equipment has, whereas only a few researches concerning the effects of the vibration on coolant flow has been performed. In a boiling water reactor (BWR), the coolant flow rate and void fraction will fluctuate under the oscillating acceleration. It will cause the fluctuation of the core power through the void-reactivity feedback and induce the core instability. Hirano et al. (1996), have modified the best estimate code, TRAC-BF1, to take into account the external acceleration and investigated the BWR instability due to seismically induced resonance within the scope of a point kinetics model). They have displayed that the instability was caused by the resonance between the oscillating acceleration and the core-wide oscillation, of which period was about 5 seconds. Due to the nuclear-coupled thermal hydraulic instabilities. It has been clarified that the long-period and large-amplitude oscillation beyond the previous expectation will continue for a long term if the massive earthquake anticipated as in Japan occurs. In BWRs, characteristic frequencies exist related to so-called nuclear-coupled thermal hydraulic instabilities. Indeed, neutron flux oscillation events have occurred at several BWRs, e.g. at Caorso in Italy in 1982 (Gialdi et al., 1985), at LaSalle-2 in 1988 (Commonwealth Edison, 1988; Murphy, 1988) and recently at Washington Nuclear Project-2 (WNP-2) in 1992 (WPPSS, 1992) in the USA. The oscillations, which occurred at LaSalle-2 and WNP-2, involved a core-wide (in-phase) oscillation, where the neutron flux over the whole core oscillates in the same phase.

A period of this range may be long for a seismic wave, but the power spectrum of seismic waves with this range of period is not negligibly small. Therefore, nuclear-coupled instabilities can be excited due to resonance, even though the plant is stable. On this topic, Shaug et al. (1987) have performed an

analysis with the TRACG code and concluded that the response is minimal and results in power oscillations of approximately 2% of rated.

It is important to evaluate the core instability under such oscillating condition from the viewpoint of plant integrity. The behaviours of the core and coolant are calculated in the various parameters of acceleration. The effects of the frequency, amplitude, time constant and enthalpy reactivity constant are discussed.

In this situation, the vertical seismic motion may have a much larger effect than the horizontal motion. Thus, in this study, only the vertical motion was taken into consideration. The vertical seismic acceleration was simply represented by one sine curve, and the effects of the frequency and amplitude of the sine wave and the degree of instability of the initial state, which is dependent on the power-to-flow ratio at the core, the axial power distribution and so forth, were investigated. This paper describes the methods and models applied and the major calculated results obtained.

The primary objective of this study was to supply quantitative information useful for determining to determine the significant effects of seismic wave on SCWR system using LPM. In order to meet the objective, the transient thermal hydraulic in-house code is used after modified to take into account external acceleration in addition to gravity.

8.2 Technique & methods

Assuming that the plant oscillates as a whole like a rigid body, we can introduce the external acceleration term by adding to the gravitational acceleration term in the motion equation ((Hirano and Tamakoshi, 1996). An analysis model is composed by considering 1-dimensional components (e.g. pressure tube, fuel rod). For the 3-dimensional components, the external acceleration vector is directly added to the gravitational acceleration vector. The 1-dimensional differential form of the momentum equation can be written as,

$$\frac{\partial G}{\partial t}+\frac{\partial}{\partial z}\left(\frac{G^2}{\rho}\right)=-\frac{\partial p}{\partial z}-\rho(g-a_z)-\left[\frac{f}{D_h}+2K_{in}\delta(z)+2K_{ex}\delta(z-L)\right]\frac{G^2}{2\rho} \quad 8.1$$

The non-dimensional equation form of the above momentum equation is

$$\frac{\partial G^*}{\partial t^*}+\frac{\partial}{\partial z^*}\left(\frac{G^{*2}}{\rho^*}\right)=-\frac{\partial p^*}{\partial z^*}-\frac{\rho^*}{N^*N_{Fr}}-[N_{Eu}+K_{in}\delta^*(z^*)+K_{ex}\delta^*(z^*-1)]\frac{G^{*2}}{\rho^*} \quad 8.2$$

Where, $N^{*-1}=\frac{a_z}{\omega}$; *where ω is peak sesmic oscillation frequency*

8.3 Input model

Three initial conditions were prepared. In case 1, the core power and mass flow rate were assumed to be 49% and 30% of each respective rated value. The axial power profile shown in Figure 2 was applied (Hirano and Tamakoshi, 1996), condition corresponds to the maximum power condition to which a stability analysis is performed in the licensing process of reactors. In case 2, the power and mass flow rate were the same as those in case 1, but the axial power profile was assumed to be fiat. In case 3, the core power was increased to 54% with fiat axial power profile. Therefore, case 1 is the most stable and case 3 the most unstable of the three.

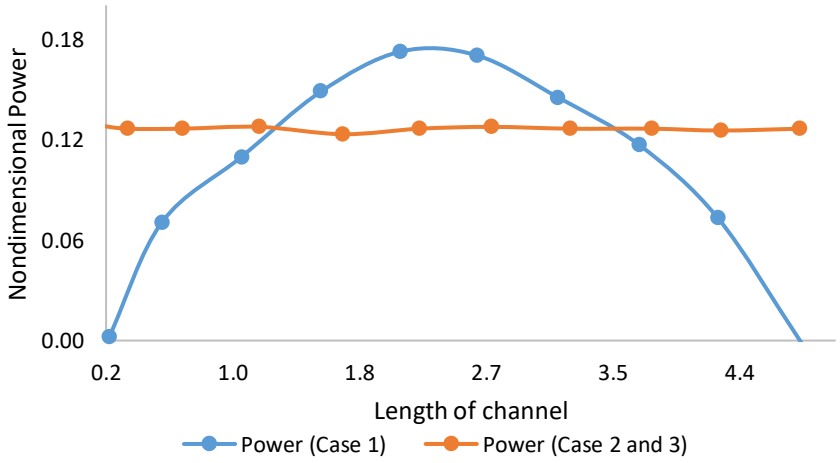

Figure 8-1: Input power profile distribution at steady state

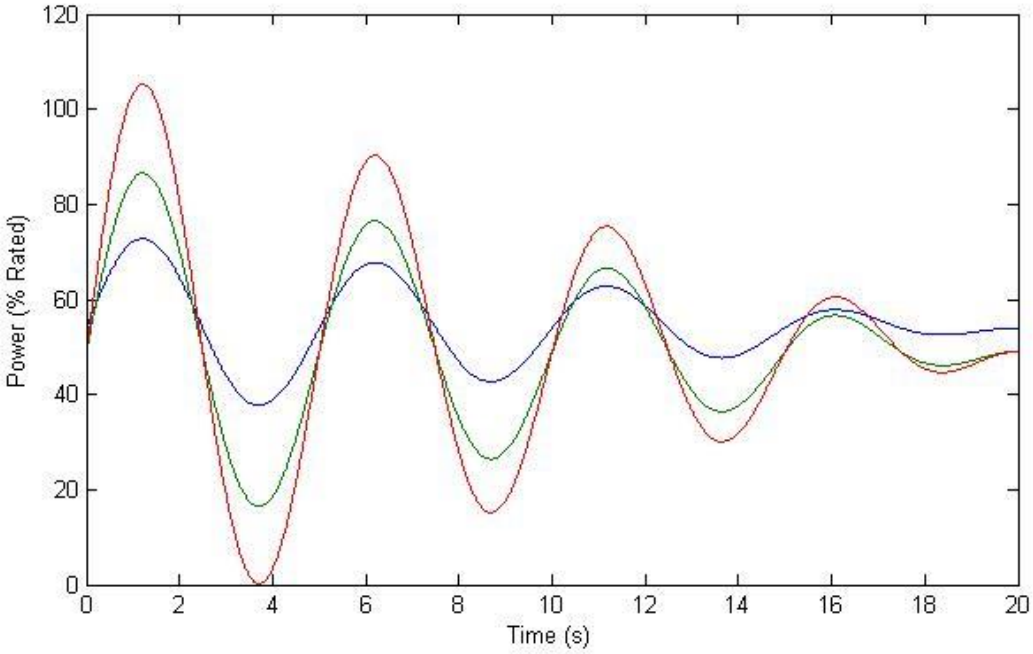

Figure 8-2: Core power transients after step change in pressure in BWR analysis

In order to characterize the degree of stability, the power response to the step change in pressure at the steam outlet was calculated for the three cases. The results are shown in Figure 8-3, where the pressure was increased by 0.07 MPa (Hirano and Tamakoshi, 1996) at time zero. From this figure, the decay ratio R, which is defined as the ratio of the second peak height to the first peak height, was estimated. The estimated values of the decay ratios are 0.44, 0.63 and 0.74 for cases 1, 2 and 3 respectively. As expected, case 1 is the most stable and case 3 is the most unstable. It should be noted that the characteristic periods of these three cases could be identified from this figure as approximately 5 s. These initial states are summarized in Table 8-1.

8.4 Modelling of seismic acceleration:

In order to avoid any complexity, a sine curve was assumed for the external acceleration in the vertical. In order to avoid any complexity, a sine curve was assumed for the external acceleration in the vertical direction as,

$$a_z = a^* \sin(\frac{2\pi}{\tau} t) \quad (8\text{-}1)$$

Where, a_z is the seismic acceleration and a^* is the amplitude of oscillation. It is difficult to define a realistic range of the seismic amplitude a^*, since the power spectrum of the amplitude quickly decreases as the period increases to several seconds and not enough reliable data exist in this range of period. However, Ishida et al, (1989) formulated a velocity response spectrum by assuming Magnitude 8 and an epicentre distance of 50 km for an input seismic motion to study a seismically isolated fast breeder reactor where the maximum velocity was defined to be 100 kine (cm-s $^{-1}$) in the period range of 2-10 s as a conservative value. This value gives 0.13g if it is multiplied by ω assuming τ = 5 s. Based on this information, a^* =0.1 is applied as a base case value and the maximum 0.15 is taken into consideration in the sensitivity calculation in this study.

Table 8-1: Summary of initial steady state conditions

Item	**Case1**	**Case2**	**Case3**
Core power (% rate)[a]	49.0	49.0	54.0
Core mass flow rate (% rated)[b]	30.0	30.0	28.2
Power-to-flow ratio (%/%)	1.63	1.63	1.91
Axial power distribution	Curve	Flat	Flat
Core inlet temperature	560	560	553
Characteristic period (s)	5	5	5

[a]Rated power, 3575 MW.

[b]Rated core mass flow rate, 1.843 x 10^4 kg s^{-1}

8.5 Results and discussion

8.5.1 Sensitivity calculations on the degree of stability and amplitude of acceleration:

Using the input data for case 3, which is the most unstable, sensitivity calculations were performed on τ setting a * = 0.1 in Eq. (8-1). The case with on τ = 5 s, which corresponds to the characteristic period of the peak. This also implies that if the period is much shorter, for example 0.2 s, the seismic amplitude may be much larger than 0.1g in reality, but the effect may be small.

The core power assuming τ = 5 s with a* = 0.1 for cases 1, 2 and 3 is given in Table 8-1. As expected, the highest peak was calculated to occur in case 3. The heights of the first, second and third power peaks are plotted as a function of the decay ratio in Figure 8-3. It is shown that the peak heights are largely dependent on the decay ratio. This figure implies that, if the decay ratio is nearly unity, a significantly large reactivity insertion could occur. The calculated peak power heights are shown as a function of the amplitude in Figure 8-4 for case 3. It is shown that the peak power is also largely dependent on the amplitude of the imposed acceleration. It should be noted here that the height of the power peak may be largely dependent on the mesh cell width in the core region due to the effect of numerical diffusion. It was confirmed that the height increased when the number of meshes was increased. In spite of this fact, the present results do not lose any physical meaning within the scope of the present study.

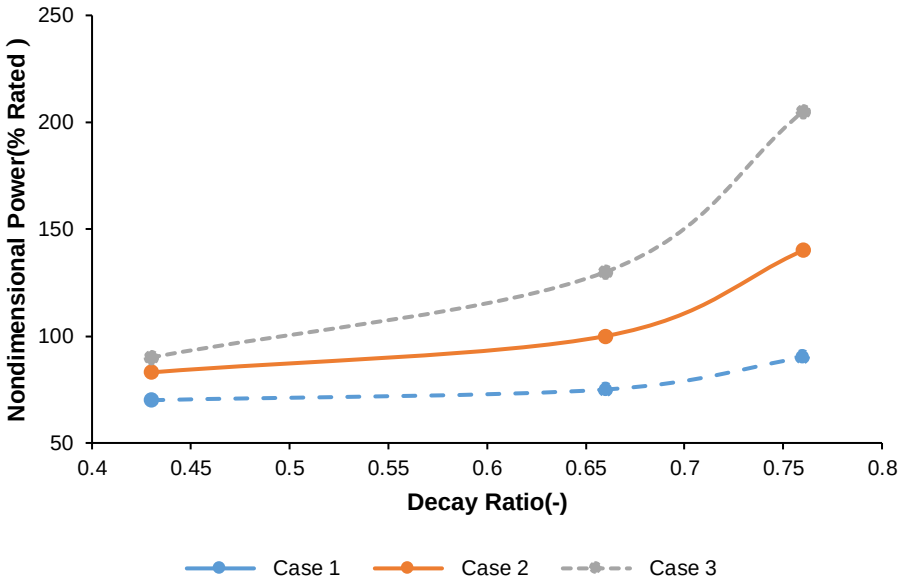

Figure 8-3: Peak power height as a function of decay ratio

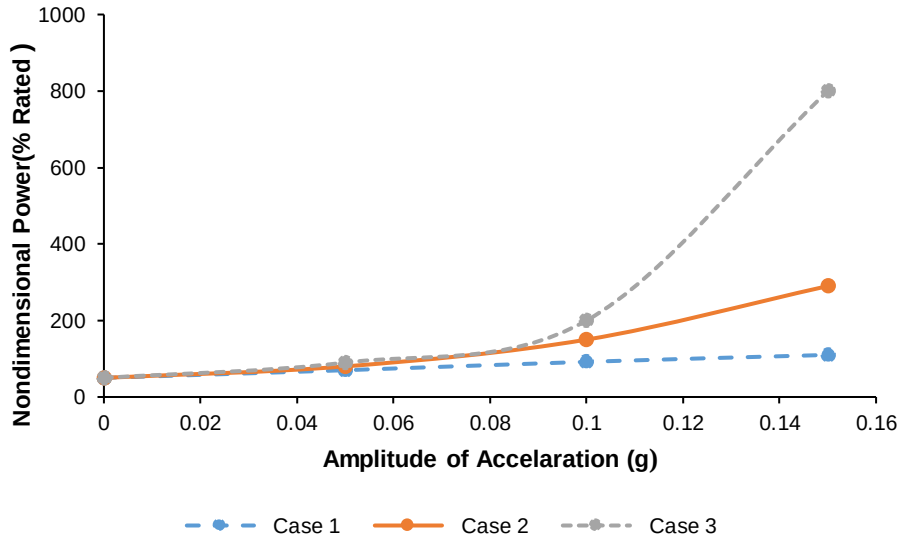

Figure 8-4: Peak power height as a function of the amplitude of the external acceleration

8.5.2 Neutronics behaviour

The system is simulated for an earthquake having a magnitude 8 and an epicentre distance of 50 km for an input seismic motion to study a seismically effect on the neutronics part of the system.

8.5.2.1 Effect of fuel time constant:

The effect of fuel time constant on the stability of SCWR is shown in Figure 8-5. The fuel time constant, in the present analysis, has been varied

over a considerable range from its normal operating value to study its influence on the stability. It has been observed that the stability of the reactor decreases with increase in fuel time constant (Figure 8-5). Previous (van Bragt and van der Hagen, 1998; Jiyun. Zhao et al.,2006) studies on BWR and SCWR have shown that changes in fuel time constant have both stabilising effect (Figure 8-6 and Figure 8-7) corresponding to point A (Figure 8-5) and destabilising effects (Figure 8-9 and Figure 8-10) corresponding to point B (Figure 8-5) respectively. Figure 8-8 shows the MSB corresponding to point C in Figure 8-5. It was found that the stabilising effect is due to the inherent filtering of high frequency oscillations, and the destabilising effect is due to the phase delay to the feedback, these are the similar effects, which has been observed in the previous study. For the moderate frequency thermohydraulic oscillations observed in the SCWR, the phase delay is more significant to destabilise the reactor for an increase in fuel time constant than the filtering effect.

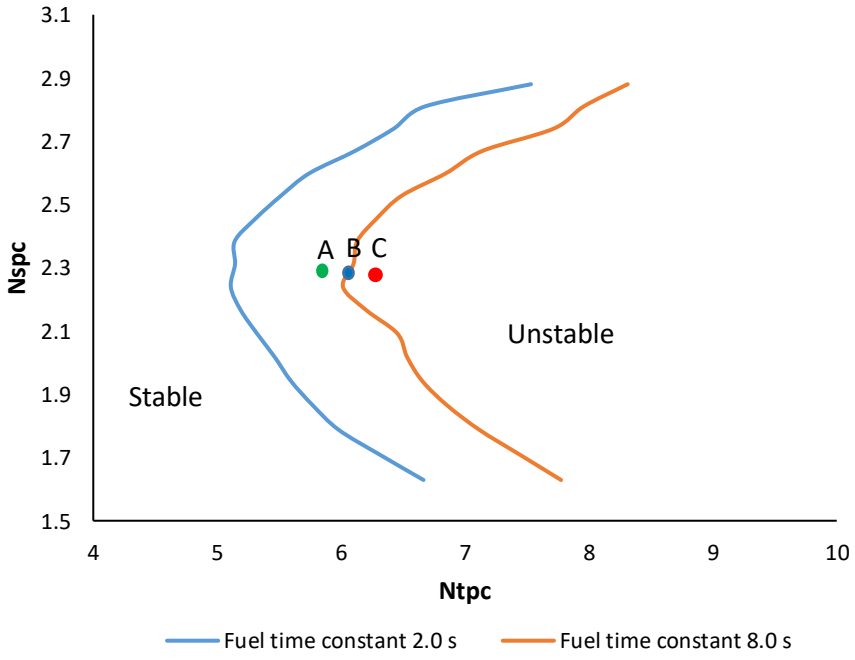

Figure 8-5: Stability map of two different Fuel Time Constants

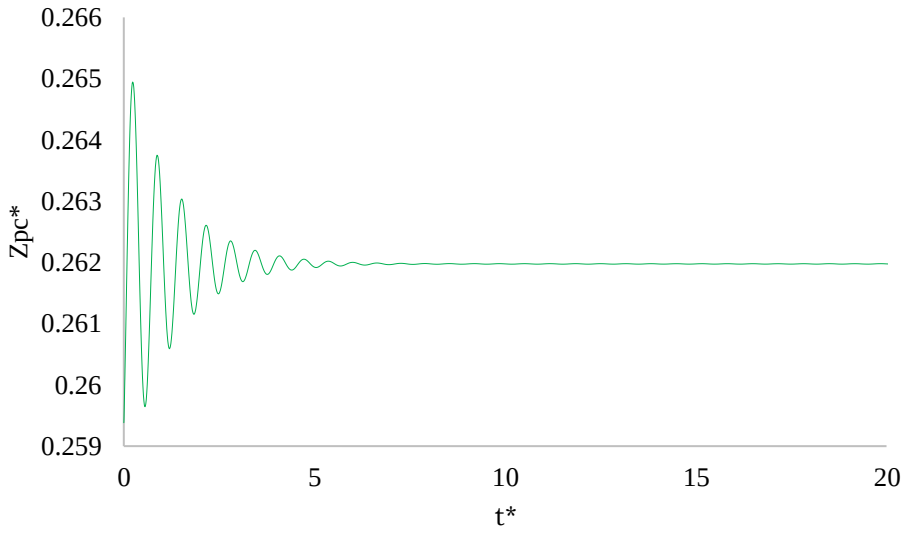

Figure 8-6: Transient plot of Z_{PC} in stable zone*

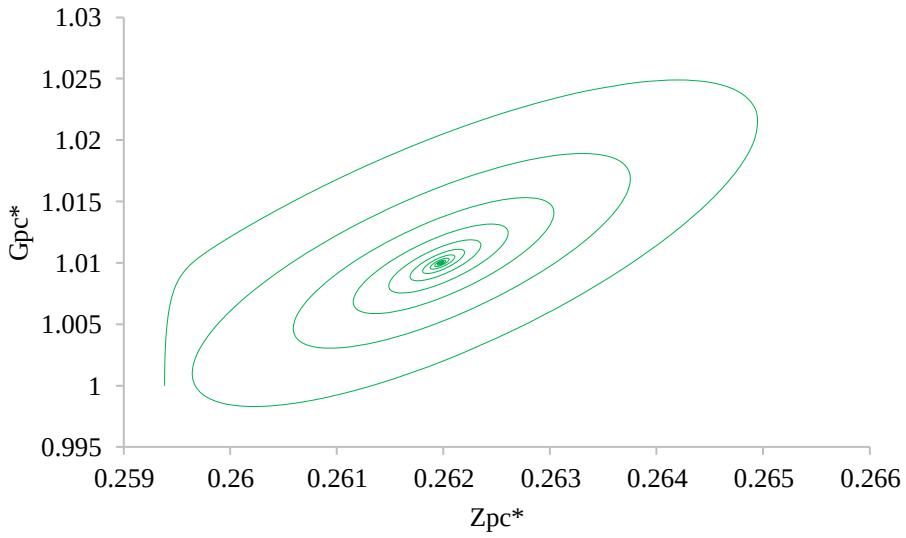

Figure 8-7: Phase portrait of Z_{PC} vs G_{PC}* in stable zone*

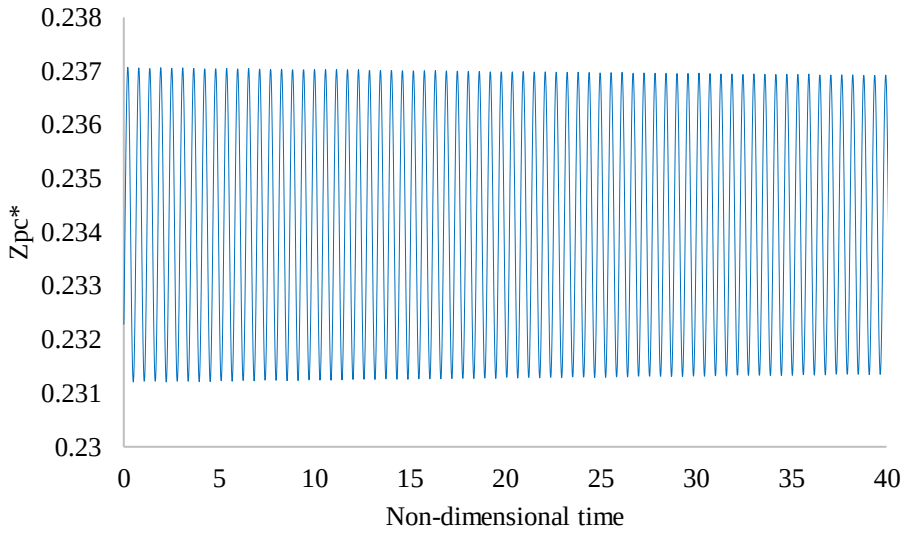

Figure 8-8: Transient plot of Z_{PC} at marginal stable boundary*

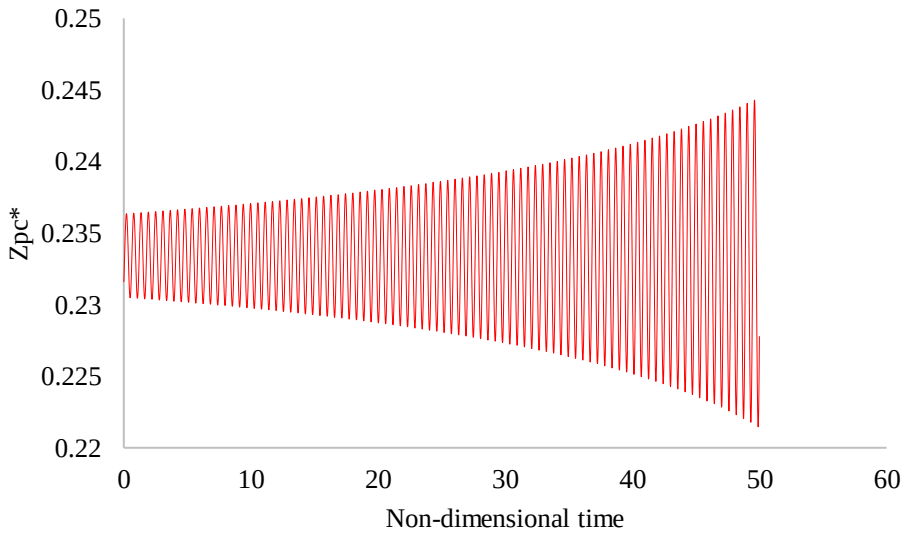

Figure 8-9: Transients plot of Z_{PC} in unstable zone*

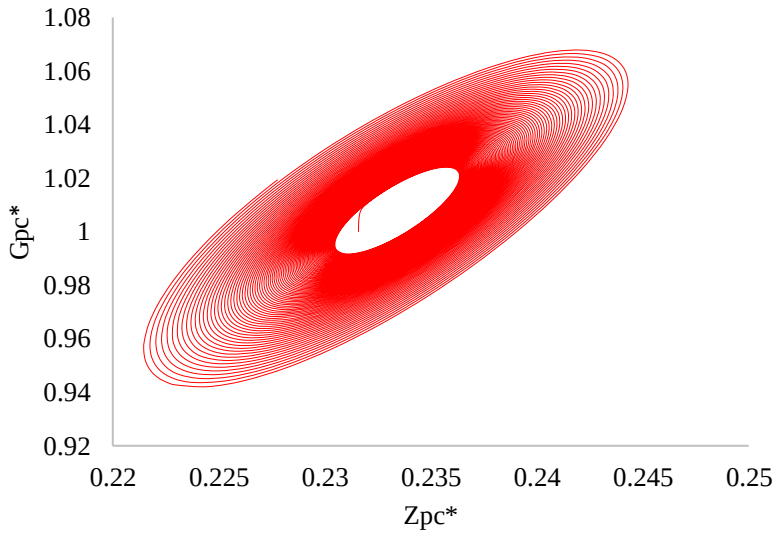

Figure 8-10: Phase portrait of GPC vs ZPC* in unstable zone*

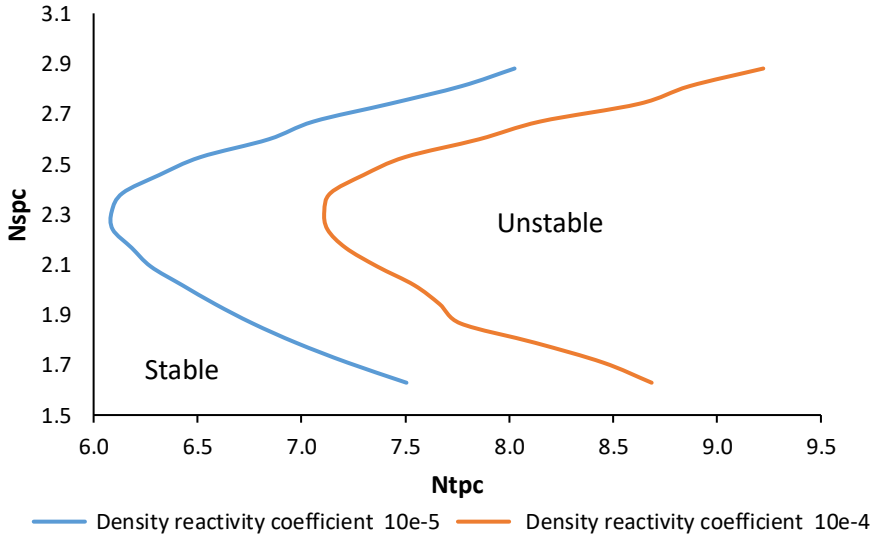

Figure 8-11: Density reactivity coefficient at fuel time 2 s.

8.5.2.2 Effect of density reactivity coefficient

The nuclear-coupled feedback has an unstable effect for the system with a large time constant. With an increase of density reactivity coefficient, periodic and chaotic oscillations may appear on further evaluates the effects of different density reactivity feedback coefficient on system stability (Figure 8-11). The results indicate that unstable regions quickly expand as the density reactivity feedback coefficient is increased. A system with a large

reactivity feedback coefficient would enhance unstable nuclear-coupled density-wave oscillations. From the viewpoint of plant control, it should not be too large or too small. If it is too large, the SCWR is unstable and the manageability is worse because the power is more sensitive to the flow rate. On the other hand, if it is too small, the manageability is also worse because the density feedback is smaller and then the main steam temperature is more sensitive to the flow rate.

8.5.2.3 Power control by feed water flow rate

The feasibility of another control system is studied, in which the control rods control the main steam temperature and the core power and the feed water pumps, respectively. This control system can also keep the SCWR stable (Satou et al., 2011). It is observed that there are not many significant changes occurred due to seismic effect.

8.6 Kanai–Tajimi model

After using, the simple sinusoidal model to simulate the artificial ground wave, an another more realistic earthquake model, which is Kanai-Tajimi model, has been used to see the more realistic analysis of SCWR. This model has non-stationary amplitude and frequency, which is able to accurately capture the non-stationary features of actual earthquake accelerograms. Most of the earthquake characterization models presented in literature have used the Kanai-Tajimi (Rofooei et al., 2001) power spectral density (PSD) function, or its variations, to generate the acceleration time history. The Kania-Tajimi power spectral density function is in the following form.

$$D(w) = a\left[\frac{\left\{1 + 4b^2\left(\frac{w}{c}\right)^2\right\}}{\left\{1 - \left(\frac{w}{c}\right)^2\right\}^2 + 4b^2\left(\frac{w}{c}\right)^2}\right]D_0 \qquad 8.3$$

$D(w)$ is a PSD function, where w is the natural frequency of linear oscillator which ranges 2.1 rad/sec- 21 rad/sec corresponding to natural time period

T=3.0 s- 0.3 s, a= 0.2196/t; t= equivalent duration of strong motion earthquake = 30 sec; b=0.64; c= 15.56.

The Figure 8-12 and Figure 8-13 shows the artificial seismic wave simulation using Kania-Tajimi model. A Matlab function is created which generate one-time series corresponding to acceleration record from a seismometer. The function requires seven inputs, and gives two outputs. The time series is generated in two steps: First a stationary process is created based on the Kanai- Tajimi spectrum, then an envelope function is used to transform this stationary time series into a non-stationary record (Guo and Kareem, 2016; Rofooei et al., 2001). From Figure 8-12, it has been observes that peak amplitude of the earthquake lasts for 5 second. Based on the given model further study has been made.

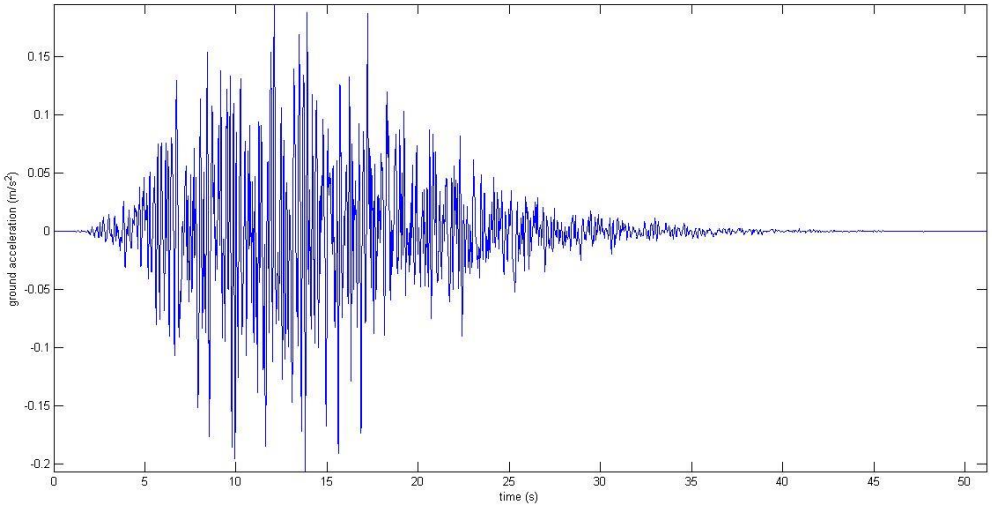

Figure 8-12: Transient Ground acceleration plot using Kania-Tajimi power spectral density

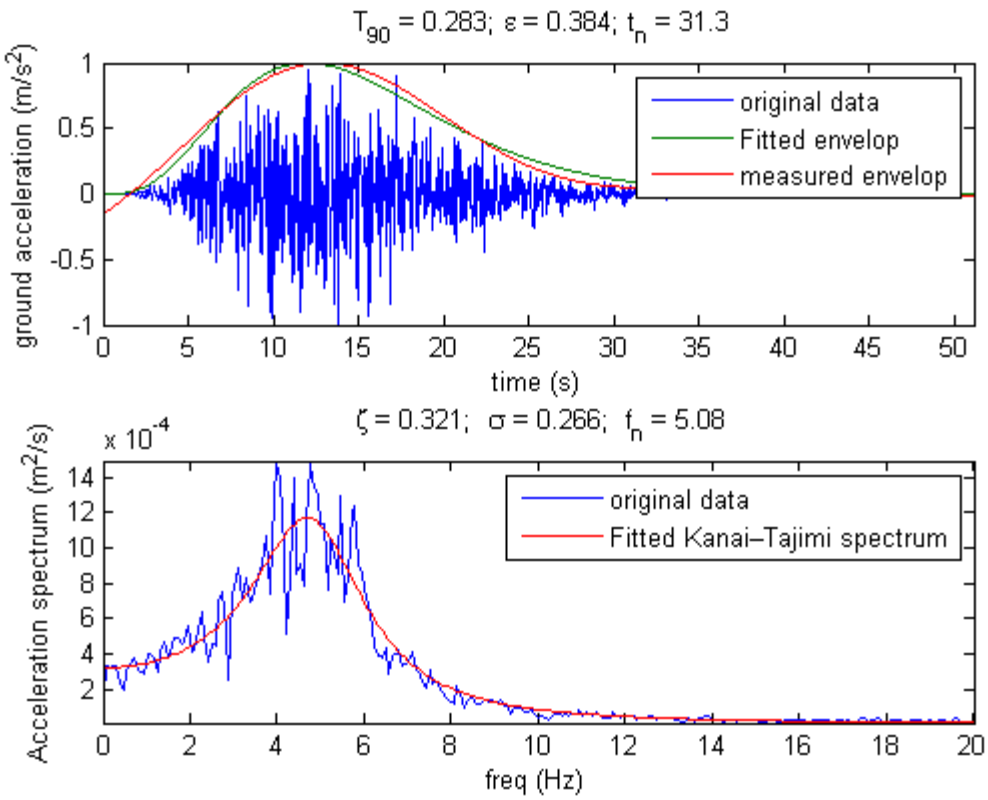

Figure 8-13: Fitted envelop on orifinal data an particular parametric value

8.7 Simulation of ground acceleration record

Time series of acceleration records are simulated using a stationary process that is "weighted" by an envelope function. The initial signal is used as a "Fitted Envelop"(Guo and Kareem, 2016; Rofooei et al., 2001). The function that fulfils this procedure is further simulated. Then, try to retrieve the parameters of the simulated seismic.

8.7.1 Effect of density reactivity constant

As discussed in section (8.5.2.2), the nuclear-coupled feedback has an unstable effect for the system with a smaller time constant. With an increase of density reactivity coefficient, periodic and chaotic oscillations may appear on further evaluates the effects of different density reactivity feedback coefficient on system stability (Figure 8-14). The results indicate that unstable regions quickly expand, as the density reactivity feedback coefficient is decreases. Figure 8-15 and Figure 8-16 shows the behaviour of point 'A' in Figure 8-14. The two figures are corresponding phase portrait and transient

of two state variables. Similarly, Figure 8-17 and Figure 8-18 are the phase portrait and transient plot of state variables corresponding to point 'B' of Figure 8-14. A different behaviour of density reactivity coefficient has been observed here. The system blow-off at the design value of density reactivity coefficient, but shows the dynamical behaviour of the system at considerable smaller value of this coefficient.

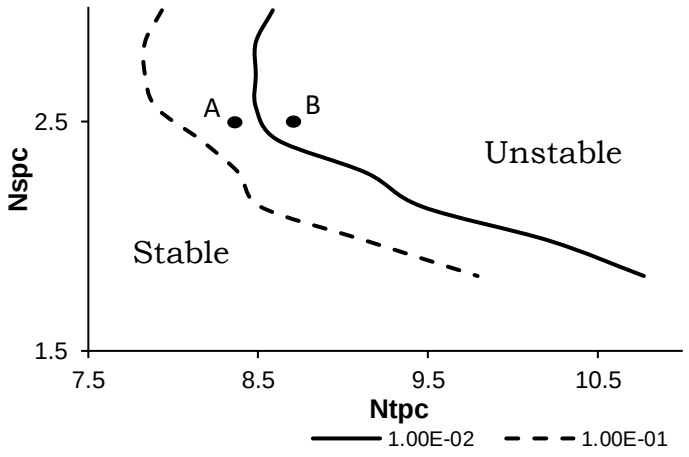

Figure 8-14: Stability map of Density reactivity constant

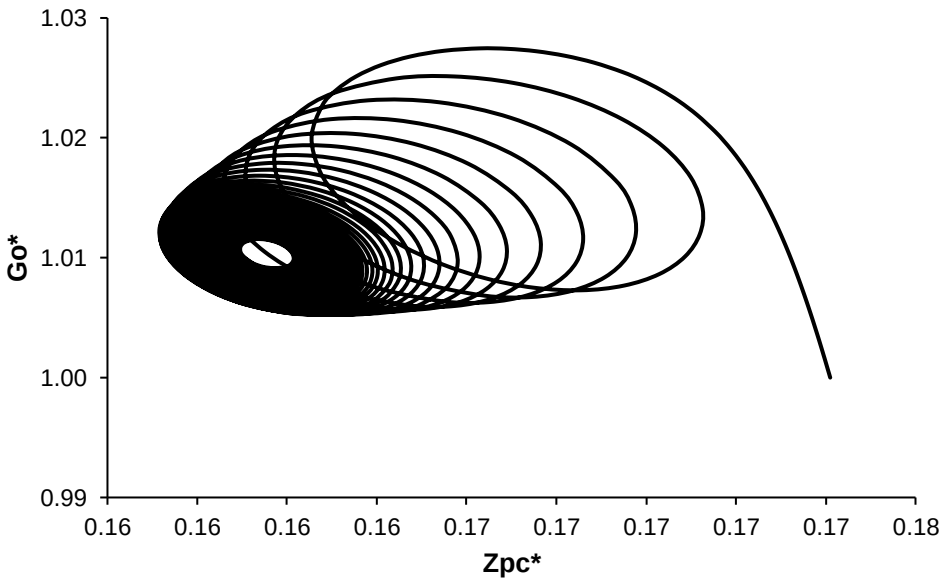

Figure 8-15: Phase potrate of G_O and Z_{PC}* corresponding to point "A"*

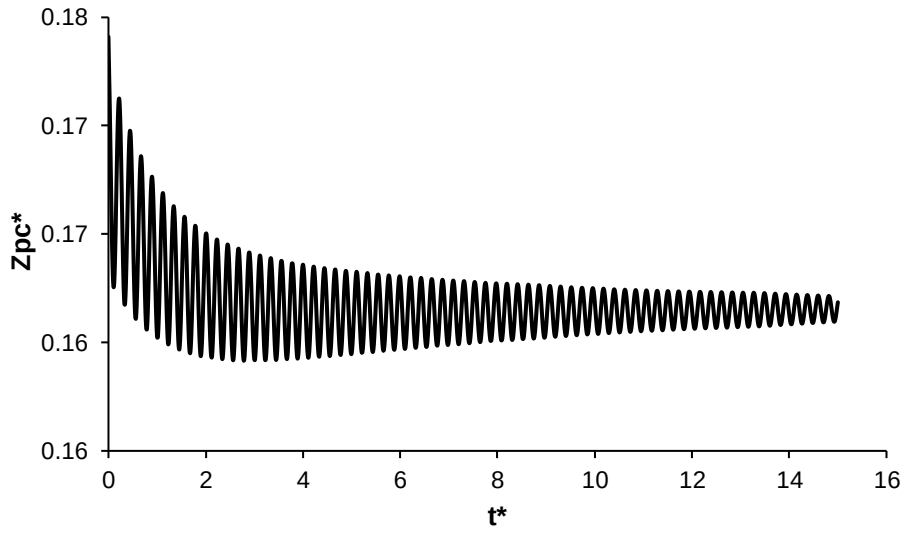

Figure 8-16: Transient of Z_{PC} corresponding to point "A"*

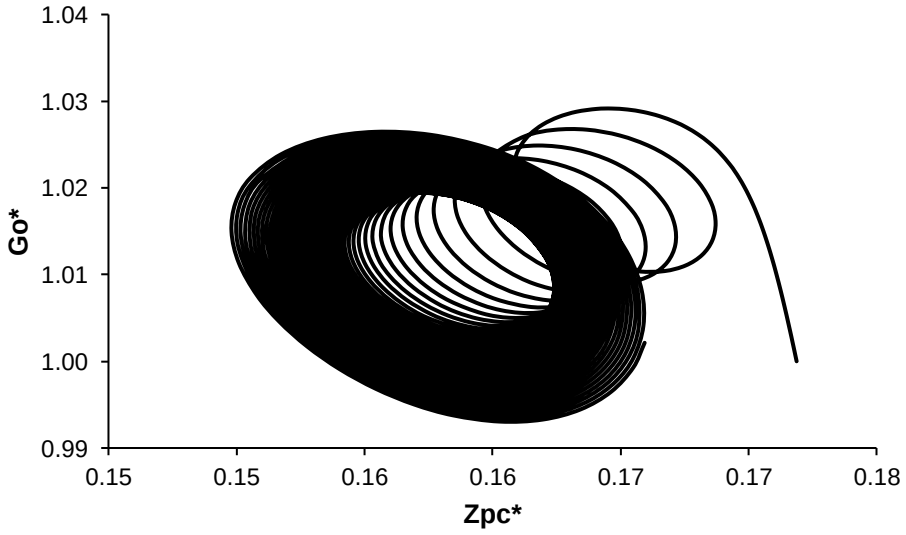

Figure 8-17: Phase potrate of G_O and Z_{PC}* corresponding to point "B"*

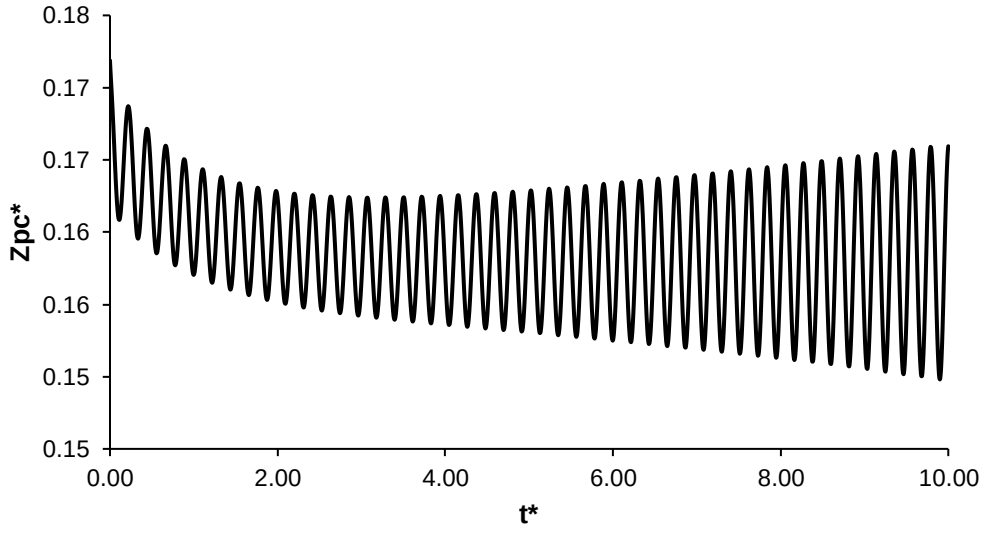

Figure 8-18: Transient of Z_{PC} corresponding to point "B"*

8.8 Conclusions

When a nuclear power plant is subjected to a huge earthquake, the seismic vibration propagates through the core internals and shakes the coolant water with measurable oscillating acceleration compared with the gravitational one. Hence, in this work, a preliminary effort is made which is based on the stability analysis on SCWR due to two different seismic oscillation models; finally, following observations have been established.

a) LPM is used to study the transient response of the system when external forcing, in this case seismic wave is applied.
b) LPM is used first time to study Seismic effect on SCWR.
c) Results can be used as a preliminary data for further stability analysis.
d) More realistic modal has been used for stability analysis of SCWR. In which the real seismic data has been used for the simulations
e) Coupled neutronics and thermal hydraulic stability analysis has been done.
f) Stability map has been plotted for T-H and neutronics parameters.
g) Most of the thermal hydraulic and neutronics parametric study giver traditional nature of stability.

h) System with a large density reactivity feedback coefficient in Kanai–Tajimi model would enhance unstable.

Chapter 9 SUMMARY AND CONCLUSIONS

Present thesis work primarily focuses on the analysis of flow instability in one of the most powerful concepts under the Generation-IV nuclear reactor; SCWR. The work mainly consists of numerical studies on flow instabilities in a forced circulation supercritical system. Thermal-hydraulic as well as coupled neutronics-thermohydraulic instabilities. Linear, Nonlinear oscillations, and bifurcations have also been investigated. Parametric effects on the stability, oscillation modes, bifurcation characteristics, in supercritical forced circulation reactors have been investigated. Furthermore, a downscaled model is developed to study the complex phenomena in laboratory conditions; moreover, a scaled method is proposed which is useful for the study of both the natural as well as the forced circulation system. For further analysing about the stability of the system, a simple and effective model has been developed as the Lumped Parameter Model (LPM). Using LPM, a linear and well nonlinear stability analysis has been done for the various parametric conditions. Finally, the stability analysis due to the seismic effect on SCWR has also been considered by using the same LPM.

9.1 Summary

- ✓ Performing experiment at the lab with supercritical water, particularly for the stability analysis, is a difficult task, due to the high level of pressure and temperature involved. That necessitates scaling analysis for the development of reduced-scale models to simulate true-scale prototype under lab condition. The study, therefore, attempts to develop a scaling methodology focused on stability analysis and to identify a less-restrictive model fluid, while proposing generalized scaling rules pre-serving the phenomenological physics. US reference design of SCWR is selected as the prototype. Four characterizing dimensionless groups are recognized from the non-dimensional conservation equations un-der imposed pressure boundary condition, while the

system pressure for the model fluid is identified noting the region of similarity on the plane of non-dimensional density and non-dimensional pressure. Two-zone LPM is used encompassing the thermal-hydraulic, fuel dynamics and power dynamics equations, which are subsequently employed for linear stability analysis and transient simulations. Both approaches produced the same stability maps, leading to a generalized representation. Several other model fluids have been studied, such as CO2, Ammonia and R23 and R134a. Among all R134a is concluded to be the most suitable model fluid from both power and pressure point of view.

- ✓ The dynamic characteristics of SCWR is different from existing reactors due to the supercritical conditions of the coolant. This necessitates the study of the stability behaviour of SCWR, which requires a dynamic model of the reactor. A simple unsteady LPM for coupled neutronics-thermohydraulic transients for SCWR has been developed. The LPM includes point reactor kinetics for neutron balance and a two-region model for fuel and coolant thermal hydraulics. The results of dynamic simulation and linear stability analysis are shown by plotting stability maps. These results show good agreement with each other. Furthermore, to study the effect of parameters on the stability of the system, variations of some geometric, control and neutronics parameters are analyzed. The stability maps predicted by the LPM are also compared with those obtained with RELAP5 code and are found to show similar trends.
- ✓ It is very difficult to study the stability of a complex system such as SCWR by linear stability analysis. It is valid for local stability analysis; nonlinear stability analysis is essential for the global stability analysis. Therefore, a simple unsteady LPM for SCWR has been used. It includes point reactor kinetics for neutron balance and a two-region model for fuel and coolant thermal hydraulics. Regions of stable and unstable operation are identified in the parameter space by linear stability analysis. Bifurcation analysis is carried out to capture the non-linear

dynamics of the system. Generalized Hopf (GH) points are, and parameter ranges for supercritical (soft and safe), and subcritical (hard and dangerous) Hopf bifurcations are identified. The type of transient behavior of the system for finite (though small) perturbations are predicted based on this analysis. The existence of predicted limit cycles is confirmed by numerical simulation of the nonlinear ODEs, using the shooting technique in case of unstable limit cycles. Furthermore, the effects of geometric, control and neutronics parameters on the stability of the system are studied.

- ✓ To know the extents of stability margin by increasing the numbers of nodes, the study has been done using the three-zone model. An improvement on that in the form of a three-region model is proposed, which was found to provide a similar prediction on the stability prediction of SCWR. Therefore, present study carries out a lumped parameter base stability analysis for a heated channel with supercritical fluid following three-region model. In the current model stability analysis has been done on three geometrical parameters and their detailed stability map has been plotted for locating the stable and unstable zones.
- ✓ In this study, two types of seismic model have been analysed. The vertical seismic oscillations motion is taken into consideration. The simple sinusoidal model to simulate the artificial ground wave, an another more realistic earthquake model which is Kanai-Tajimi model has been used to see the more realistic analysis of SCWR. The vertical seismic acceleration was simply represented by one sine curve, and the effects of the frequency and amplitude of the sine wave and the degree of instability of the initial state, which is dependent on the power-to-flow ratio at the core, the axial power distribution and so forth, were investigated. This paper describes the methods and models applied and the major calculated results obtained. The primary objective of this study is to supply quantitative information useful for determining the significant effects of seismic wave on SCWR system. In order to meet

the objective, the transient thermal hydraulic in-house code is used after modified to take into account external acceleration in addition to gravity.

9.2 Conclusions

As summarized in the preceding section, a detailed investigation of parametric effects on the stability, scaling methodology and nonlinear oscillation in supercritical systems has been presented in this work. Based on these results the following conclusions can be drawn

- ✓ A new scaling approach proposed exclusively for SCWRs.
- ✓ Four different fluids are compared by equating the important dimensionless groups.
- ✓ R134a is found to be the most suitable scaling fluid from temperature, pressure and power point of view. It also leads to more compact design and poses convenient chemical properties.
- ✓ Stability behavior of the prototype with water and model with R134a is compared using both linear stability analysis and transient simulations. Both approaches are found to produce identical results.
- ✓ System pressure is found to have insignificant role from stability point of view. RELAP5 is employed for validation of the developed model and the present lumped approach is observed to produce conservative estimate of the stability threshold.
- ✓ Parametric effects on the stability threshold have been investigated and major conclusions are given below. A reduced-order model, also called lumped parameter model (LPM), is proposed in the present study to ascertain the stability characteristics of SCWR.
    - Increasing the heated channel length has destabilizing effect on the system, which is quite common in boiling channels also.
    - Stabilizing effect on the system has been observed by increasing the hydraulic diameter.
    - Increase in inlet orifice coefficient has stabilizing effect whereas the reverse can be observed for the outlet orifice.

- System pressure is found to have negligible effect on the non-dimensional stability threshold.
- The stability of the reactor decreases with increase in fuel time constant.
- The stability of the reactor is found to increase with an increase in negative enthalpy reactivity coefficient.

✓ Parametric trends in 3-zone model for heated channel length, hydraulic diameter and orifice coefficients are similar to 2-zone model and the difference in the MSB is 2-8%, therefore, 2-zone model is more suitable for further study.

✓ Linear as well non-linear stability analysis of SCWR has been carried out by employing a LPM, considering thermal hydraulics as well as neutronics of the system. Based on the study, major findings are the following.

- Generalized Hopf (GH) bifurcation is observed from non-linear analysis of the system.
- The range of unstable limit cycle is obtained by predicting its boundary through the shooting technique.
- The stability of the reactor deteriorates with increase in fuel time constant.
- The stability of the reactor is found to improve marginally with increase in density reactivity coefficient.
- Increasing the heated channel length and area ratio has destabilizing effect on the system, which is quite common in boiling channels also.
- Reduction in the mass flow rate has destabilizing effect on SCWR, similar to BWR and CANDU SCWR.

9.3 Future works

Although a lots of work have been carried out by different researchers in different field of SCWR, but still a lot of effort can be done in this field for

improvement. Few of the observations and suggestions, which may be useful in future extensions of the present work, is given below.

1. This thesis presents a detailed analysis of instabilities and scaling in forced circulation systems. The knowledge generated by this study is likely to be useful for the design and operation of SCWR for further study. Based on these studies, a suitable combination of geometrical, feedback, and neutronics parameters can be designed.

2. Scaling method**,** a unified model can be made for both natural circulation (NC) and forced circulation (FC) system. SCWR safety including power at start-up and during set-down.

3. Start-up transients need to be investigated using nonlinear dynamics methods. Extensive research has been done on linear analysis of instabilities in natural circulation, there is a scope for nonlinear analysis of instabilities using the techniques of nonlinear dynamics and bifurcation theory.

4. The knowledge gained from nonlinear analysis can be used for designing better control systems and safety measures. Study of transient behaviour of SCW and scaled fluid at SC pressure. Unified stability map covering the entire parameter space and all types of instabilities.

5. Many numerical codes have been developed to simulate neutronics and thermal hydraulics, but development of user-friendly software with graphic user interface remains to be done. This will facilitate extensive numerical simulations of instabilities and thus help in improving reactor safety.

6. In the present study a high pressure lumped parameter model is used. The fluid properties are evaluated at constant system pressure. This restricts the use of this model to high pressure conditions and operational transients. In order to investigate the nonlinear dynamics

of start-up-transients, a lumped parameter model in which fluid properties are evaluated at local pressure is to be used. This needs a further study.

7. Nonlinear dynamic analysis of the SCWR using MATLAB tools and Shooting method. Using these stable and unstable limit cycle has been predicated. More detailed analysis can be possible by using some advance nonlinear codes.

LIST OF PUBLICATIONS

Journals

1. Shankar, D., Basu, D.N., Pandey, M., 2017. Development and Analysis of a Novel Scaling Methodology for Stability Appraisal of Supercritical Flow Channels. Nucl. Eng. Des. 323, 46–55
2. Shankar, D., Pandey, M., Basu, D.N., 2018. Parametric Effects on Coupled Neutronic Thermohydraulic Stability Characteristics of Supercritical Water Cooled Reactor. Ann. Nucl. Energy 112, 120–131
3. Shankar, D., Pandey, M. & Basu, D.N., 2017. Nonlinear analysis of nuclear coupled density wave instability in time domain for SCWR. Ann. Nucl. Energy (Under Revision).
4. Shankar, D., Basu, D.N., Pandey, M., 2017. Neutron-Coupled Thermal Hydraulic Calculation of SCWR Under Seismic Wave Acceleration. Nucl. Eng. Des. (Under Preparations)

Conferences

1. Shankar, D., Basu, D. N., Pandey, M., Study on Design of Scaled Down Test Facilities for Investigation of Instabilities in Supercritical Water Reactor. ICONE21-16638, In: Proceedings of 16th International conference on Nuclear Engineering ICONE-21, Chengdu, China, July 29-Aug 2, 2013.
2. Shankar, D., Basu, D. N., Pandey, M., Lumped Parameter Analysis for A Supercritical Water Cooled Reactor Following Three-Region Model, IHMTC2017-13-0950, Proceedings of the 24th National and 2nd International ISHMT-ASTFE, Heat and Mass Transfer Conference (IHMTC-2017), December 27-30, 2017, BITS Pilani, Hyderabad, India.
3. Shankar, D., Pandey, M., Basu, D. N., Coupled-Neutronic-Thermalhydraulic Stability Appraisal of Supercritical Forced Flow Channels Following Lumped Parameter Approach, Proceedings of the 16th International Heat Transfer Conference (IHTC16-23961), IHTC-16, August 10-15, 2018, Beijing, China

APPENDIX-A

Flow chart of stability analysis of SCWR

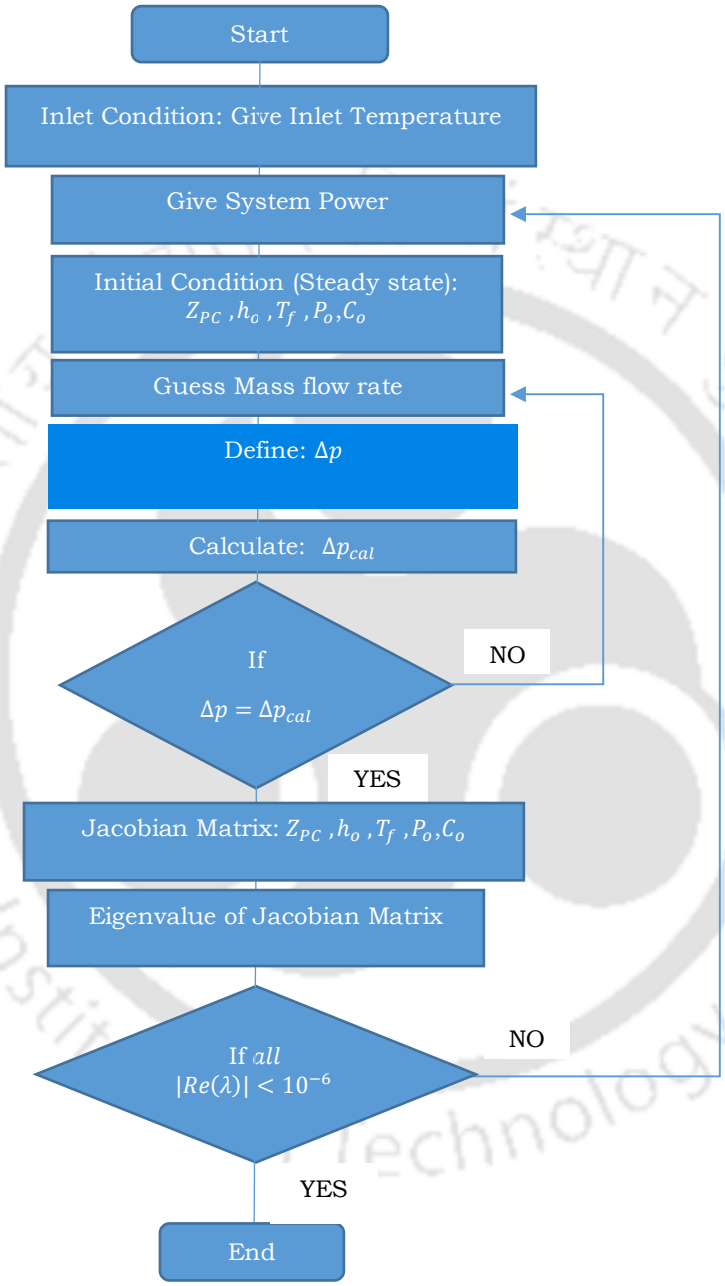

REFERENCES

Abram, T., Ion, S., 2008. Generation-IV nuclear power: A review of the state of the science. Energy Policy 36, 4323–4330. https://doi.org/10.1016/j.enpol.2008.09.059

Ambrosini, W., 2008. Lesson learned from the adoption of numerical tec niques in the analysis of nuclear reactor thermal-hydraulic phenomena. Prog. Nucl. Energy 50, 866–876. https://doi.org/10.1016/j.pnucene.2008.02.008

Ambrosini, W., Ferreri, J.C., 2006. Analysis of basic phenomena in boiling channel instabilities with different flow models and numerical schemes. In: 14th International national Conference on Nuclear Engineering (ICONE 14), Miami, Florida, USA, July 17–20.

Ambrosini, W., Sharabi, M., 2008. Dimensionless parameters in stability analysis of heated channels with fluids at supercritical pressures. Nucl. Eng. Des. 238, 1917–1929. https://doi.org/10.1016/j.nucengdes.2007.09.008

Ambrosini, W., Di Marco, P. and Ferreri, J. C., 2000. Linear and nonlinear analysis of density-wave instability phenomena. Heat and Technology, 18(1), pp. 27–36.

Ampomah-amoako, E., Akaho, E.H.K., Nyarko, B.J.B., Ambrosini, W., 2013. Annals of Nuclear Energy CFD analysis of the dynamic behaviour of a fuel rod subchannel in a supercritical water reactor with point kinetics. Ann. Nucl. Energy 59, 211–223. https://doi.org/10.1016/j.anucene.2013.04.008

Anishchenko, V.S., Vadivasova, T.E., Strelkova, G.I., 2014. Deterministic Nonlinear Systems. https://doi.org/10.1007/978-3-319-06871-8

Barragán-Martínez, A.M., Martin-Del-Campo, C., François, J.L., Espinosa-Paredes, G., 2013. MCNPX and HELIOS-2 comparison for the neutronics calculations of a Supercritical Water Reactor HPLWR. Ann. Nucl. Energy 51, 181–188. https://doi.org/10.1016/j.anucene.2012.08.013

Blázquez, J., Montalvo, C., García-berrocal, A., Balbás, M., 2013. Annals of Nuclear Energy Searching the beginning of BWR power instability events with the Hilbert Huang transform. Ann. Nucl. Energy 54, 281–288. https://doi.org/10.1016/j.anucene.2012.09.005

Boure, J.A., Bergles, A.E., Tong, L.S., 1973. Review of two-phase flow instability. Nucl. Eng. Des. 25, 165–192. https://doi.org/10.1016/0029-5493(73)90043-5

Cai, J., Ishiwatari, Y., Ikejiri, S., Oka, Y., 2009. Thermal and stability considerations for a supercritical water-cooled fast reactor with downward-flow channels during power-raising phase of plant startup. 239, 665–679. https://doi.org/10.1016/j.nucengdes.2008.12.010

Chatoorgoon, V., 2001. Stability of supercritical fluid flow in a single-channel natural-convection loop. Int. J. Heat Mass Transf. 44, 1963–1972. https://doi.org/10.1016/S0017-9310(00)00218-0

Chaudri, K.S., Tian, W., Su, Y., Zhao, H., Zhu, D., Su, G., Qiu, S., 2013. Coupled analysis for new fuel design using and UC for SCWR. Prog. Nucl. Energy 63, 57–65. https://doi.org/10.1016/j.pnucene.2012.11.001

Cheng, X., Schulenberg, T., 2001. Heat Transfer at Supercritical Pressures - Literature Review and Application to an HPLWR.

Commonwealth Edison Co., 1988. Reactor scram on high average power monitor flux level due to the personal valvingerror, LER 88-003-00.

Colombo, M., Cammi, A., Papini, D., Ricotti, M.E., 2012. RELAP5/MOD3.3 study on density wave instabilities in single channel and two parallel channels. Prog. Nucl. Energy 56, 15–23. https://doi.org/10.1016/j.pnucene.2011.12.002

Debrah, S.K., Ambrosini, W., Chen, Y., 2013. Discussion on the stability of natural circulation loops with supercritical pressure fluids. Ann. Nucl. Energy 54, 47–57. https://doi.org/10.1016/j.anucene.2012.10.015

Dhooge, a., Govaerts, W., Kuznetsov, Y. a., 2003. MATCONT: A MATLAB package for numerical bifurcation analysis of ODEs. ACM Trans. Math. Softw. 29, 141–164. https://doi.org/10.1145/779359.779362

Dutta, G., Maitri, R., Zhang, C., Jiang, J., 2015a. Numerical models to predict steady and unsteady thermal-hydraulic behaviour of supercritical water flow in circular tubes Atomic Energy of Canada Limited. Nucl. Eng. Des. 289, 155–165. https://doi.org/10.1016/j.nucengdes.2015.04.028

Dutta, G., Zhang, C., Jiang, J., 2015b. Analysis of flow induced density wave oscillations in the CANDU supercritical water reactor. Ann. Nucl. Energy 83, 264–273. https://doi.org/10.1016/j.anucene.2015.04.023

Durga Prasad, G.V., Pandey, M., 2008. Stability analysis and nonlinear dynamics of natural circulation boiling water reactors. Nucl. Eng. Des. 238, 229–240. https://doi.org/10.1016/j.nucengdes.2007.05.004

Dykin, V., Demazière, C., Lange, C., Hennig, D., 2013. Annals of Nuclear Energy Investigation of local BWR instabilities with a four heated-channel Reduced Order Model. Ann. Nucl. Energy 53, 320–330. https://doi.org/10.1016/j.anucene.2012.07.022

E. Gialdi, S. Grifoni, C. Parmeggiani and C. Tricoli, 1985. Core stability in operating BWR: operating experience. Prog. Nucl. Energy, 15, 447-459.

Fu, S.W., Liu, X.J., Zhou, C., Xu, Z.H., Yang, Y.H., Cheng, X., 2012. Annals of Nuclear Energy Modification and application of the system analysis code ATHLET to trans-critical simulations. 44, 40–49. https://doi.org/10.1016/j.anucene.2012.02.005

Gajev, I., Ma, W., Kozlowski, T., 2013. Annals of Nuclear Energy Space – time convergence analysis on BWR stability using TRACE / PARCS. Ann. Nucl. Energy 51, 295–306. https://doi.org/10.1016/j.anucene.2012.08.018

Guo, Y., Kareem, A., 2016. System identification through nonstationary data using Time – Frequency Blind Source Separation. J. Sound Vib. 371, 110–131. https://doi.org/10.1016/j.jsv.2016.02.011

Guido, G., Converti, J. and Clausse, A., 1991. Density-wave oscillations in paraUel channels - an analytical approach. Pb hb', 125, pp. 121–136.

Henry, A.F., 1975. Nuclear Reactor Analysis. MIT, Cambridge. International Atomic Energy Agency, 1999. Basic Safety Principles for Nuclear Power Plants 1. INSAG 12. IAEA.

Hirano, M., Tamakoshi, T., 1996. An analytical study on excitation of nuclear coupled thermal hydraulic instability due to seismically induced resonance in BWR. Nucl. Eng. Des. 162, 307–315. https://doi.org/10.1016/0029-5493(95)01128-5

Hou, D., Lin, M., Liu, P., Yang, Y., 2011. Stability analysis of parallel-channel systems with forced flows under supercritical pressure. Ann. Nucl. Energy 38, 2386–2396. https://doi.org/10.1016/j.anucene.2011.07.021

Hou, X., Sun, Z., Fan, G., Wang, L., 2017. Experimental and analytical investigation on the flow characteristics in an open natural circulation system. Appl. Therm. Eng. 124, 673–687. https://doi.org/10.1016/j.applthermaleng.2017.05.201

Ikejiri, S., Ishiwatari, Y., Oka, Y., 2010. Safety analysis of a supercritical-pressure water-cooled fast reactor under supercritical pressure. Nucl. Eng. Des. 240, 1218–1228. https://doi.org/10.1016/j.nucengdes.2009.12.034

Ishii, M., 1971. Thermally induced flow instabilities in two-phase mixtures in thermal equilibrium. PhD. Georg. Inst. Technol.

Ishiwatari, Y., Oka, Y., Koshizuka, S., 2003. Control of a High Temperature Supercritical Pressure Light Water Cooled and Moderated Reactor with Water Rods. J. Nucl. Sci. Technol. 40, 298–306. https://doi.org/10.1080/18811248.2003.9715359

J.C. Shaug, J.T. Tatsumi, J.G.M. 1987. Analysis of fluid dynamics in a boiling water reactor in a varying acceleration field, Forum on Unsteady Fluid Flow. ASME Winter Annual Meeting, Boston, USA, October.

Jäger, W., Sánchez Espinoza, V.H., Hurtado, A., 2011. Review and proposal for heat transfer predictions at supercritical water conditions using existing correlations and experiments. Nucl. Eng. Des. 241, 2184–2203. https://doi.org/10.1016/j.nucengdes.2011.03.022

Jackson, J.D., Hall, W.B., 1979. Influence of Buoyancy on Heat Transfer to Fluids in Vertical Tubes under Turbulent Conditions, Turbulent Forced Convection in Channels and Bundles. Hemishpere, New York, pp. 613–640.

Jain, R., 2005. Thermal-hydraulic instabilities in natural circulation flow loops under supercritical conditions. PhD thesis, University of Wisconsin-Madison.

Jain, V., Nayak, A.K., Vijayan, P.K., Saha, D., Sinha, R.K., 2010. Experimental investigation on the flow instability behavior of a multi-channel boiling natural circulation loop at low-pressures. Exp. Therm. Fluid Sci. 34, 776–787. https://doi.org/10.1016/j.expthermflusci.2010.01.007

Jain, P.K., Rizwan-uddin, 2008. Numerical analysis of supercritical flow instabilities in a natural circulation loop. Nucl. Eng. Des. 238, 1947–1957. https://doi.org/10.1016/j.nucengdes.2007.10.034

Joen, C.T., Gilli, L., Rohde, M., T'Joen, C., Gilli, L., Rohde, M., Joen, C.T., Gilli, L., Rohde, M., 2011. Sensitivity analysis of numerically determined linear stability boundaries of a supercritical heated channel. Nucl. Eng. Des. 241, 3879–3889. https://doi.org/10.1016/j.nucengdes.2011.07.005

K. Fukuda and T. Kobori., 1979. Classification of two-phase flow instabilities by density-wave oscillation model. J. Nucl. Sci. Technol. 16(2), 95, 18.

Kakac, S., Bon, B., 2008. A Review of two-phase flow dynamic instabilities in tube boiling systems. Int. J. Heat Mass Transf. 51, 399–433. https://doi.org/10.1016/j.ijheatmasstransfer.2007.09.026

Khabensky, V., Gerliga, V., 2012. Coolant Flow Instabilities in Power Equipment. https://doi.org/10.1201/b13658

Kiss, A., Balaskó, M., Horváth, L., Kis, Z., Aszódi, A., 2017. Experimental investigation of the thermal hydraulics of supercritical water under natural circulation in a closed loop. Ann. Nucl. Energy 100, 178–203. https://doi.org/10.1016/j.anucene.2016.09.020

Kotlyar, D., Shaposhnik, Y., Fridman, E., Shwageraus, E., 2011. Coupled neutronics thermo-hydraulic analysis of full PWR core with Monte-Carlo based BGCore system. Nucl. Eng. Des. 241, 3777–3786. https://doi.org/10.1016/j.nucengdes.2011.07.028

Kozmenkov, Y., Rohde, U., Manera, A., 2012. Validation of the RELAP5 code for the modeling of flashing-induced instabilities under natural-circulation conditions using experimental data from the CIRCUS test facility. Nucl. Eng. Des. 243, 168–175. https://doi.org/10.1016/j.nucengdes.2011.10.053

Kurganov, V.A., Zeigarnik, Y.A., Maslakova, I. V, 2012. Heat transfer and hydraulic resistance of super-critical-pressure coolants. Part I : Specifics of thermophysical properties of supercritical pressure fluids and turbulent heat transfer under heating con-ditio. Int. J. Heat Mass Transf. 55, 3061–3075. https://doi.org/10.1016/j.ijheatmasstransfer.2012.01.031

Lahey, R.T., 1986. Advance in the Analytical Modeling of Linear and Nonlinear Density-Wave Instability Modes. Nucl. Eng. Des. 95, 5–34.

Lee, J. Der, Pan, C., 2005. Nonlinear analysis for a nuclear-coupled two-phase natural circulation loop. Nucl. Eng. Des. 235, 613–626. https://doi.org/10.1016/j.nucengdes.2004.09.008

Lewins, J., 1961. Nuclear reactor kinetics and control. https://doi.org/10.1007/978-4-431-54195-0

Li, H. bo, Zhao, M., Hu, Z. xiao, Zhang, Y., Wang, F., 2018. Experimental study of supercritical water heat transfer deteriorations in different channels. Ann. Nucl. Energy 119, 240–256. https://doi.org/10.1016/j.anucene.2018.05.009

Li, S., Chatoorgoon, V., Ormiston, S.J., 2018. Numerical study of oscillatory flow instability in upward flow of supercritical water in two heated parallel channels. Int. J. Heat Mass Transf. 116, 16–29. https://doi.org/10.1016/j.ijheatmasstransfer.2017.08.115

Licht, J., 2009. Heat Transfer and Fluid Flow Characteristics in Supercritical 131, 1–14. https://doi.org/10.1115/1.3090817

Manera, A., Zboray, R., Van Der Hagen, T.H.J.J., 2003. Assessment of linear and non-linear auto-regressive methods for BWR stability monitoring. Prog. Nucl. Energy 43, 321–327. https://doi.org/10.1016/S0149-1970(03)00005-2

Marcel, C.P., Rohde, M., Masson, V.P., Hagen, T.H.J.J. Van Der, 2009. Fluid-to-fluid modeling of supercritical water loops for stability analysis. Int. J. Heat Mass Transf. 52, 5046–5054. https://doi.org/10.1016/j.ijheatmasstransfer.2009.03.022

March-Leuba, J., Rey, J., 1993. Coupled thermohydraulic-neutronics instabilities in boiling water nuclear reactors: a review of the state of the art. Nucl. Eng. Des. 145, 97–111. https://doi.org/10.1016/0029-5493(93)90061-D

Mcevoy, E., 2009. Using Matlab to integrate Ordinary Differential Equations (ODEs) 45, 1–9.

Meijer, H., 2008. Matcont Tutorial : ODE GUI version Getting started / Installation 14, 1–9.

Meloni, P., Polidori, M., 2007. A neutronics -thermalhydraulics model for preliminary studies on TRADE dynamics 237, 1704–1717. https://doi.org/10.1016/j.nucengdes.2007.03.014

Merroun, O., Almers, A., Bardouni, T. El, Bakkari, B. El, Chakir, E., 2009. Analytical benchmarks for verification of thermal-hydraulic codes based on sub-channel approach 239, 735–748. https://doi.org/10.1016/j.nucengdes.2009.01.005

Mishra, A.M., Singh, S., 2016. Non linear stability analysis of parallel channels with natural circulation. Nucl. Eng. Des. 309, 136–150. https://doi.org/10.1016/j.nucengdes.2016.09.002

Monti, L., Starflinger, J., Schulenberg, T., 2011. Development of a coupled neutronic-thermal-hydraulic tool with multi-scale capabilities and applications to HPLWR core analysis. Nucl. Eng. Des. 241, 1579–1591. https://doi.org/10.1016/j.nucengdes.2011.02.012

Mousavian, S.K., Misale, M., D'Auria, F., Salehi, M.A., 2004. Transient and stability analysis in single-phase natural circulation. Ann. Nucl. Energy 31, 1177–1198. https://doi.org/10.1016/j.anucene.2004.01.005

G.A. Murphy, 1988. Selected safety-related events, Nucl. Safety, 29 (3), 356-362

Nakatsuka, T., Oka, Y., Koshizuka, S., 1998. Control of a fast reactor cooled by super- critical light water. Nuclear Technology 121 (1), 81–92.

Nayak, A.K., Vijayan, P.K., Saha, D., Raj, V.V., 2000. Analytical study of nuclear-coupled density-wave instability in a natural circulation pressure tube type boiling water reactor. Nucl. Eng. Des. 195, 27–44.

Nayfeh AH, Balachandran B., 1992. Cyclic motions near a Hopf bifurcation of a four-dimensional system. Nonlinear Dyn. 1, 19–39.

Ortega, T.G., Class, A., Jr, R.T.L., Schulenberg, T., 2008. Stability analysis of a uniformly heated channel with super-critical water. Nucl. Eng. Des. 238, 1930–1939. https://doi.org/10.1016/j.nucengdes.2007.10.031

Pandey, M., 1996. Nonlinear Reactivity Interactions in Fission Reactor Dynamical Systems. Ph.D. Thesis, Indian Institute of Technology, Kanpur.

Pandey, M., Kumar, C.N., 2007. Lumped parameter modeling and stability analysis of supercritical water-cooled reactor. In the 12th International Topical Meeting on Nuclear Reactor Thermal Hydraulics (NURETH-12) Sheraton Station Square, Pittsburgh, Pennsylvania, U.S.A. pp. 1–11.

Pandey, V., Singh, S., 2016. A bifurcation analysis of boiling water reactor on large domain of parametric spaces. Commun. Nonlinear Sci. Numer. Simul. 38, 30–44. https://doi.org/10.1016/j.cnsns.2016.01.018

Paruya, S., Maiti, S., Karmakar, A., Gupta, P., Sarkar, J.P., 2012. Lumped parameterization of boiling channel — Bifurcations during density wave oscillations. Chem. Eng. Sci. 74, 310–326. https://doi.org/10.1016/j.ces.2012.02.039

Papini, D., Cammi, A., Colombo, M., Ricotti, M.E., 2012. Time-domain li ear and non-linear studies on density wave oscillations. Chem. Eng. Sci. 81, 118–139. https://doi.org/10.1016/j.ces.2012.06.005

Paul, S., Singh, S., 2014. Analysis of sub- and supercritical Hopf bifurcation with a reduced order model in natural circulation loop. Int. J. Heat Mass Transf. 77, 344–358. https://doi.org/10.1016/j.ijheatmasstransfer.2014.05.033

Peng, S.J., Podowski, M.Z., Lahey, R.T., 1986. BWR linear stability analysis. Nucl. Eng. Des. 93, 25–37. https://doi.org/10.1016/0029-5493(86)90192-5

Pioro, I.L., Duffey, R.B., 2005. Experimental heat transfer in supercritical water flowing inside channels (survey) 235, 2407–2430. https://doi.org/10.1016/j.nucengdes.2005.05.034

Prasad, G.V.D., Pandey, M., Kalra, M.S., 2007. Review of research on flow instabilities in natural circulation boiling systems. Prog. Nucl. Energy 49. https://doi.org/10.1016/j.pnucene.2007.06.002

Pucciarelli, A., Ambrosini, W., 2016. Fluid-to-fluid scaling of heat transfer phenomena with supercritical pressure fluids: Results from RANS analyses. Ann. Nucl. Energy 92, 21–35. https://doi.org/10.1016/j.anucene.2016.01.028

Rao, Y.F., Fukuda, K., Kaneshima, R., 1995. Nuclear Engineering and Design Analytical study of coupled neutronic and thermodynamic instabilities in a boiling channel 133–144.

Regis, C.R., Cotta, R.M., Su, J., 2000. Improved lumped analysis of transient heat conduction in a nuclear fuel rod. Int. Commun. Heat Mass Transf. 27, 357–366. https://doi.org/10.1016/S0735-1933(00)00116-0

Reiss, T., Fehér, S., Czifrus, S., 2008. Coupled neutronics and thermohydraulics calculations with burn-up for HPLWRs. Prog. Nucl. Energy 50, 52–61. https://doi.org/10.1016/j.pnucene.2007.12.002

Roberto, T.D., Silva, M.A.B. Da, Lapa, C.M.F., 2016. Development of a test facility for analyzing transients in supercritical water-cooled reactors by fractional scaling analysis. Nucl. Eng. Des. 296, 9–18. https://doi.org/10.1016/j.nucengdes.2015.10.025

Rofooei, F.R., Mobarake, A., Ahmadi, G., 2001. Generation of artificial earthquake records with a nonstationary Kanai-Tajimi model. Eng. Struct. 23, 827–837. https://doi.org/10.1016/S0141-0296(00)00093-6

Rohde, M., Marcel, C.P., T'Joen, C., Class, A.G., Van Der Hagen, T.H.J.J., 2011. Downscaling a supercritical water loop for experimental studies on system stability. Int. J. Heat Mass Transf. 54, 65–74. https://doi.org/10.1016/j.ijheatmasstransfer.2010.09.063

Roy, R.P., Jain, P., Kalra, S.P., 1988. Dynamic instability experiments in a boiling flow system. Int. J. Heat Mass Transf. 31, 1947–1952. https://doi.org/10.1016/0017-9310 (88)90209-8

Rohde, M., Marcel, C.P., T'Joen, C., Class, A.G., Van Der Hagen, T.H.J.J., 2011. Downscaling a supercritical water loop for experimental studies on system stability. Int. J. Heat Mass Transf. 54, 65–74. https://doi.org/10.1016/j.ijheatmasstransfer.2010.09.063

Ruspini, L.C., Marcel, C.P., Clausse, A., 2014. Two-phase flow instabilities: A review. Int. J. Heat Mass Transf. 71, 521–548. https://doi.org/10.1016/j.ijheatmasstransfer.2013.12.047

Saha, P., Ishii, M., Zuber, N., 1975. Experimental Investigation of The Thermally Induced Flow Oscillations. In Two-Phase Systems. Am. Soc. Mech. Eng. 8.

Satou, A., Watanabe, T., Maruyama, Y., Nakamura, H., 2011. Neutron-Coupled Thermal Hydraulic Calculation of BWR under Seismic Acceleration 2, 120–124.

Schmitt, T., Rodriguez, J., Leyva, I.A., Candel, S., 2012. Experiments and numerical simulation of mixing under supercritical conditions. Phys. Fluids 24. https://doi.org/10.1063/1.3701374

Schmidt, E., Eckert, E., Grigull, U., 1946. Heat Transfer by Liquids near the Critical State. Wright Field, Air Materiel Command.

Schulenberg, T., Leung, L.K.H., Oka, Y., 2014. Review of R&D for supercritical water-cooled reactors. Prog. Nucl. Energy 77, 282–299. https://doi.org/10.1016/j.pnucene.2014.02.021

Shan, J., Zhang, B., Li, C., Leung, L.K.H., 2009. SCWR subchannel code ATHAS development and CANDU-SCWR analysis. Nucl. Eng. Des. 239, 1979–1987. https://doi.org/10.1016/j.nucengdes.2009.05.008

Shampine, L.F. and Reichelt, M.W., 1997. The MATLAB ODE suit. SIAM J. Sci. Compt. 18, 1, 1-22.

Shang, Z., Lo, S., 2010. Numerical investigation of supercritical water-cooled nuclear reactor in horizontal rod bundles. Nucl. Eng. Des. 240, 776–782. https://doi.org/10.1016/j.nucengdes.2009.10.029

Sharabi, M., Ambrosini, W., 2009. Discussion of heat transfer phenomena in fluids at supercritical pressure with the aid of CFD models. Ann. Nucl. Energy 36, 60–71. https://doi.org/10.1016/j.anucene.2008.10.006

Sharabi, M., Ambrosini, W., He, S., Jackson, J.D., 2008. Prediction of turbulent convective heat transfer to a fluid at supercritical pressure in square and triangular channels. Ann. Nucl. Energy 35, 993–1005. https://doi.org/10.1016/j.anucene.2007.11.006

Sharma, M., Pilkhwal, D.S., Vijayan, P.K., Saha, D., Sinha, R.K., 2010. Steady state and linear stability analysis of a supercritical water natural circulation loop. Nucl. Eng. Des. 240, 588–597. https://doi.org/10.1016/j.nucengdes.2009.10.0

Sharma, M., Vijayan, P.K., Pilkhwal, D.S., Asako, Y., 2013. Steady state and stability characteristics of natural circulation loops operating with carbon dioxide at supercritical pressures for open and closed loop boundary conditions. Nucl. Eng. Des. 265, 737–754. https://doi.org/10.1016/j.nucengdes.2013.07.023

Shen, Z., Yang, D., Wang, S., Wang, W., Li, Y., 2017. Experimental and numerical analysis of heat transfer to water at supercritical pressures. Int. J. Heat Mass Transf. 108, 1676–1688. https://doi.org/10.1016/j.ijheatmasstransfer.2016.12.081

Shi, S., Lin, Y., Yang, W.S., 2015. Experimental Stability Maps for a BWR-type Small Modular Reactor. NURETH-16, Chicago 5498–5511.

Shitsi, E., Debrah, S. K., Agbodemegbe, V. Y. and Ampomah-Amoako, E. 2018. Effect of axial power distribution on flow instability in parallel channels with water at supercritical pressures. Annals of Nuclear Energy. Elsevier Ltd, 112, pp. 109–119. doi: 10.1016/j.anucene.2017.10.003

Su, Y., Feng, J., Zhao, H., Tian, W., Su, G., Qiu, S., 2013. Theoretical study on the fl ow instability of supercritical water in the parallel channels. Prog. Nucl. Energy 68, 169–176. https://doi.org/10.1016/j.pnucene.2013.06.005

Suárez, L.E., Montejo, L.A., 2005. Generation of artificial earthquakes via the wavelet transform. In International Journal of Solids and Structures. pp. 5905–5919. https://doi.org/10.1016/j.ijsolstr.2005.03.025

Sun, P., Jiang, J. and Shan, J. 2011. Construction of dynamic model of CANDU-SCWR using moving boundary method. Nuclear Engineering and Design. Elsevier B.V., 241(5), pp. 1701–1714. doi: 10.1016/j.nucengdes.2011.02.017.

Swapnalee, B.T., Vijayan, P.K., Sharma, M., Pilkhwal, D.S., 2012. Steady state flow and static instability of supercritical natural circulation loops.

Nucl. Eng. Des. 245, 99–112. https://doi.org/10.1016/j.nucengdes.2012.01.002

Parker, T.S., Chua, L.O., 1989. Practical Numerical Algorithms for Chaotic Systems. Springer-Verlag.

T. Ishida and I. Tomiai, 1992. Development of an analysis code for thermal hydrodynamics of marine reactor under multi-dimensional ship motions, Proc. 5th Int. Topical Meeting on Reactor Thermal Hydraulics, NURETH-5, Salt Lake City, USA.

Tian, X., Tian, W., Zhu, D., Qiu, S., Su, G., Xia, B., 2012. Annals of Nuclear Energy Flow instability analysis of supercritical water-cooled reactor CSR1000 based on frequency domain. Ann. Nucl. Energy 49, 70–80. https://doi.org/10.1016/j.anucene.2012.06.023

T'Joen, C., Rohde, M., 2012. Experimental study of the coupled thermo-hydraulic-neutronics stability of a natural circulation HPLWR. Nucl. Eng. Des. 242, 221–232. https://doi.org/10.1016/j.nucengdes.2011.10.055

Theler, G. G. and Bonetto, F. J., 2010. On the stability of the point reactor kinetics equations. Nuclear Engineering and Design, 240(6), pp. 1443–1449. doi: 10.1016/j.nucengdes.2010.03.007.

Todreas, E, N. and Kazimi, M. S. (2001) Nuclear Systems II: Elements of Thermal Hydraulic Design.

Uehiro, M., Rao, Y.F., Fukuda, K., 1996. Linear stability analysis on instabilities of in-phase and out-of-phase modes in boiling water reactors. J. Nucl. Sci. Technol. 33, 628–635.

van Bragt, D.D.B., van der Hagen, T.H.J.J., 1998. Stability of natural circulation boiling water reactors: Part I. Description stability model and theoretical analysis in terms of dimensionless groups. Nucl. Technol. 121, 40–51.

Wahi, P., Kumawat, V., 2011. Nonlinear stability analysis of a reduced order model of nuclear reactors : A parametric study relevant to the advanced heavy water reactor. Nucl. Eng. Des. 241, 134–143. https://doi.org/10.1016/j.nucengdes.2010.11.006

Wang, H., Bi, Q., Wu, G., Yang, Z., 2018. Experimental investigation on pressure drop of supercritical water in an annular channel. J. Supercrit. Fluids 131, 47–57. https://doi.org/10.1016/j.supflu.2017.08.014

Wang, H., Wang, W., Bi, Q., 2017. Experimental investigation on boiling heat transfer of high pressure water in a SCWR sub-channel. Int. J. Heat Mass Transf. 105, 799–810. https://doi.org/10.1016/j.ijheatmasstransfer.2016.09.088

WPPSS, 1992. Unusual reactor scram due to core instability, Revision I, LER 92-037

Xiong, T., Yan, X., Huang, S., Yu, J., Huang, Y., 2013. International Journal of Heat and Mass Transfer Modeling and analysis of supercritical flow instability in parallel channels. HEAT MASS Transf. 57, 549–557. https://doi.org/10.1016/j.ijheatmasstransfer.2012.08.046

Xiong, T., Yan, X., Xiao, Z., Li, Y., Huang, Y., Yu, J., 2012. Experimental study on flow instability in parallel channels with supercritical water. Ann. Nucl. Energy 48, 60–67. https://doi.org/10.1016/j.anucene.2012.05.018

Xi, X., Xiao, Z., Yan, X., Xiong, T., et al., 2014a. Numerical simulation of the flow instability between two heated parallel channels with supercritical water. Annals of Nuclear Energy, 64, pp. 57–66.
doi: 10.1016/j.anucene.2013.09.017.

Xi, X., Xiao, Z., Yan, X., Li, Y., et al., 2014b. An experimental investigation of flow instability between two heated parallel channels with supercritical water. Nuc. Eng. and Des., 278, pp. 171–181.
doi: 10.1016/j.nucengdes.2014.06.034.

Xu, W., Cai, J., Liu, S., Tang, Q., 2015. Analysis of the influences of thermal correlations on neutronic-thermohydraulic coupling calculation of SCWR. Nucl. Eng. Des. 284, 50–59. https://doi.org/10.1016/j.nucengdes.2014.11.043

Xu, Y., Downar, T., Walls, R., Ivanov, K., Staudenmeier, J., March-lueba, J., 2009. Application of TRACE / PARCS to BWR sta-bility analysis. Ann. Nucl. Energy 36, 317–323. https://doi.org/10.1016/j.anucene.2008.12.022

Yamaji, A., Kamei, K., Oka, Y., Koshizuka, S., 2005. Improved core design of the high temperature supercritical-pressure light water reactor. Ann. Nucl. Energy 32, 651–670. https://doi.org/10.1016/j.anucene.2004.12.006

Yang, W.S., Yang, W.S., 2005. Initial Implementation of Multi-Channel Thermal-Hydraulics Capability in Frequency Domain SCWR Stability Analysis Code SCWRSA. Argonne National Laboratory.

Yang, W.S., Zavaljevski, N., 2003. Preliminary stability analysis for super-critical water reactor. In Global 2003: Atoms for Prosperity: Updating Eisenhowers Global Vision for Nuclear Energy.

Yang, X., Su, G.H., Tian, W., Wang, J., Qiu, S., 2010. Numerical study on flow and heat transfer characteristics in the rod bundle channels under super critical pressure condition. Ann. Nucl. Energy 37, 1723–1734. https://doi.org/10.1016/j.anucene.2010.07.008

Yang, Z., Shan, Y., 2018. Experimental study on the onset of flow instability in small horizontal tubes at supercritical pressures. Appl. Therm. Eng. 135, 504–511. https://doi.org/10.1016/j.applthermaleng.2018.02.092

Yi, T.T., Koshizuka, S., Oka, Y., 2004. A Linear Stability Analysis of Supercritical Water Reactors, (I) Thermal-Hydraulic Stability. J. Nucl. Sci. Technol. 41, 1166–1175.

Yoo, J., Ishiwatari, Y., Oka, Y., Liu, J., 2006. Conceptual design of compact supercritical water-cooled fast reactor with thermal hydraulic coupling. Ann. Nucl. Energy 33, 945–956. https://doi.org/10.1016/j.anucene.2006.07.004

Yoshikawa, S., Smith, R.L., Inomata, H., Matsumura, Y., Arai, K., 2005. Performance of a natural convection circulation system for supercritical fluids. J. Supercrit. Fluids 36, 70–80. https://doi.org/10.1016/j.supflu.2005.02.007

Yu, J., Che, S., Li, R., Qi, B., 2011. Analysis of Ledinegg flow instability in natural circulation at supercritical pressure. Prog. Nucl. Energy 53, 775–779. https://doi.org/10.1016/j.pnucene.2011.04.001

Yu, J., Che, S., Li, R., Qi, B., Werner, B., Vijayan, P.K., Nayak., 2003. Application of a momentum integral model to the study of parallel channel boiling flow oscillations. Ann. Nucl. Energy 238, May 13-18, Nice, France. https://doi.org/10.1063/1.4823195

Yu, K. L. and Glusker B.N., 1965. Flow stability investigation in parallel coils with up flow down flow of the fluid at subcritical and subcritical pressures. CKTI Proceeding, Leningrad, issue 59, pp. 198-217.

Zahlan, H., Groeneveld, D.C., Tavoularis, S., 2014. Fluid-to-fluid scaling for convective heat transfer in tubes at supercritical and high subcritical pressures. Int. J. Heat Mass Transf. 73, 224–283. https://doi.org/10.1016/j.ijheatmasstransfer.2014.02.018

Zhang, R.J., Wang, W.Q., Hou, S.H., Chan, C.K., 2001. Seismic analysis of nuclear reactor core. Comput. Struct. 79, 1395–1404.

Zhang, Y., Li, H., Li, L., Wang, T., Zhang, Q., Lei, X., 2015. A new model for studying the density wave instabilities of supercritical water flows in tubes. Appl. Therm. Eng. 75, 397–409. https://doi.org/10.1016/j.applthermaleng.2014.09.029

Zhao, J., Saha, P., Kazimi, M.S., 2007. Core-Wide (In-Phase) Stability of Supercritical Water- Cooled Reactors-II: Comparison with Boiling Water Reactors. Nucl. Technol. 161, 124–139.

Zhao, J., Saha, P., Kazimi, M.S., 2006a. Hot-Channel Stability of Supercritical Water-Cooled Reactors-II: Effect of Water Rod Heating and Comparison with BWR Stability. Nucl. Technol. 158, 174–190.

Zhao, J., Saha, P., Kazimi, M.S., 2006a. Hot-Channel Stability of Supercritical Water Cooled Reactor-1: Steady State and Sliding Pressure Startup. Nucl. Technol. 158, 158–173.

Zhao, J., Saha, P., Kazimi, M.S., 2005. Stability of Supercritical Water-Cooled Reactor During Steady-State and Sliding Pressure Start-Up, in: The 11th International Topical Meeting on Nuclear Reactor Thermal-Hydraulics (NURETH-11) Popes' Palace Conference Center, Avignon, France, October 2-6, 2005. pp. 1–21.

Zhao, J., Saha, P., Kazimi, M.S., 2006b. Coupled Neutronics and Thermal-Hydraulic Out-Of-Phase Stability Of Supercritical Water- Cooled Reactors. Nucl. Technol. 164, 20–33.

Zhao, J., Tso, C.P., Tseng, K.J., 2011. SCWR single channel stability analysis using a response matrix method. Nucl. Eng. Des. 241, 2528–2535. https://doi.org/10.1016/j.nucengdes.2011.04.026

Zuber, N., 1966. An analysis of thermally induced flow oscillations in the near-critical and Supercritical thermodynamic region.